

Thesis Report

Flight Dynamics Simulation for the Preliminary Design of a Lift + Cruise eVTOL aircraft

Master Thesis AE

Jasper L'Ortije

Delft University of Technology



Thesis Report

Flight Dynamics Simulation for the Preliminary Design of a Lift + Cruise eVTOL aircraft

by

Jasper L'Ortije

to obtain the degree of Master of Science
at the Delft University of Technology,
to be defended publicly on Monday July 3, 2023 at 10:00 AM.

Student number: 4809521
Project duration: December 1, 2022 – July 3, 2023
Thesis committee: Dr. M.D.Pavel, TU Delft, supervisor
F.Olivero, TU Delft
A.Bombelli, TU Delft

This thesis is confidential and cannot be made public until December 31, 2024.

Cover: EVE V3 render by Embraer (from Embraer website)
Style: TU Delft Report Style

Preface

This report has been created by Jasper L'Ortije for the thesis on a flight dynamics model for Lift + Cruise eVTOL aircraft with the example of the EVE V3 aircraft by Embraer. In this report, information can be found on the subject of VTOL aircraft including research about the design and operations of such aircraft. This report is part of the Aerospace Engineering Master at the Technical University of Delft. This report has been created thanks to the help of by Dr. Marilena Pavel from the TU Delft who supervised the project.

*Jasper L'Ortije
Delft, June 2023*

Contents

Preface	i
Nomenclature	viii
1 Introduction	1
1.1 Research Questions	2
2 The eVTOL Market	3
2.1 eVTOL aircraft	3
2.2 Lift + Cruise	5
2.2.1 AIR AIR ONE	5
2.2.2 Airbus CityAirbus Nextgen	6
2.2.3 Volocopter VoloConnect/VoloRegion	6
2.3 Market Summary	7
2.4 Key Players	7
2.5 Preliminary Data Analytics	9
3 Case Study: Generic Lift + Cruise Aircraft	10
3.1 The EVE V3 eVTOL	10
3.2 Requirements	11
3.3 Planform Dimensions	11
3.4 Wing Sizing	12
3.4.1 Empennage Sizing	12
3.4.2 Airfoil selection	13
3.4.3 Drag Calculation	14
3.5 Fuselage Sizing	14
3.5.1 Top Fuselage Drag	14
3.5.2 Front Fuselage Drag	15
3.6 Battery Sizing	15
3.7 Engine Sizing	17
3.7.1 Power Calculation	17
3.7.2 Propeller Design	19
3.8 Class II Mass Estimation	20
3.9 Center of Gravity	21
3.10 N.P location	23
3.11 Moment of Inertia	23
3.12 Final Parameter values for EVE V3	24
4 The eVTOL aircraft Model	27
4.1 Assumptions	27
4.2 Phases of Flight	29
4.3 Coordinate System	29
4.4 Flight Conditions	30
4.5 Forces and Moments on the Model	31
4.5.1 Wings Forces and Moments	31
4.5.2 Fuselage Forces and Moments	33
4.5.3 Thrust Forces and Moments	34
4.5.4 Other Forces and Moments	35
4.6 Total Forces and Moments	35
4.7 Acceleration, Velocity, and Position	36
4.7.1 Transnational Motion	36

5	The Flight Dynamics Loop	38
5.1	Total Program Overview	38
5.2	Inputs and Outputs	39
5.3	Initialisation Sequence	41
5.3.1	Initialise Variables	41
5.3.2	Check Parameters	42
5.4	Plane Preliminary Calculations	42
5.4.1	Center of Gravity (C.G.)	42
5.4.2	Neutral Point (N.P.)	43
5.4.3	Moment of Inertia	43
5.4.4	Heading in Flight	43
5.5	Program Capabilities	43
5.6	The Flight Loop	44
5.7	Control Loops	45
5.7.1	Control Overview	45
5.7.2	Phase 1: Vertical Take-Off	45
5.7.3	Phase 2: Transition 1	46
5.7.4	Phase 3: Climb	47
5.7.5	Phase 4: Cruise	48
5.7.6	Phase 5: Descent	48
5.7.7	Phase 6: Transition 2	49
5.7.8	Phase 7: Vertical Landing	49
6	Optimisation of the VTOL and Output	51
6.1	General Output Graphs	51
6.1.1	Planform	52
6.1.2	Forces and Phases Panel	52
6.1.3	Stability Panel	53
6.1.4	Moment in X	54
6.1.5	Propeller Pitch	54
6.2	Optimisation	55
6.2.1	Concept Explanation	55
6.3	Flightpath and Limitations files	55
6.3.1	Class II Weight Estimation	56
6.3.2	Parameter Dimensions	58
6.3.3	Empennage Control Surfaces	59
6.3.4	Wing Control Surfaces	59
6.3.5	Optimised Engines	60
6.3.6	Optimised Battery	61
6.3.7	Convergence Plots	62
6.4	Range Effects	63
7	Conclusion	65
	References	69
A	EVE V3 Parameter text file	72
B	Limitations text file	77
C	Flightpath text file	78
D	EVE V3 Data	79
E	Other eVTOLS	81
E.1	Airbus NextGen	81
E.1.1	Input Parameter File	81
E.1.2	Output Plots	86
E.2	Korean KUS	92
E.2.1	Input Parameter File	92

- E.2.2 Output Plots 96
- E.3 Wisk Cora 102
 - E.3.1 Input Parameter File 102
 - E.3.2 Output Plots 106

List of Figures

1.1	The JSF-35B [2] and V-22 Osprey [3]	1
2.1	Render of the AIR ONE VTOL aircraft [10]	5
2.2	Renders of the Airbus CityAirbus Nextgen [13]	6
2.3	Render of the VoloRegion [15]	6
2.4	Market Share of eVTOL categories [17]	7
2.5	Speed and Range for various VTOL aircraft	9
3.1	Subscale test model of Eve [21]	10
3.2	Another render of the EVE V3 [21]	11
3.3	Planform with dimensions of the EVE V3	12
3.4	Clark Y airfoil data	13
3.5	Fuselage Drag (Helicopter Lecture 8, slide 18), [31]	15
3.6	CL and Mt graph used to find CDp	18
3.7	Power Calculation for EVE V3	19
3.8	Electric motor power density regression model [36]	19
3.9	Upwards Propeller Design	20
3.10	Values for the upward engine propeller	20
3.11	Forward Propeller Design	20
3.12	Values for the upward engine propeller	20
3.13	Planform with mass locations of the EVE V3	22
4.1	MATLAB Program Coordinate System	29
4.2	Flightpath angle and Track angle for the EVE aircraft	30
4.3	Lift and Drag diagram for the EVE aircraft	32
4.4	Aileron deflection angle for the EVE aircraft	33
4.5	Fuselage Drag diagram angle for the EVE aircraft	34
4.6	Pitch and Thrust Coefficient graph [53]	34
4.7	Thrust diagram for the EVE aircraft	35
5.1	MATLAB Program Overview	38
5.2	MATLAB Program Inputs and Outputs	39
5.3	MATLAB Program Inputs	39
5.4	MATLAB Program Initialisation	41
5.5	MATLAB Program Parameter Check	42
5.6	MATLAB Program Flight Loop	44
5.7	Phase 1 Flight Loop Diagram	45
5.8	Phase 2 Flight Loop Diagram	46
5.9	Phase 3 Flight Loop Diagram	47
5.10	Phase 4 Flight Loop Diagram	48
5.11	Phase 5 Flight Loop Diagram	49
5.12	Phase 6 Flight Loop Diagram	49
5.13	Phase 7 Flight Loop Diagram	50
6.1	Trajectory of EVE V3	51
6.2	Planform of EVE V3	52
6.3	Transition 1 forces in Z of EVE V3	52
6.4	Transition 1 forces in X of EVE V3	53
6.5	Trim Panel of EVE V3	53

6.6	Transition 1 moments in X of EVE V3	54
6.7	Pitch of the forward propeller of EVE V3	54
6.8	Optimization loop	55
6.9	Optimum Mass of EVE V3	57
6.10	Optimum Mass of EVE V3	58
6.11	Optimum Empennage Control Surfaces of EVE V3	59
6.12	Values for Transition Conditions	60
6.13	Values for Cruise Conditions	60
6.14	Optimum Wing Control Surfaces of EVE V3	60
6.15	Optimum Engines of EVE V3	60
6.16	Optimum Battery of EVE V3	61
6.17	Optimum Convergence of EVE V3	62
6.18	Mass and Range of EVE V3	63
7.1	MATLAB program file structure	66
D.1	Velocities/RPS for EVE V3	79
E.1	Optimum Path of Airbus NextGEN	86
E.2	Optimum Battery of Airbus NextGEN	87
E.3	Optimum Masses of Airbus NextGEN	88
E.4	Optimum Dimensions of Airbus NextGEN	89
E.5	Optimum Stabiliser of Airbus NextGEN	90
E.6	Optimum Engines of Airbus NextGEN	91
E.7	Optimum Path of Korean KUS	96
E.8	Optimum Battery of Korean KUS	97
E.9	Optimum Masses of Korean KUS	98
E.10	Optimum Dimensions of Korean KUS	99
E.11	Optimum Stabiliser of Korean KUS	100
E.12	Optimum Engines of Korean KUS	101
E.13	Optimum Path of Wisk Cora	106
E.14	Optimum Battery of Wisk Cora	107
E.15	Optimum Masses of Wisk Cora	108
E.16	Optimum Dimensions of Wisk Cora	109
E.17	Optimum Stabiliser of Wisk Cora	110
E.18	Optimum Engines of Wisk Cora	111

List of Tables

2.1	Different VTOL categories, [7] [8] [9] [10]	4
2.2	Volocopter 2X	4
2.3	Scorpion 3	4
2.4	Joby S4	4
2.5	AIR AIR ONE	4
2.6	Performance of the AIR AIR ONE [11]	5
2.7	Performance of the Airbus CityAirbus Nextgen [13]	6
2.8	Performance of the VoloRegion [15]	6
2.9	Different VTOL players, [18] [7] [9] [19] [20] [21]	8
3.1	Performance of the EVE (V3) [21]	11
3.2	System requirements for EVE	11
3.3	Lift Surface parameters for EVE V3	14
3.4	Drag Surface parameters for EVE V3	14
3.5	Parameters used for the Power Required [32]	17
3.6	Parameters used for the Power Required	18
3.7	Motor Data [37][38][39]	19
3.8	Design Parameter Values	21
3.9	Converged Mass Values	21
3.10	C.G. relative Location of EVE V3 Components	23
3.11	Text file Input Parameters for EVE V3 (Part 1)	25
3.12	Text file Input Parameters for EVE V3 (Part 1)	26
3.13	Calculated Parameters	26
4.1	Engine Parameters for EVE V3	27
5.1	Program System requirements	40
5.2	General Parameters for EVE V3	42
5.3	General Parameters for EVE V3	43
5.4	Control Options for each phase of flight	45
5.5	Values in Equation 5.7.4 and Equation 5.7.4	47
5.6	Values in Equation 5.7.4 and Equation 5.7.4	48
6.1	Flightpath Text File Values	56
6.2	Limitations Text File Values	56
6.3	Input Mass Values	56
6.4	Optimised Mass Values	56
6.5	Final Values for EVE V3, 1	62
6.6	Final Values for EVE V3, 2	62
6.7	Mass values for different flight ranges	63
D.2	Engine values for different flight ranges	79
D.3	Battery values for different flight ranges	79
D.1	Range and Mass Values for EVE V3	80

Nomenclature

Abbreviations

Abbreviation	Definition
AAM	Advanced Air Mobility
ATM	Air Traffic Management
APU	Auxiliary Power Unit
BLDC	Brushless DC Electric Motors
DEP	Distributed Electric Propulsion
eVTOL	electrical Vertical Take-Off and Landing
Li-Ion	Lithium-Ion
MaaS	Mobility as a Service
PAV	Personal Air Vehicles
RPM	Rotations Per Minute
UAM	Urban Air Mobility
UN	United Nations
UATM	Urban Air Traffic Management
VTOL	Vertical Take-Off and Landing

Symbols

Symbol	Definition	Unit
a_x	Acceleration in X	$[m/s^2]$
a_y	Acceleration in Y	$[m/s^2]$
a_z	Acceleration in Z	$[m/s^2]$
AR	Aspect ratio	$[-]$
b	Wingspan	$[m]$
b_h	Horizontal Tail Wingspan	$[m]$
c	Chord length	$[-]$
c_{MAC}	Mean Aerodynamic Chord	$[-]$
C	Rate of climb	$[-]$
C_D	Drag coefficient	$[-]$
$C_{D,t}$	Transition Drag coefficient	$[-]$
C_{D0}	Zero lift drag coefficient	$[-]$
$C_{D_{front}}$	Front Fuselage drag coefficient	$[-]$
$C_{D_{top}}$	Front Fuselage drag coefficient	$[-]$
C_{Dp}	Profile drag coefficient	$[-]$
C_L	Lift coefficient	$[-]$
C_{L0}	Zero AoA Lift coefficient	$[-]$
C_T	Thrust coefficient	$[-]$
C_{VT}	Vertical Tail volume coefficient	$[-]$
D	Drag	$[N]$
d_{prop}	Propeller Diameter	$[m]$
e	Oswald efficiency factor	$[-]$
E_x	Specific phase battery energy	$[-]$
g	Earth Gravity constant	$[m/s^2]$

Symbol	Definition	Unit
GED	Gravimetric Energy Density	[Wh/kg]
h_b	Battery Height	[m]
h_f	Fuselage Height	[m]
ki	Induced power factor	[-]
l_b	Battery Length	[m]
l_f	Fuselage Length	[m]
l_v	Distance to vertical tail	[m]
L	Lift	[N]
m	Aircraft Mass	[kg]
MAC	Mean Aerodynamic Chord	[m]
M_a	Aileron Moment	[Nm]
M_e	Elevator Moment	[Nm]
M_r	Rudder Moment	[Nmb]
M_t	Tip Mach number	[-]
M_{wing}	Wing Pitching Moment	[Nm]
n_A	Upward engines after C.G.	[-]
n_B	Upward engines before C.G.	[-]
$N_{bl,u}$	Number of prop. blades Upwards,	[-]
$N_{bl,f}$	Number of prop. blades Forwards,	[-]
$N_{mot,u}$	Number of motors Upwards,	[-]
$N_{mot,f}$	Number of motors Forwards,	[-]
N_{pax}	Number of Passengers,	[-]
p	Air pressure	[Pa]
p_0	Sea Level Air pressure	[Pa]
p_{T_A}	After C.G. position	[m]
p_{T_B}	Before C.G. position	[m]
P_{climb}	Power required for climb	[W]
PM	Power Margin	[%]
P_{cruise}	Power required for cruise	[W]
P_d	Drag power	[N]
$P_{descent}$	Power required for descent	[W]
P_{hover}	Power required for hover	[W]
P_i	Induced power	[N]
$P_{i,hover}$	Induced drag power for hover	[W]
P_{max}	Fuselage section perimeter	[m]
P_{par}	Parasite power for vertical climb	[W]
p_T	Upward engine position	[-]
P_{prof}	Profile power	[W]
r	Rotor radius	[m]
\ddot{R}	Rotational Acceleration	[deg/s ²]
\dot{R}	Rotational Velocity	[deg/s]
R_A	After C.G. Ratio	[-]
R_B	Before C.G. Ratio	[-]
R	Rotational Position	[deg]
Re	Reynolds number	[-]
RPS	Rotations per Second	[-]
S	Wing surface area	[m ²]
$S_{V,tail}$	V-Tail surface area	[m ²]
SED	Battery specific energy density	[Wh/kg]
SOC_{min}	Minimum State of Charge	[%]
T	Thrust	[N]
V	Velocity	[m/s]
V_f	Forward Velocity	[m/s]
V_t	Transition Velocity	[m/s]

Symbol	Definition	Unit
v_x	X-direction Velocity	[<i>m/s</i>]
v_y	Y-direction Velocity	[<i>m/s</i>]
v_z	Z-direction Velocity	[<i>m/s</i>]
VEC	Volumetric Energy Density	[<i>Wh/L</i>]
W	Weight	[<i>N</i>]
w_b	Battery Width	[<i>m</i>]
w_f	Fuselage Width	[<i>m</i>]
x	Position in X	[<i>m</i>]
y	Position in Y	[<i>m</i>]
z	Position in Z	[<i>m</i>]
α	Angle of Attack	[<i>deg</i>]
α_{eff}	Effective Angle of Attack	[<i>deg</i>]
ρ	Density	[<i>kg/m³</i>]
η	Thrust Efficiency	[–]
η_b	Battery Efficiency	[–]
δ_a	Aileron Deflection	[<i>deg</i>]
δ_e	Elevator Deflection	[<i>deg</i>]
δ_r	Rudder Deflection	[<i>deg</i>]
μ	Advance ratio	[–]
σ	Blade solidity	[–]
λ	Wing Taper Ratio	[–]
Λ	Wing Sweep Angle	[<i>deg</i>]
Γ	Wing Dihedral Angle	[<i>deg</i>]
ω	Propeller velocity	[<i>RPS</i>]
$\ddot{\phi}$	Rotational Acceleration in X	[<i>deg/s²</i>]
$\dot{\phi}$	Rotational Velocity in X	[<i>deg/s</i>]
ϕ	Rotational Position in X	[<i>deg</i>]
$\ddot{\theta}$	Rotational Acceleration in Y	[<i>deg/s²</i>]
$\dot{\theta}$	Rotational Velocity in Y	[<i>deg/s</i>]
θ	Rotational Position in Y	[<i>deg</i>]
$\ddot{\psi}$	Rotational Acceleration in Z	[<i>deg/s²</i>]
$\dot{\psi}$	Rotational Velocity in Z	[<i>deg/s</i>]
ψ	Rotational Position in Z	[<i>deg</i>]
ζ	Wing Coefficient	[–]

1

Introduction

A study conducted by the United Nations (UN) on world urbanisation in 2022 reports that 54% of the world population lives in an urban environment. This is expected to increase to 66% by 2050 as another 2.5 billion people would move to urban areas [1]. This increase will create numerous challenges as cities will have to adapt their infrastructure to accommodate more people. As a result, many startups are racing to develop aerial ways of transportation in urban areas, as roads are congested most of the time. There is a very relevant quote by Elon Musk as he said: "having 2D streets and 3D buildings means bad traffic forever".

The solution is to create efficient urban air transport with modern VTOL aircraft (Vertical Take-off and Landing). One of the main concerns when designing an VTOL is the vertical take-off and landing options. Very few aircraft like the F35-B or V-22 Osprey are currently capable of such performance. Both aircraft are top of the line military projects by the government of the United States and cost 100 million dollars and 60 million dollars respectively [2][3]. The fact that even these expensive projects have had major drawbacks as the V-22 Osprey, since becoming operational in 2007, has had eight crashes resulting in 16 fatalities and several minor incidents reinforces the complexity of VTOL aircraft design.



Figure 1.1: The JSF-35B [2] and V-22 Osprey [3]

While these military projects use various types of combustion engines, this report focuses on electric VTOL aircraft (eVTOL) as these are these eVTOL aircraft could be used as an alternative to using public transport or other automotive solutions in cities. The increase in computing capacity which is needed to control aircraft in very complex transitions as well as the technological advancements in battery technology has opened up a new market: the urban electric VTOL market. Many companies are trying to make the best possible eVTOL that can be used in large, congested cities. The urban eVTOL market is expected to grow at a rate of 40% per year until at least 2032 [4]. As a result, many new startups will develop their own eVTOL aircraft that will be able to transport goods or passengers in large, congested metropolitan areas. A tool for the preliminary design of a eVTOL is therefore necessary in order to enhance the quality of the first iteration of such an aircraft. This is done by simulating a full flight in

MATLAB using a flight dynamics model that is flexible to the user's inputs (wings dimensions, airfoil choice, weight of battery and many others) which will be defined at a later stage in this report.

This thesis will investigate the flight dynamics of such a eVTOL aircraft by taking the example of EVE V3, an eVTOL aircraft developed by Embraer, the third-largest aircraft manufacturer in the world. The end goal is to have a program that outputs the optimal engine blade sizing, size of the control surfaces (elevator, ailerons, and rudder) for a given set of requirements as inputs which include the cruise velocity and cruise altitude for example. The eVTOL will be able to follow these inputs and fly in all 6 dimensions: three forces and three moments around the centre of gravity of the plane. The MATLAB program will be able to simulate a flight for any given Lift + Cruise eVTOL aircraft (input) and optimize the mentioned parameters.

In chapter 2, the eVTOL market is described along with the explanation of the three main eVTOL categories: Multicopter, Vectored Thrust and Lift + Cruise. The latter is the main focus of the report as it concerns the eVTOL, on which the MATLAB program is based on. EVE V3, the Lift + Cruise aircraft made by Embraer is sized and analysed in chapter 3. Then, in chapter 4, the force model used by the MATLAB program is addressed in detail, and the preliminary calculations are showcased. The next step is to explain how the flight loop of the program works, which is done in chapter 5. At last, the output plots made by the MATLAB program are shown and discussed in chapter 6.

1.1. Research Questions

The thesis aims to create a preliminary design tool in MATLAB for Lift + Cruise eVTOLs, covering all aspects of flight in order to be able to optimise a certain aspect of the aircraft. The thesis focuses on making a flight dynamics model of the EVE V3 eVTOL aircraft created by Embraer. This flight model will later on be generalised to Lift + Cruise aircraft with the ability to change the number of engines, wing size and many other parameters.

As a result, how can the flight dynamics of Lift + Cruise eVTOLs be accurately modelled in MATLAB? What are the key design considerations for optimizing a specific aspect of the Lift + Cruise eVTOL aircraft, such as efficiency or range? What are the critical parameters that need to be considered when generalizing the flight dynamics model to accommodate different aircraft configurations? How does the number of engines impact the flight performance and stability of Lift + Cruise eVTOLs? How can the MATLAB design tool find an optimal aircraft for a given mission, and a given aircraft configuration? What are the trade-offs involved in optimizing Lift + Cruise eVTOLs for different objectives?

These research questions will guide the development and exploration of a preliminary design tool for the Lift + Cruise eVTOL in MATLAB. By addressing these issues, this work should contribute to understanding the complex flight dynamics of eVTOL aircraft and provide valuable insights for optimizing their performance. Accurately modelling flight dynamics in MATLAB will allow designers to simulate and evaluate the behaviour of different eVTOL configurations under different conditions.

2

The eVTOL Market

In this chapter, which is based on the literature study, the eVTOL market is described starting with the definition of an eVTOL. The three eVTOL categories are outlined in section 2.1. Then, the Lift + Cruise is explored in detail in section 2.2. This chapter concludes with a market overview and an overview of the key eVTOL players in section 2.3.

2.1. eVTOL aircraft

Vertical take-off and landing (VTOL) aircraft are a type of aircraft that are capable of taking off and landing vertically, without the need for a runway. This allows them to operate in a wide range of environments, including urban areas, forests, and other locations where traditional aircraft may not be able to land or take off. VTOL aircraft typically use a combination of rotors, fans, and other propulsion systems to generate the lift and thrust needed for vertical flight. They may also have the ability to transition from vertical to horizontal flight, allowing them to fly like a traditional airplane once they are airborne.

The development of VTOL aircraft has been an area of intense research and innovation in recent years, with many companies and organizations working on designs that offer new capabilities and improved performance. Some of the key challenges in the development of VTOL aircraft include the need to design a propulsion system that can provide enough lift for vertical flight, while also being efficient enough to allow the aircraft to fly horizontally. Additionally, VTOL aircraft are typically more complex and expensive to design and manufacture than traditional aircraft, which can limit their development and adoption.





Despite these challenges, VTOL aircraft have the potential to revolutionize air travel and transportation, offering new capabilities and greater flexibility than conventional aircraft. They can operate in a wide range of environments, including urban areas for example or forests, and other locations where traditional aircraft may not be able to land or take off. Additionally, VTOL aircraft can be used for a variety of missions, including transportation, surveillance, search and rescue, and other operations that require the ability to take off and land vertically. The focus of this report as well as most of the current research is electric vertical take-off and landing aircraft that will be deployed in urban areas as part of the future of mobility in big metropolises.

Electric vertical take-off and landing aircraft (eVTOL) are currently being developed all around the globe. They can serve many purposes including mobility-as-a-service (MaaS), enable Advanced Air Mobility (AAM) [5], that could include on-demand air taxi services, regional air mobility, freight delivery, and personal air vehicles (PAVs). Advanced Air Mobility, as outlined by NASA, is a vision of a safe, accessible, automated and affordable air transportation system for passengers and cargo in urban and rural locations [6]. This vision is slowly becoming a reality with various companies including Uber, Joby Aviation, Volocopter and Airbus among many others, developing an eVTOL aircraft.

Due to the limited battery capacities, range is the biggest problem for VTOL aircraft. As a result, most VTOL aircraft are designed for short flights, as a replacement for cars in congested areas. Certain

attempts are being made in order to make a regional VTOL aircraft. There are many ways to design a eVTOL aircraft that will satisfy the above-mentioned mission profile with vertical take-off and landing. These categories include the Multicopter, Hoverbike, Vectored Thrust and Lift + Cruise. Each category has their own benefits and drawbacks highlighted in Table 2.1.

Table 2.1: Different VTOL categories, [7] [8] [9] [10]

Category	Example	Benefits (+)	Drawbacks (-)
Multicopter	 <p>Volocopter 2X</p>	<ul style="list-style-type: none"> • Hovering Efficiency • Compactness (Size) 	<ul style="list-style-type: none"> • Rotor failure consequences • Energy consumption in Cruise
Hoverbike	 <p>Scorpion 3</p>	<ul style="list-style-type: none"> • Price • Size and Weight 	<ul style="list-style-type: none"> • No Safety pod • Rotor failure consequences • 1 Passenger (or 2 maximum)
Vectored Thrust	 <p>Joby S4</p>	<ul style="list-style-type: none"> • Cruise Performance • Safety 	<ul style="list-style-type: none"> • Complexity of tilting rotors • Weight
Lift + Cruise	 <p>AIR AIR ONE</p>	<ul style="list-style-type: none"> • Cruise Performance • More simple than V.Thrust 	<ul style="list-style-type: none"> • Drag from unused rotors • Compromise between hover and cruise

Wingless (Multicopter)

Multicopter are the simplest form of eVTOL aircraft. These aircraft strongly resemble helicopters but instead of having one with rotor with a swashblade, these eVTOLs use multiple rotors with propellers in order to provide enough thrust to lift up the aircraft. The development of electric rotors has created opportunities to use many rotors on one aircraft which was previously not the case as helicopters with multiple rotors are very complex, since they also need multiple heavy engines.

Hover Bikes

Hoverbikes could be compared to motorcycles as they not come with any structural protection for the passenger. These hover bikes are designed for short commutes. This category is not covered in

detail as it is too far away from the main research point but it can still be interesting to look at their performance.

Vectored Thrust

This category is the most complex and currently most researched eVTOL type, Vectored thrust. These VTOL aircraft are capable of changing the pitch of their propellers in order to transition from providing an upwards force in order to hover into a forward force at higher speeds. These aircraft often also make use of wings to provide additional lift. As the tilting rotor system is often very complex, this configuration will not be used in the simulation.

Lift + Cruise

Lift + Cruise is an interesting category, it is a compromise between the fully vertical multicopter design and the thrust vectoring design. In this category, the rotors that are used for vertical flight are turned off in cruise and visa-versa. This creates unnecessary drag, but the main advantage is the simplicity of non-tilting rotors, which can have an impact on the weight and therefore the range of the aircraft. EVE, the subject of this thesis, is part of the Lift + Cruise category. When compared to Vectored Thrust eVTOLs, the transitions are much simpler since the upward facing engines and forward facing engine's rotations per minute (RPM) can be varied independently. Lift + Cruise eVTOLs thrive in urban areas where the distances flown for each flight is small. The added drag of the upward engines in flight is less important for short metropolitan flights and the reduced complexity of this category when compared to Vectored Thrust also leads to less complex control systems and hence a safer aircraft.

2.2. Lift + Cruise

Lift + Cruise is the chosen eVTOL category for this thesis, it is a compromise between the fully vertical multicopter design and the thrust vectoring design. In this category, the rotors that are used for vertical flight are turned off in cruise and visa-versa. This creates unnecessary drag, but the main advantage is the simplicity of non-tilting rotors, which can have an impact on the weight and therefore the range of the aircraft. EVE, the subject of this literature study, is part of the Lift + Cruise category.

2.2.1. AIR AIR ONE

An example of Lift + Cruise eVTOL aircraft is the AIR AIR ONE made by AIREV, a company from Israel founded in 2018. The VTOL aircraft is designed for personal use and uses the company's "fly by intent" controls. While little information is available on the control system, the company wants to make the controls as easy as possible, so this aircraft can be used as a personal vehicle. This aircraft is not yet in production, but it is one of the leaders in the VTOL market.



Figure 2.1: Render of the AIR ONE VTOL aircraft [10]

Table 2.6: Performance of the AIR AIR ONE [11]

Performance	Value	Unit
Number of Rotors	8	-
Blades per Rotor	3	-
Max Speed	250	[km/h]
Cruise Speed	161	[km/h]
Range	177	[km]
Passengers	2	-

A full scale AIR AIR ONE completed a successful hover test in Q2 of 2022, [12]. The aircraft controls itself at low speeds using a difference in RPM (Rotations per Minute) in each of the rotors, for high speeds, control surfaces are used on the wings. The aircraft is powered by eight electric motors, and uses eight pairs of rotors to fly at a max speed of 249 [km/h] and a max range of 177 [km]. While being a vectored thrust VTOL aircraft, the wing and rotors do not tilt. As a result, the aircraft is relatively light at 970 [kg] with its passengers.

2.2.2. Airbus CityAirbus Nextgen

The Nextgen is Airbus' second iteration of a VTOL aircraft. Contrary to the first CityAirbus which is a multicopter eVTOL, this VTOL has a Lift + Cruise configuration. This concept was revealed in September 2021. The aircraft holds 4 passengers and has a cruise speed of 120 $[km/h]$ and a range of 80 $[km]$. It is interesting to notice is that on top of the V-tail, the Nextgen has a horizontal stabiliser with an elevator that is clearly visible on Figure 2.2.



Figure 2.2: Renders of the Airbus CityAirbus Nextgen [13]

The aircraft has 8 rotors with 4 blades each. The fact that there are no vertical rotors for cruise conditions is quite surprising. While there is limited information on this question, the 2 angled rotors on the V-tail could be active during cruise and the 6 propellers on the wings could be turned off. CityAirbus NextGen is in a detailed design phase right now, and the prototype's first flight is planned for 2023. The prototype will pave the way for certification, and certification is expected around 2025. Also, Airbus Helicopters has started building a dedicated test center for its CityAirbus NextGen eVTOL aircraft within its existing site at Donauwörth in southern Germany [14].

Table 2.7: Performance of the Airbus CityAirbus Nextgen [13]

Performance	Value	Unit
Number of Rotors	8	-
Blades per Rotor	4	-
Cruise Speed	120	$[km/h]$
Range	80	$[km]$
Passengers	4	-

2.2.3. Volocopter VoloConnect/VoloRegion

Volocopter, most known for its Volocopter 2X model which is a multicopter, is developing a regional aircraft. This aircraft is in the Lift + Cruise configuration and has a range of 100 $[km]$, a cruise speed of 180 $[km/h]$. It holds 4 passengers and is expected to be piloted fully autonomously when on the market.



Figure 2.3: Render of the VoloRegion [15]

Table 2.8: Performance of the VoloRegion [15]

Performance	Value	Unit
Number of Rotors	6+2	-
Blades per Rotor	2	-
Cruise Speed	180	$[km/h]$
Range	100	$[km]$
Passengers	4	-

The VoloRegion originally debuted as VoloConnect. The name change from VoloConnect to VoloRegion took place in 2022. Volocopter announced that its VoloConnect fixed-wing eVTOL performed its first flight in May 2022 [16]. The aircraft has 6 rotors and 2 ducted fans for forward flight. The program is able to optimise all above-mentioned aircraft.

2.3. Market Summary

The market share summary of all the categories paints an interesting picture. As can be seen in Figure 2.4, the Vectored Thrust category has the advantage with a market share of 52%, followed by Lift + Cruise with 26% and Multicopter with 22%. [17]

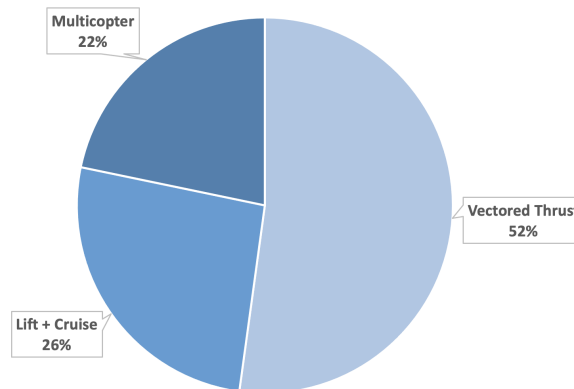












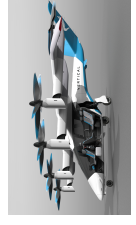

Figure 2.4: Market Share of eVTOL categories [17]

The reason Vectored Thrust is most popular is mainly due to its overall lower drag and thus higher range capabilities because the upward and forward facing engines are the same, the engines merely rotate during transition. Since the eVTOL market is developing, many startups are able to get enough funding in order to attempt to create the best possible eVTOL aircraft with the most advanced control systems possible.

2.4. Key Players

While there are hundreds of eVTOL concepts available, only a handful are serious contenders for an entry in service in the near future. The research done on the current developments of VTOL aircraft are summarized in Table 2.9. Clear leaders of this developing markets are Airbus, Volocopter, Joby, Archer, Vertical and Embraer with its EVE aircraft. These companies are mostly startups, except Airbus, which is a well-established aviation player. Embraer's EVE project is listed on the stock market under a separate company than its main operations, under the ticker NYSE:EVEX. Joby, Archer, Vertical and Embraer are currently testing their prototypes. It is interesting to notice that all these concepts feature 4 passengers plus 1 pilot. It seems that it would take a few more years or even decades for fully autonomous VTOL aircraft to come on the market. Airbus' and Volocopter's concepts are fully autonomous, but these two companies are only in the early stages of design for now.

Table 2.9: Different VTOL players, [18] [7] [9] [19] [20] [21]

Name	Airbus	Volocopter	Joby	Archer	Vertical	Embraer (Eve)
Logo	 AIRBUS	 VOLOCOPTER	 Joby	 ARCHER	 VERTICAL	 EMBRAER
Stock ticker	EPA: AIR	Private	NYSE: JOBY	NYSE: ACHR	NYSE: EVTL	NYSE:EVEX
Aircraft						
Name	NextGen	VoloRegion	Joby S4	Midnight	VX-4	EVE V3
Established Players	✓	X	X	X	X	✓
Category	Lift + Cruise	Lift + Cruise	Vectored Thrust	Vectored Thrust	Vectored Thrust	Lift + Cruise
Number of Passengers	4	4	4+1	4+1	4+1	4+1
Cruise Speed [km/h]	120	180	250	240	241	200
Range [km]	80	100	250	100	160	100
Controls	Autonomous	Autonomous	Pilot	Pilot	Pilot	Pilot

2.5. Preliminary Data Analytics

It is very interesting to plot the cruise speed and range of each different VTOL aircraft. The Hoverbikes were ignored because of their limited capabilities in terms of speed and range.

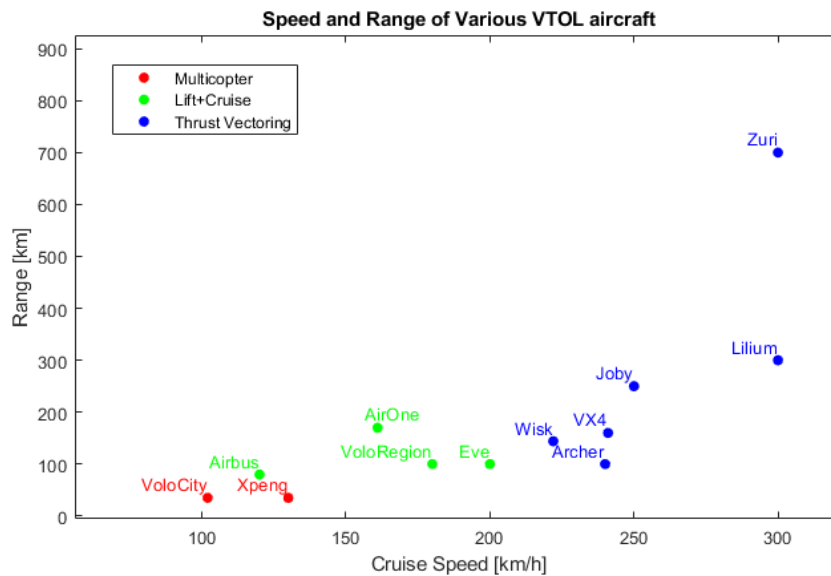


Figure 2.5: Speed and Range for various VTOL aircraft

It is important to notice that all aircraft in Figure 2.5 are able to accommodate 5 passengers, except for the Multicopters and AIR AIR ONE which is a 2 passenger eVTOL. There is a clear range and cruise speed difference when comparing the three different VTOL categories: Multicopter, Lift + Cruise and Thrust Vectoring. The Multicopter design has a relatively low range, which makes it a good candidate for short urban flights. The Lift + Cruise VTOL aircraft have relatively better performance, with EVE achieving the highest cruise speed of 200 [km/h]. This higher cruise speed could result in lower travel times for the passengers. At last, the Thrust Vectoring aircraft have the highest range and cruise speeds. The Zuri 2.0 aircraft has a range of 700 [km], but this also due to its hybrid propulsion system as it has a "old-fashioned" turbine in the back in addition to its 8 electric rotors.

Since the eVTOL market has now been described, it is now time to take an in depth look at the EVE V3 Lift + Cruise eVTOL create by Embraer. The next chapter covers the sizing of the eVTOL as well as further information about Lift + Cruise aircraft.

3

Case Study: Generic Lift + Cruise Aircraft

This chapter covers the sizing process of a generic Lift + Cruise aircraft. As an example, the EVE V3 aircraft made by Embraer is chosen. In this chapter the wing is sized in section 3.4 followed by the sizing of the fuselage in section 3.5, the battery sizing in section 3.6 and the engine sizing in section 3.7. At last, a Class II mass estimation is performed in order to have an exact mass value for EVE V3 in section 3.8.

3.1. The EVE V3 eVTOL

EVE V3 is the aircraft that has been chosen in order to build the flight dynamics program in MATLAB. This Lift + Cruise eVTOL aircraft has been chosen because of its many rotors. The fact that it has 8 upward rotors and 2 forward rotors helps with control in every direction. The system is even over-controlled, so decisions will have to be made about what engines control what motions later on in the process (see Figure 4.5.1). The aircraft is currently being tested by Embraer and is expected to enter the market at the end of 2025. The EVE concept is designed to provide urban air mobility solutions, including transportation of passengers and cargo. The aircraft features electric propulsion and vertical takeoff and landing capabilities, enabling it to operate in densely populated urban areas with limited infrastructure.

Embraer is the third-biggest aircraft manufacturer in the world, behind Airbus and Boeing. It was founded in 1969 and its main headquarters are based in São Paulo, Brazil. EmbraerX is the disruptive innovation subsidiary of the Embraer Group, is based in the USA and is the business group in charge of developing their eVTOL aircraft for Urban Air Mobility (UAM). This subsidiary has conceptualised EVE, a sustainable mode of transportation in an urban scenario. The EVE project was also put on the US stock market in order to gather equity in December 2021 (*NYSE : EVEX*).



Figure 3.1: Subscale test model of Eve [21]

On July 17, 2022, the company unveiled its first full-sized cabin mock-up of their EVE eVTOL passenger air taxi aircraft at the Farnborough International Airshow trade exhibition. Embraer performed a successful sub-scale hover test a EVE in 2021, there is limited information on this test available, most certainly because of it would reveal sensitive information about the EVE project to the public.



Figure 3.2: Another render of the EVE V3 [21]

Table 3.1: Performance of the EVE (V3) [21]

Performance	Value	Unit
Number of Rotors	8+2	[-]
Blades per Rotor	2	[-]
Cruise Speed	200	[km/h]
Range	100	[km]
Passengers	4+1	[-]

In order to create a simulation model of EVE, the dimensions of the aircraft, wings, blades and airfoils will have to be determined. EVE is designed to have a cruise speed of 200 [km/h] and a range of 100 [km]. The aircraft can hold 4 passengers and 1 pilot. EVE V3 has 8 upward facing rotors for horizontal flight and 2 forward facing rotors for vertical flight.

3.2. Requirements

Any mission needs boundaries under the form of requirements. These requirements are given to the MATLAB code in order to set limits on every aspect of the aircraft during flight.

Table 3.2: System requirements for EVE

Identification	Requirement	Explanation
EVE-PERF-01	EVE shall be able to take off vertically	VTOL characteristics
EVE-PERF-02	EVE shall be able to land vertically	VTOL characteristics
EVE-PERF-03	EVE shall be able to cruise in horizontal flight	VTOL characteristics
EVE-PERF-04	EVE shall be able to land vertically	VTOL characteristics
EVE-PERF-05	EVE shall have a range of 100 [km]	Embraer
EVE-PERF-06	EVE shall have a cruise speed of 200 [km/h]	Embraer
EVE-PERF-07	EVE shall have a cruise altitude of 2000 [m]	Personal
EVE-PERF-08	EVE shall have a vertical climb rate of 10 [m/s]	Personal
EVE-PERF-09	EVE shall have a climb rate of 8 [m/s]	Personal
EVE-PERF-10	EVE shall have a descent rate of -12 [m/s]	Personal
EVE-PERF-11	EVE shall have a roll rate of 20 [deg/s]	Personal
EVE-PROP-01	EVE shall have the same 10 electric rotors	Embraer
EVE-PROP-02	EVE shall have 8 rotors used for vertical motion	Embraer
EVE-PROP-03	EVE shall have 2 rotors used for horizontal motion	Embraer
EVE-MASS-01	EVE shall have an empty mass of 1500 [kg]	Embraer
EVE-MASS-02	EVE shall accommodate up to 5 passengers	Embraer
EVE-MASS-03	EVE's passengers shall each weigh 80 [kg]	Personal
EVE-MASS-04	EVE's passengers shall carry up to 20 [kg] of luggage	Personal

3.3. Planform Dimensions

The first step is to determine the dimensions of the EVE aircraft. Since little is known about EVE's dimensions, the following top plan has been created for EVE V3. The planform dimensions are taken

from the available renders of EVE V3. The dimensions of the aircraft are fixed for the thesis and can not change. Except for the rotor diameter and that is one of the parameters to be optimized during the thesis. This will be done in the optimization part of the MATLAB code. The aircraft has two wings, two stabilisers including a V-Tail and a rudder. Regarding the propulsion system of EVE V3, the aircraft has eight upward facing engines and two forward facing engines.

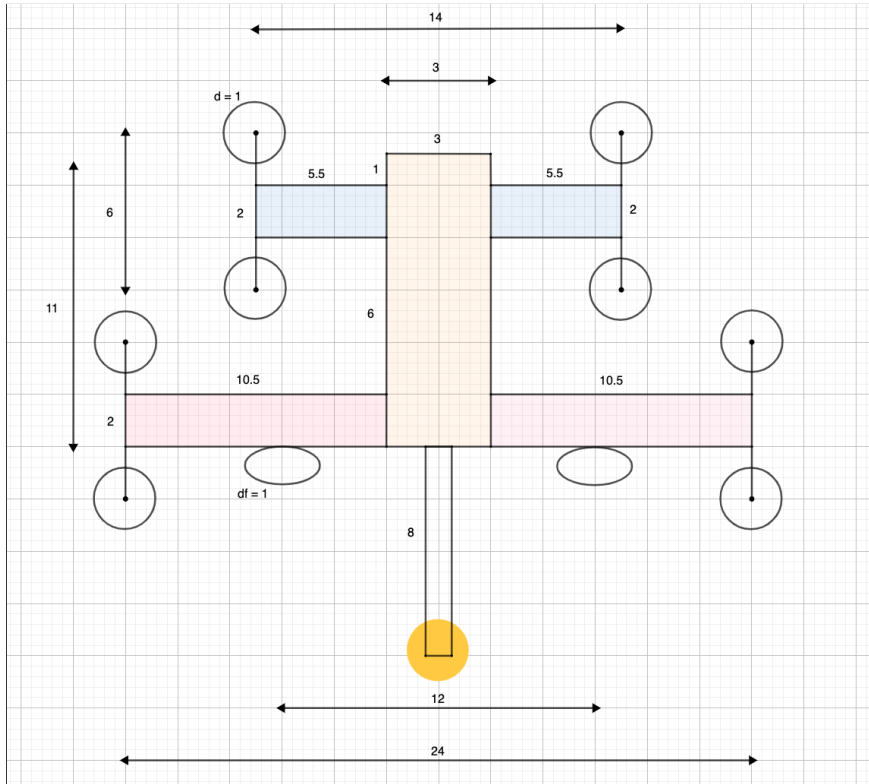


Figure 3.3: Planform with dimensions of the EVE V3

EVE's eight upward engines have a diameter of 1 [m] and the two forward engines also have a diameter of 1 [m]. The fuselage has a length of 11 [m], a width of 3 [m] and a height of 2.5 [m]. The Empennage is represented by a yellow circle, and its dimensions are explored further in subsection 3.4.1. The small wing has a wing span of 14 [m] and the bigger wing has a wing span of 24 [m]. The small wing will be referred to as Wing 2 in the report, the bigger wing is named Wing 1. This is due to the fact that the program places the ailerons on Wing 1, and it would be logical to have the aileron on the higher wing span wing in order to create a bigger roll moment with a certain aileron deflection.

3.4. Wing Sizing

In this section, the wing of EVE V3 is sized. This encompasses the sizing of the empennage which is a V-Tail plus an inverted rudder, the lift calculations, the drag calculations as well as the sizing of the control surfaces.

3.4.1. Empennage Sizing

The choice of a V-Tail for EVE is evident, the exhaust from the forward propellers prevent a conventional or T-tail design. In order to size a V-tail, the horizontal tail and vertical tail are sized independently and are then combined together using the following formula [22]. From renders, one can also see that EVE has an inverted rudder, which means that the empennage consists of a V-Tail and a rudder:

$$S_{Vtail} = S_V + S_H \quad (3.1) \quad angle_V = \arctan \sqrt{S_V/S_H} \quad (3.2)$$

Considering the fact that EVE has two wings, the vertical tail sizing is most important, since EVE has sufficient control over its pitch angle for controllability in most phases of flight where RPM control is

used. For stability, the following equations can be used to size the horizontal tail:

$$b_h = \sqrt{AR \cdot S_h} = AR \cdot MAC \quad (3.3) \quad c_{r_h} = \frac{3}{2} MAC \frac{1 + \lambda_h}{1 + \lambda_h + \lambda_h^2} \quad (3.4)$$

It is common to select an aspect ratio that is half that of the main wing, leading to an AR of 4. Regarding, the MAC, 1 meter is selected, and the taper ratio is within the 0.4-0.5 range from statistics [23]. Now, by using Equation 4.1 and Equation 4.2, the size of the V-tail can be determined. This leads to a V-tail size of **9.46** [m^2]. The angle of the V-tail is **55.44** degrees. The next step is the vertical tail (rudder):

$$S_v = \frac{C_{VT} b S}{l_v} \quad (3.5)$$

The value for the tail volume coefficient is selected to be 0.04 [24]. The length of the vertical tail is 2 meters. This leads to a vertical tail area of 5.6 [m^2].

3.4.2. Airfoil selection

EVE V3 has a relatively low design cruise speed of 200 [km/h] and a relatively high total wing surface area of 76 [m^2]. As a result, the lift coefficient needed for cruise is quite low, in the range of a lift coefficient for all wings that is approximately 0.2. However, during the transition from vertical flight to horizontal flight, the aircraft accelerates at a relatively low angle of attack to generate lift. The speed at which the aircraft transitions is calculated as follows:

$$V_t = \sqrt{\frac{mg}{\frac{1}{2}\rho_t (\cos \Gamma_1 Cl_{0_1} S_1 + \cos \Gamma_2 Cl_{0_2} S_2 + \cos \Gamma_3 Cl_{0_3} S_3 + \cos \Gamma_4 Cl_{0_4} S_4)}} \quad (3.6)$$

The velocity needs to be inferior to the cruise velocity as the density at transition level is higher than at cruise level, this means that the zero angle of attack lift coefficient needs to be around 0.15. As a result, the airfoil needs to be cambered in order to have a positive lift coefficient around zero angle of attack. With these two main criteria in mind, the Clark Y airfoil was chosen for EVE V3:

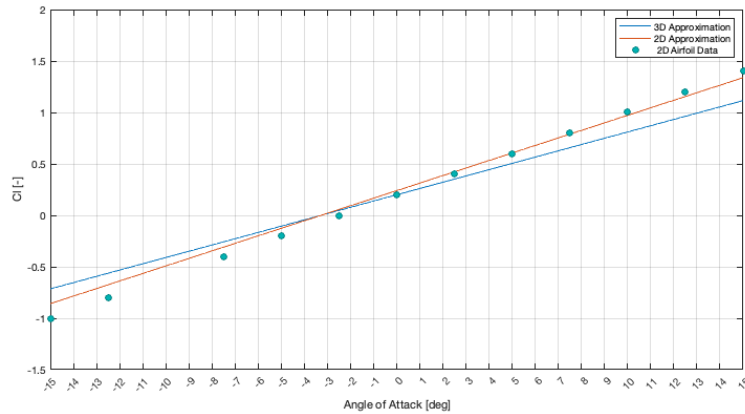


Figure 3.4: Clark Y airfoil data

The data for the Clark Y airfoil [airfoil] is compared to the Prandtl's Classic Lifting-Line Theory [25] approximation, which will be used by the program in order to accommodate all Lift + Cruise aircraft. This approximation is very close to the actual Clark Y performance, and the user is able to change the zero angle of attack lift coefficient (Cl_{0_x}) in the input text file of the program.

$$Cl_x = \frac{AR_x * 0.11}{AR_x + 18.25 * 0.11} * (\alpha) + Cl_{0_x} \quad (3.7)$$

Regarding the empennage (both the V-tail and the inverted Rudder), the airfoil selected is the NACA 2411. This NACA airfoil has a thickness to ratio of 12 and the point of maximum camber is located at 40% of its chord. Its design lift coefficient is in the range of 0.3-0.4 and therefore is sufficient for stability

(this is verified in the neutral point calculation in section 3.10). Due to its symmetry, the zero angle of attack lift coefficient (Cl_{0_x}) is 0. It is also important to have a look at the downwash caused by the wings, as this will change the effective angle of attack perceived by the wings behind [26]. It has been estimated that the downwash change per change in angle of attack is 0.05 for Wing 1 which is behind Wing 2 and 0.1 for both stabilisers at the back of the aircraft [27]. As a result, each wing has a different effective angle of attack:

$$\alpha_{eff} = \left(1 - \frac{\delta_e}{\delta_\alpha}\right) \alpha \quad (3.8)$$

It is also important to discuss the stall angles of the aircraft. The Clark Y airfoil stalls at -15 and 15 [deg] angle of attack at a Reynolds number of 2000000 [28]. This information is also added to the plane parameter text file. Here are the final lift slope values for each of the lift surfaces of EVE V3:

Surface	AR [-]	Slope [deg^{-1}]	Cl_{0_x} [-]	$\frac{\delta_e}{\delta_\alpha}$ [-]
Wing 1	12	0.0942	0.15	0.05
Wing 2	7	0.0855	0.15	0
Stab 1 (V-Tail)	2.5	0.0610	0	0.1
Stab 2 (Rudder)	2.5	0.0610	0	0.1

Table 3.3: Lift Surface parameters for EVE V3

3.4.3. Drag Calculation

Now that the lift coefficient of each of the wings has been determined, the next step is to calculate the drag coefficients for both wings, the V-tail and the rudder. The Oswald efficiency factor calculated using an approximation from Raymer for close to straight wings [29] [30]:

$$e = 1.78 \cdot (1 - 0.045 \cdot AR_x^{0.68}) - 0.64 \quad (3.9)$$

Using , the values for the Oswald efficiency factor are as follows:

Surface	AR [-]	e [-]
Wing 1	12	0.706
Wing 2	7	0.839
Stab 1 (V-Tail)	2.5	0.991
Stab 2 (Rudder)	2.5	0.991

Table 3.4: Drag Surface parameters for EVE V3

All parameters have been found in order to be able to calculate the drag of each wing using the following equation:

$$C_{d_x} = C_{d_0} + \frac{C_{l_x}^2}{e\pi AR_x} \quad (3.10)$$

3.5. Fuselage Sizing

The Fuselage produces drag during the whole flight. The drag equation is the same as the drag equation for a wing, the difference being in the drag coefficient. As a result, in this section, the fuselage drag coefficients are calculated.

3.5.1. Top Fuselage Drag

A top drag force needs to be accounted for in the Vertical phases of flight (Phase 1: *Vertical Take-Off* and Phase 7: *Vertical Descent*) in order for the aircraft to have a terminal velocity. This force is only active in those phases, as without it the aircraft would accelerate to infinity. The difficulty is to find the drag coefficient for the fuselage from a top/bottom view. The fuselage is assumed to be cylindrical, and the wings are modelled as flat plates from the top view.

$$C_{D_{top}} = \frac{\sum A_i C_{D_i}}{A} = \frac{33 * 0.68 + 22 * 1.1 + 42 * 1.1}{97} = 0.96 \quad (3.11)$$

From literature, the drag coefficient over a cylinder is 0.68 and the drag coefficient over a flat plate in 3D is 1.1. As a result, a weighted average can be found for the overall shape, the total surface area is equal to 97 [m²]. The calculated top fuselage drag coefficient is **0.96**.

3.5.2. Front Fuselage Drag

While a VTOL aircraft creates many types of drag depending on its flight phase, let's start off by determining the front fuselage drag coefficient. From the top view in Figure 3.3, the width of the fuselage is 3 [m].

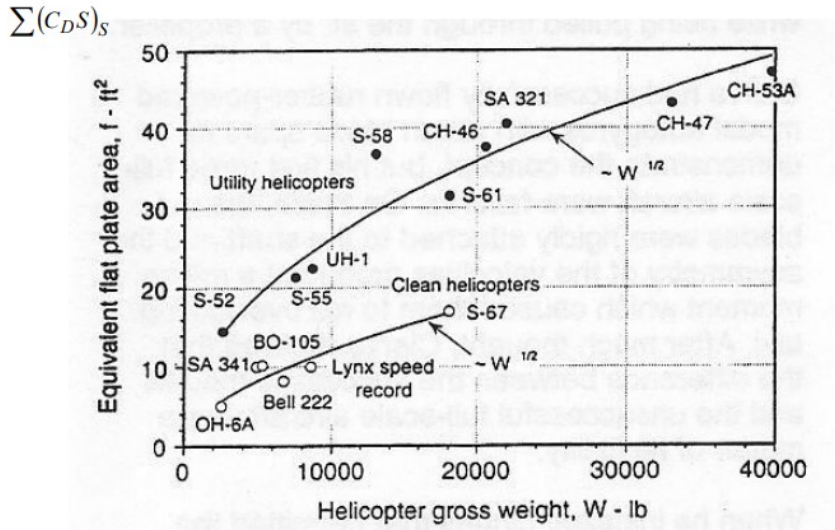


Figure 3.5: Fuselage Drag (Helicopter Lecture 8, slide 18), [31]

While this graph is made for helicopters, the fuselage shape of EVE V3 strongly resembles the shape of a helicopter and thus the same drag values can be applied. The drag of the wings and stabilisers is calculated in the wing forces of each lifting surface and is independent of the front fuselage drag force. With the height of the fuselage being equal to 2.5 [m], the frontal surface of EVE equates to 7.5 [m²] (or 80.73 [ft²]). The mass of EVE is set to 2000 [kg] (or 4409 [lb]) and is set by Embraer (EVE-PERF-07). The fuselage of EVE is similar to that of a utility helicopter (due to its VTOL specific design) so using Figure 4.5, this results in a fuselage drag coefficient of 0.245. The location of the application of the force is specified in detail in subsection 4.5.2.

3.6. Battery Sizing

The aircraft is assumed to have a mass of 2000 [kg] since the empty mass is 1500 [kg] and there are 5 passengers on board each weighing 80 [kg] with 20 [kg] of luggage. For the calculation of the weight of the battery, the transition phases are not taken into account, the aircraft takes off vertically at a set vertical rate of climb (10 [m/s] for EVE V3) up to a transition altitude (300 [m] in the case of EVE V3). Then, the aircraft climbs at a certain rate of climb (8 [m/s] for EVE V3) up to a cruise altitude (2000 [m] for EVE V3). The aircraft cruises for its design range (250 [km] for EVE V3) and then descends in order to transition and land vertically with a vertical descent rate (-2 [m/s] for EVE V3). The fact that the transitions are not taken into account over sizes the battery a little, since the lift produced in the transition phases is not counted.

Vertical Take-Off

The Vertical flight phase takes the aircraft up to 300 meters using the 8 upwards facing rotors all working together to obtain a vertical climb rate of 10 [m/s] for EVE V3. For now, the radius of all the 10 rotors is fixed to 0.5 meters. This results in the disk area of:

$$A = \pi * r^2 = 0.7854 \text{ [m}^2\text{]} \tag{3.12}$$

The thrust for each flight phase can now be calculated. The Thrust produces by all 8 engines in vertical flight is calculated as:

$$T_v = n * \rho * A * \eta * RPS^2 = 27476.4 \text{ [N]} \quad (3.13)$$

Since the upwards velocity in this configuration is 10 [m/s] (as per requirement EVE-PERF-10), the power of the vertical phase up until the 300-meter altitude is:

$$P_v = T_v * V = 274.764 \text{ [kW]} \quad (3.14)$$

The time needed to get to an altitude of 300 meters with the RPM and radius of the rotors is 88.5 seconds. So the energy needed for the vertical phase is:

$$E_v = P_v * t_v = 6716.5 \text{ [Wh]} \quad (3.15)$$

Climb

The same process is repeated for the climb phase. The forward engines are on and the upwards engines are off since the aircraft has transitioned. The Thrust produced by all 2 engines in climbing flight is calculated as, the RPS_f setting calculation is explained in subsection 5.7.4:

$$T_c = n_f * \rho * A * \eta * RPS_f^2 = 12469 \text{ [N]} \quad (3.16)$$

This results in the following power value:

$$P_c = T_c * V_c = 685.795 \text{ [kW]} \quad (3.17)$$

The time needed to get to an altitude of 300 meters with the RPM and radius of the rotors is 72 seconds. So the energy needed for the vertical phase is:

$$E_c = P_c * t_c = 38480.7 \text{ [Wh]} \quad (3.18)$$

Cruise

In cruise, EVE V3 flies at a cruise velocity of 200 [km/h] as per requirement EVE-PERF-06. For this velocity, the cruise RPS is found to be 76.9 for both forward engines. At this RPS, they produce a thrust force of:

$$T_{cr} = n_f * \rho_{cr} * A * \eta * RPS_f^2 = 7450 \text{ [N]} \quad (3.19)$$

So at a velocity of 200 [km/h] (which is 55.56 [m/s]), the power is:

$$P_{cr} = T_{cr} * V_{cr} = 413.881 \text{ [kW]} \quad (3.20)$$

The cruise phase lasts for 30 minutes since the aircraft moves at a speed of 200 [km/h] for a total range of 100 km as per requirement EVE-PERF-05. This consumes the following amount of energy.

$$E_{cr} = P_{cr} * t_{cr} = 206940 \text{ [Wh]} \quad (3.21)$$

Descent

In Descent, the aircraft glides at a maximum L/D ratio, so all engines are off. The reason for an unpowered descent is that the battery is not used during the entire descent phase. This may change in later phases of aircraft development due to safety reasons. The battery is not using any energy, and it could even be possible to have an energy recuperation system to recharge the batteries in the descent phase.

Vertical Descent

In vertical descent, EVE V3 has a descent velocity of -2 [m/s]. The forward engines are still off and the upward engines are on. The upwards engines' thrust is therefore:

$$T_v = n * \rho * A * \eta * RPS^2 = 22167 \text{ [N]} \quad (3.22)$$

So at a velocity of -2 [m/s], the power is:

$$P_v = T_v * V_v = 44.334 \text{ [kW]} \quad (3.23)$$

The vertical descent phase lasts for 149 seconds as the aircraft descends from an altitude of 300 [m] to the ground:

$$E_c = P_v * t_v = 1970.411 \text{ [Wh]} \quad (3.24)$$

Total Energy

The total energy is simply the sum of the energies needed for all the three different flight phases. These energies can be summed up in the following table.

Flight Phase	Power [kW]	Time [s]	Energy [Wh]
Vertical Take-Off	274.8	88.5	6716.5
Climb	685.8	202	38480.7
Cruise	413.8	1800	206940
Vertical Descent	44.3	160	1970.4

Table 3.5: Parameters used for the Power Required [32]

After having completed a full flight, the aircraft has consumed a total energy of:

$$E = \sum_{j=1}^n P_j t_j = E_v + E_c + E_{cr} + E_d = 254107.6 \text{ [Wh]} \quad (3.25)$$

The State of Charge is set to 20% which means that the battery is only allowed to use 80% of its capacity in order to preserve its lifespan. Also, the battery has an efficiency of 85% which is in line with current technology. [33]

$$m_b = \frac{E (1 + \text{SoC}_{\min})}{\text{SED} \eta_b} = 597.9 \text{ [kg]} \quad (3.26)$$

With an energy density of the battery of 500 [Wh/kg], the battery has a total mass of **597.9 [kg]**. Since the transitions are not taken into account, the aircraft will not use all the energy from the battery in a flight as the wing will produce lift in the take-off and transition phase of the flight as the aircraft will have a forward velocity starting at 300 meter altitude, leading to less thrust required by the upwards engines. The chosen battery density of 600 [Wh/kg] is high, but that is because with the current battery technology and a density of 200 [Wh/kg], the battery would weigh 1500 [kg] which is more than half of the operational empty weight. With the current technological advancements, it is estimated that the chosen battery capacity is available on the market in 2026. [34]

3.7. Engine Sizing

The engine sizing is a critical part of the design process, as EVE V3 needs to have sufficient thrust in order to be able to reach its velocity targets during flight. The mass of the engines is found by calculating the power needed during flight and taking the maximum power of the engine and by multiplying it with a safety factor.

3.7.1. Power Calculation

Power calculations are important in order to be able to size and estimate the mass of the upward and forward facing engines of EVE V3.

The first step in the power calculations is to calculate the induced velocity. At sea level, the induced velocity from hover is as follows:

$$V_{i_{hov}} = \sqrt{\frac{W}{2\rho n\pi R^2}} = \sqrt{\frac{\frac{1500}{8} * 9.81}{2 * 1.225 * 3.14 * 0.5^2}} = 30.9176 \text{ [m/s]} \quad (3.27)$$

According to Blade Element theory [35], in forward flight, as can be seen in Equation 3.28, the Power Required is composed of Induced Power, Rotor Parasite power (times 8 since there are 8 upwards rotors) and Rotor Profile drag Power, Fuselage Drag Power and Miscellaneous Power.

$$P = 8 * P_i + 8 * (P_p + P_d) + P_{par} + P_{misc} = 8 * k T v_i + 8 * \frac{\sigma \bar{C}_{DP}}{8} \rho (\Omega R)^3 \pi R^2 (1 + 4.65 \mu^2) + \sum (C_D S)_S \frac{1}{2} \rho V^3 + P_{misc} \quad (3.28)$$

Some parameters used in Equation 3.28 are found in Table 3.6, others will be calculated and explained separately.

Parameter	Value	Unit
Weight	14715	[N]
Ω	50	[RPS]
Radius	0.5	[m]
ρ	1.225	[kg/m ³]
k	1.15	[-]

Table 3.6: Parameters used for the Power Required

The fuselage drag times the surface (which is equal to $7.5 * 0.245 = 1.8375$) is taken from Figure 4.5. In addition to the values provided in Table 3.6, the values for the solidity, σ is:

$$\sigma = \frac{N * c}{\pi * R} = \frac{5 * 0.27}{\pi * 0.5} = 0.8594 \quad (3.29)$$

In order to find the rotor profile drag coefficient used to calculate the profile power of the EVE VTOL, the Mach number at the tip has to be found. The reason for this low Mach number is the fact that EVE V3 has 8 separate engines. Leading to lower propeller radii and therefore lower tip velocities.

$$M_t = \frac{\Omega * R}{a} = \frac{50 * 0.5}{343} = 0.07289 \quad (3.30)$$

One of the advantages of many smaller propellers is the low tip velocity and thus the low noise emissions. This value is combined with the Lift coefficient that is derived from the Thrust coefficient:

$$C_T = C_W = \frac{W}{\rho n \pi R^2 (\Omega R)^2} = 0.0478 \quad (3.31)$$

$$\bar{C}_L = \frac{6.6 C_T}{\sigma} = \frac{6.6 C_T}{\sigma} = \frac{6.6 * 0.0067}{0.8594} = 0.3671 \quad (3.32)$$

The chosen tip Mach number line used for Figure 3.6 is $M_t = 0.31$.

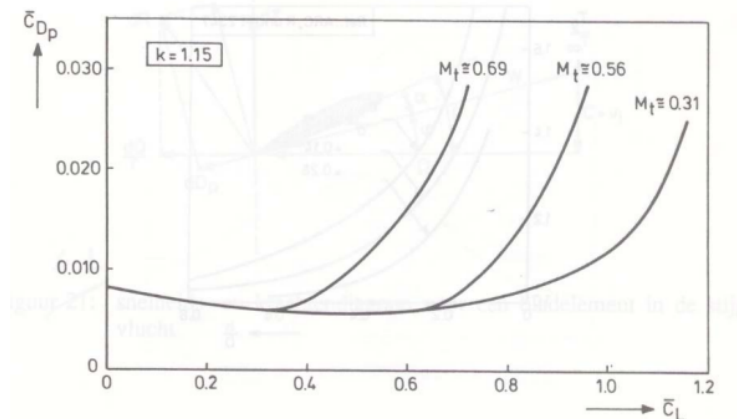


Figure 3.6: CL and Mt graph used to find CDp

As a result, according to Figure 3.6, the value for CDp is 0.010. Now that all the constants have been determined, the power components can be plotted as a function of the velocity as seen in Figure 3.7, note that this is for forward flight:

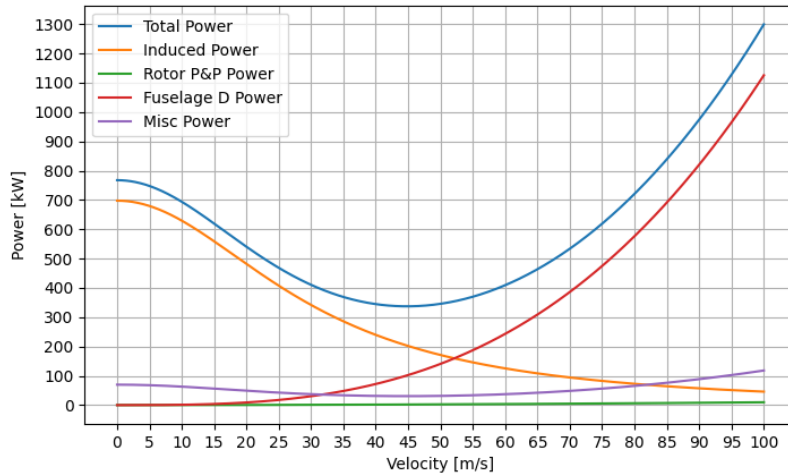


Figure 3.7: Power Calculation for EVE V3

As can be seen from Figure 3.7, the point in flight that requires the least amount of power is at 42 [m/s], for a total power of 350 [kW]. The upward engines will be sized at a power rating of 800 [kW] to enable hover and move up to 70 [m/s]. The engine weight for the total of 8 engines on board of EVE V3 is taken from a power density regression model in Figure 3.8 that is used on the dataset from Table 3.7. The continuous power needed during flight calculated in subsection 3.7.1 is 100 [kW] since the aircraft has 8 upwards facing engines.

Table 3.7: Motor Data [37][38][39]

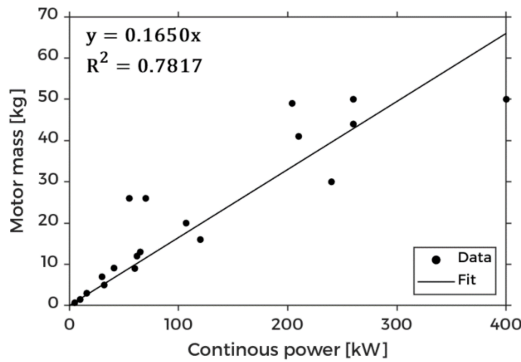


Figure 3.8: Electric motor power density regression model [36]

Motor	Power [kW]	Mass [kg]
Emrax 188	52	7
Emrax 348	380	41
MAGiDRIVE 12	12	1.5
MAGiDRIVE 150	150	16
MAGiDRIVE 6	6	0.7
Magnix magni350	350	111.5
Magnix magni650	640	200
Siemens SP260D	260	50
Siemens SP55D	72	26
Siemens SP70D	92	26
Yuneec Power 40	40	19
Yuneec Power 60	60	30

The engine mass can be modelled using the “Torenbeek propeller mass estimation method” [40][41]. This model relies on the maximum power needed in flight (P_{max}), the power margin (PM) and the number of engines (N_{mot}). This equation brings the mass of one upward engine to 24.75 [kg].

$$m_{mot} = 0.165 \frac{P_{max}(1 + PM)}{N_{mot}} \tag{3.33}$$

The same principle can be applied to the mass estimation of the forward engines, the highest power in flight is 644 [kW] (see section 3.6). This gives a mass per forward engine of 79.69 [kg].

3.7.2. Propeller Design

In order to design the propeller that will be used for forward and upward flight, the Javaprop program is used. The power needed, velocity, diameter, and number of blades is given as input. Regarding the sizing for the upward engines, from Figure 3.7, the total power needed for vertical flight is 800 [kW].

Since EVE has 8 upwards engines, this means, 100000 [W] per engine [42][43]. The upward engines have 5 blades each, when inputted in Javafoil, this gives the following propeller:

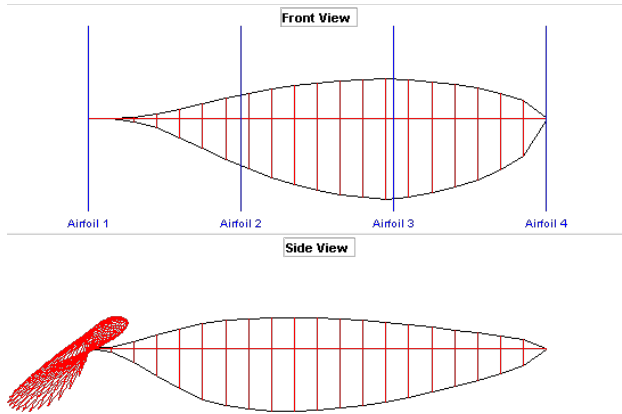


Figure 3.9: Upwards Propeller Design

The forward engine blades need to be slightly bigger as the maximum amount of power needed is 685 [kW]. The highest power amount needed is in the climb phase. Since EVE V3 has two forward facing engines, it means 342.5 [kW] per forward engine.

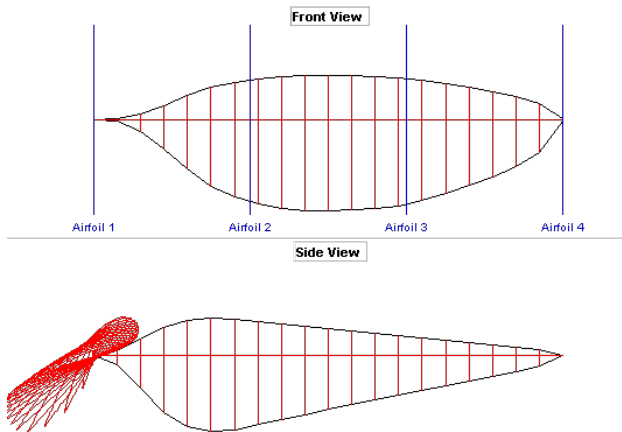


Figure 3.11: Forward Propeller Design

The maximum chord of the blade is 0.218 [m] which is higher than the maximum chord length of the upward facing propellers of 0.158 [m]. In addition, the propeller mass is calculated using the following Class II method [40]:

$$m_{\text{prop}} = 0.144 \left(d_{\text{prop}} \frac{P_{cb}}{N_{bl}} N_{bl}^{0.5} \right)^{0.782} \quad (3.34)$$

With d_{prop} , the diameter of the propeller and N_{bl} the number of blades on each engine. This gives a starting mass for the upwards propellers of 4.29 [kg] and a propeller mass for each forward engine of 24.70 [kg]. This brings the total upward propeller mass for all 8 engines to 34.32 [kg] and the total forward propeller mass for the 2 engines to 49.41 [kg].

3.8. Class II Mass Estimation

In order to accurately estimate the mass of the aircraft, a Class II weight estimation is used [40]. The fuselage length (l_f), the maximum fuselage section perimeter (P_{max}) and number of occupants (N_{pass}). The mass also depends on the total mass (m) of the aircraft. This applies to all equations presented in

Figure 3.10: Values for the upward engine propeller

Blade characteristics		
Number of blades	5	[–]
Airfoil	Clark Y	[–]
β at 75%	30.1	[deg]
Max Chord	0.158	[m]
Solidity	0.503	[–]

Figure 3.12: Values for the upward engine propeller

Blade characteristics		
Number of blades	5	[–]
Airfoil	Clark Y	[–]
β at 75%	35.9	[deg]
Max Chord	0.218	[m]
Solidity	0.694	[–]

this section. The equation for the mass of the fuselage from Roskam [40] for an unpressurised cabin and a maximum cruising speed of 370 [km/h] can be expressed as:

$$m_f = 14.86m^{0.144} \frac{l_f}{P_{\max}}^{0.778} l_f^{0.383} N_{\text{pax}}^{0.455} \quad (3.35)$$

EVE has two straight wings that each have their own respective mass. The mass of each lifting surface is calculated as a function of the total mass (m) of the aircraft, the surface area of the wing (S_x), the design load factor of the wing (η_x) and the aspect ratio (AR_x):

$$m_w = 0.04674m^{0.397} S_x^{0.360} \eta_x^{0.397} AR_x^{1.712} \quad (3.36)$$

Regarding the horizontal and vertical tails, the Roskam Class II weight estimation equation is a function of the tail area (S_x), tail aspect ratio (AR_x), tail root chord ($c_{r,x}$) and tail quarter chord sweep angle ($\Lambda_{0.25,x}$). Since EVE has a V-tail, for the mass estimation, the horizontal tail surface area and vertical tail surface areas calculated in the empennage sizing (see subsection 3.4.1) are taken.

$$m_{t,h} = \frac{3.184m^{0.887} S_{t,h}^{0.101} AR_{t,h}^{0.101}}{174.04t_{r,h}^{0.223}} \quad (3.37)$$

In the case of EVE V3, the V-tail is considered the horizontal tail in the mass estimation. While the weight may be a little higher due to its dihedral angle, this is not taken into account in the calculations. The V-Tail has a mass of 50.86 [kg].

$$m_{t,v} = \frac{1.68m^{0.567} S_{t,v}^{1.249} AR_{t,v}^{0.482}}{639.95t_{r,v}^{0.747} (\cos \Lambda_{0.25,t,v})^{0.882}} \quad (3.38)$$

The Rudder mass has been calculated using Equation 4.15, the final mass after optimization is 26.8 [kg].

Table 3.8: Design Parameter Values

Design Parameter	Value	Unit
Payload	500	[kg]
Number of occupants, N_{pax}	5	[-]
Upward Motor count, $N_{\text{mot,u}}$	8	[-]
Forward Motor count, $N_{\text{mot,f}}$	2	[-]
Motor power margin, PM	50	[%]
Min. battery state of charge, SoC_{min}	20	[%]
Battery specific energy density, SED	600	[Wh/kg]
Battery system efficiency, η_b	0.85	[-]
Fuselage length, l_f	11	[m]
Fuselage section perimeter, P_{\max}	11	[m]
Number of prop. blades Up., $N_{\text{bl,u}}$	5	[-]
Number of prop. blades Fr., $N_{\text{bl,f}}$	5	[-]

Table 3.9: Converged Mass Values

Component	Value	Unit
Fuselage	258.8	[kg]
Battery	597.9	[kg]
Passengers	500	[kg]
Wing 1	414.63	[kg]
Wing 2	128.39	[kg]
Stab 1 (V-tail)	50.86	[kg]
Stab 2 (Rudder)	26.80	[kg]
Upward Engines	8*24.75	[kg]
Forward Engines	2*79.69	[kg]
Upward Propellers	8*4.30	[kg]
Forward Propellers	2*24.71	[kg]
Total	2418	[kg]

The above used efficiencies are in line with the current available technology. The power margin of 50% is quite high, but it is important to have sufficient power in order for the aircraft to get out of difficult situations. The total mass of EVE V3 is, **2418** [kg], including the five passengers that each weigh 80 [kg] and have 20 [kg] of luggage with them.

3.9. Center of Gravity

The centre of gravity is a critical part in the design of an aircraft, as all the moments are taken around the centre of gravity (C.G.). The centre of gravity also needs to be in front of the neutral point in order for the aircraft to be stable in pitch motion (see section 3.10). The position of each subcomponent can clearly be seen in Figure 3.13, due to the aircraft's symmetry around the x-axis, the C.G. is on this axis.

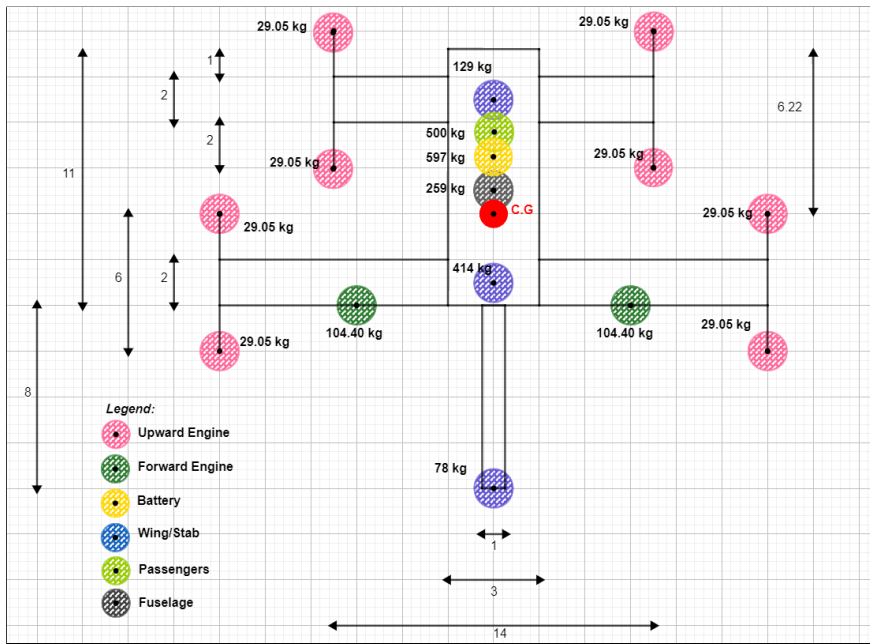


Figure 3.13: Planform with mass locations of the EVE V3

The pink mass points indicate the rotors, the weight for the rotors has been found to be 24.75 [kg] from the Class II weight estimation. The dark green circle represents the forward facing rotors. The wings' mass points are represented in blue: 129 [kg] for the small wing, 414 [kg] for the bigger wing, and 78 [kg] for the empennage of the eVTOL. The battery pack, with a weight of 597 [kg], is represented by the yellow mass point. The fuselage is represented by a grey point with a mass of 269 [kg]. At last, the 5 passengers are represented by the light green circle. The total weight of the aircraft is 2418.7 [kg]. Since the weight and location of each of the subcomponents of EVE V3 are known, the centre of gravity can be calculated as follows:

$$X_{C.G.} = \frac{\sum X_i * m_i}{\sum m_i}, Y_{C.G.} = \frac{\sum Y_i * m_i}{\sum Y_i}, Z_{C.G.} = \frac{\sum Z_i * m_i}{\sum Z_i} \quad (3.39)$$

This results in a C.G location of: 6.22 [m] from the front of the aircraft in the x-direction [44]. The C.G. location enables the program to calculate the relative position of all the forces that will act on the aircraft. These relative positions are used for the moment calculations and are shown in Table 3.10:

Component	X [m]	Y [m]	Z [m]
Fuselage	-0.08	0	-0.33
Passengers	-3.58	0	-0.33
Battery	-2.58	0	-1.08
Wing 1	4.42	0	0.92
Wing 2	-3.58	0	0.92
Stab 1	13.42	0	0.92
Stab 2	13.42	0	0.92
T_{u_1}	-6.58	-7	0.92
T_{u_2}	-0.58	-7	0.92
T_{u_3}	-6.58	7	0.92
T_{u_4}	-0.58	7	0.92
T_{u_5}	1.42	-12	0.92
T_{u_6}	7.42	-12	0.92
T_{u_7}	1.42	12	0.92
T_{u_8}	7.42	12	0.92
T_{f_1}	5.42	-6	0.92
T_{f_2}	5.42	6	0.92

Table 3.10: C.G. relative Location of EVE V3 Components

3.10. N.P location

Longitudinal stability is an important aspect of aircraft design, ensuring that the aircraft remains stable and controllable during pitching motions. Pitch motion is the movement of an aircraft about its pitch axis, which is an imaginary line that runs from wingtip to wingtip.

In a stabilized aircraft, any perturbation that causes the nose to tilt up or down will cause an automatic correction that returns the aircraft to its original pitch attitude. This self-correcting behaviour is called longitudinal stability.

The neutral point is the point along the chord where the pitching moment does not vary with the angle of attack. This is the point of aerodynamic balance, and any disturbance from that point will result in a nose up or nose down pitching moment. The neutral point is found using the following equation:

$$(\mathbf{X}_{N.P.} - l_1)\zeta(\alpha_1) + (\mathbf{X}_{N.P.} - l_2)\zeta(\alpha_2) - (\mathbf{X}_{N.P.} - l_3)\zeta(\alpha_3) - (\mathbf{X}_{N.P.} - l_4)\zeta(\alpha_4) = 0 \quad (3.40)$$

with:

$$\zeta_x = a_x S_x \cos(\Gamma) \left(1 - \left(\frac{\delta e}{\delta a} \right)_x \right) \quad (3.41)$$

The location of the neutral point is determined by the aerodynamic properties of the wing and can be modified by aircraft design parameters: a_x the lift slope, S_x the surface area, l_x the arm lengths, $\frac{\delta e}{\delta a}$ the downwash/angle of attack change and Λ_x the dihedral angle. The position of the neutral point is a key factor in determining the static margin, and ensuring that the neutral point is in front of the centre of gravity is very important for a stable aircraft. For EVE V3, the neutral point location is at 7.11 [m], which is behind the C.G. at 6.22 [m] from the front of the fuselage, the aircraft is stable in pitch.

3.11. Moment of Inertia

Moment of inertia is a measure of the aircraft's resistance to rotational motion. It depends on the mass distribution and geometry of the aircraft and plays a vital role in determining the flight characteristics of the aircraft. The moment of inertia affects the response of the aircraft to control inputs and disturbances, and is of great significance to ensure the stability and controllability of the aircraft [45].

There are several ways to determine the moment of inertia of an aircraft. One way is to use physical measurements. Weigh the plane and measure its dimensions. However, this method can be time-consuming and may not be practical for larger aircraft. Another approach is to estimate the moment of

inertia by subdividing the aircraft into different subcomponents, each with their own mass. Firstly, the moment of inertia tensor is as follows [46]:

$$I = \begin{bmatrix} I_{xx} & -I_{xy} & -I_{xz} \\ -I_{xy} & I_{yy} & I_{yz} \\ -I_{xz} & -I_{yz} & I_{zz} \end{bmatrix} = \begin{bmatrix} I_{xx} & 0 & -I_{xz} \\ 0 & I_{yy} & 0 \\ -I_{xz} & 0 & I_{zz} \end{bmatrix} \quad (3.42)$$

Using this approach, the moment of inertia can be estimated and used by the MATLAB program for the preliminary design of Lift + Cruise eVTOLs. The moment of inertia in yz-plane is zero, as the aircraft is symmetric in the yz-plane. The following values were found for the calculation of EVE V3's moment of inertia:

$$\begin{aligned} I_{xx} &= \sum (m_i \cdot z_i^2 + m_i \cdot y_i^2) = 26452.89 \text{ [kg.m}^2\text{]} \\ I_{yy} &= \sum (m_i \cdot x_i^2 + m_i \cdot z_i^2) = 45395.74 \text{ [kg.m}^2\text{]} \\ I_{zz} &= \sum (m_i \cdot x_i^2 + m_i \cdot y_i^2) = 68632.93 \text{ [kg.m}^2\text{]} \\ I_{xz} &= \sum (m_i \cdot x_i \cdot z_i) = 5356.72 \text{ [kg.m}^2\text{]} \end{aligned} \quad (3.43)$$

In order to get the principal axis of Inertia, the eigenvalues need to be calculated, the 3×3 matrix can be reduced to a 2×2 matrix as the value of I_{yy} is already the principal axis in y-direction.

$$\det |\lambda_i - I| = \det \begin{vmatrix} (\lambda_i - I_{xx}) & I_{xz} \\ I_{xz} & (\lambda_i - I_{zz}) \end{vmatrix} = 0 \quad (3.44)$$

This gives the following moment of Inertia values that are used by the MATLAB program for the eVTOL EVE V3:

$$\begin{aligned} I_x^p &= 25783.24 \text{ [kg.m}^2\text{]} \\ I_y^p &= 45395.74 \text{ [kg.m}^2\text{]} \\ I_z^p &= 69302.58 \text{ [kg.m}^2\text{]} \end{aligned} \quad (3.45)$$

3.12. Final Parameter values for EVE V3

Since the EVE V3 is still in development, it is very difficult to get accurate data of its dimensions. As a result, the dimensions for EVE have been established and the program uses the following values for the parameters of EVE V3 in the input text file explained in section 5.2.

EVE has a total wing surface of 76 [m^2] in a two wing configuration. The smaller wing has a wing span of 14 [m] and the bigger wing has a wing span of 24 [m]. Both wings have a chord length of 2 [m] and no sweep angle. EVE has 8 upward facing engines and 2 forward facing engines. As explained earlier, the locations in Table 3.11 are centred around the bottom middle front of the fuselage (0,0,0). The aircraft parameters of EVE are compiled in a text file (see Appendix A) for the program to read. To summarise all the aspect of the eVTOL, EVE V3's parameters are described below:

Table 3.11: Text file Input Parameters for EVE V3 (Part 1)

Input Parameter	Value	Unit	Input Parameter	Value	Unit
General Parameters			Stab 2		
Mass	1500	[kg]	Surface Area	5.6	[m ²]
Design Cruise Velocity	200	[km/h]	Wing Span	2	[m]
Design Range	100	[km]	SweepLE	20	[deg]
Number of Passengers	5	[-]	Taper Ratio	0.5	[-]
Number of Wings	2	[-]	Zero-Lift Drag Coefficient	0.03	[-]
Number of Stabilizers	2	[-]	Oswold Efficiency factor	0.991	[-]
Wing 1			DeDa	0.1	[-]
Surface Area	48	[m ²]	Dihedral Angle	-90	[deg]
Wing Span	24	[m]	Offset in Y	0	[m]
SweepLE	0	[deg]	Cl0 of Airfoil	0	[-]
Taper Ratio	1	[-]	Cm0 of Airfoil	0	[-]
Zero-Lift Drag	0.03	[-]	t/c max	0.1	[-]
Oswold Efficiency	0.706	[-]	stall min	-15	[deg]
DeDa	0.05	[-]	stall max	15	[deg]
Dihedral Angle	0	[deg]	Rudder Chord Length	0.5	[m]
Cl0 of Airfoil	0.2	[-]	Extra		
Cm0 of Airfoil	0.18	[-]	Empennage Connection Width	0.6	[m]
t/c max	0.1	[-]	Empennage Connection Height	0.6	[m]
stall min	-15	[deg]	Upward Engines		
stall max	15	[deg]	Number of Upward Engines	8	[-]
LS Aileron Chord Length	0.3	[m]	Diameter Upward Engines	1	[m]
LS Aileron Start %b/2	0.5	[%]	Thrust Coefficient Upward Engines	0.8	[-]
LS Aileron Stop %b/2	0.9	[%]	Wing or Fuselage Attached (0 or 1)	0	[-]
HS Aileron Chord Length	0.3	[m]	Forward Engines		
HS Aileron Start %b/2	0.2	[%]	Number of Forward Engines	2	[-]
HS Aileron Stop %b/2	0.4	[%]	Diameter Forward Engines	1	[m]
Wing 2			Thrust Coefficient Forward Engines	0.8	[-]
Surface Area	28	[m ²]	Wing or Fuselage Attached (0 or 1)	0	[-]
Wing Span	14	[m]	Fuselage		
SweepLE	0	[deg]	Fuselage Top Drag Coefficient	0.8	[-]
Taper Ratio	1	[-]	Fuselage Front Drag Coefficient	0.245	[-]
Zero-Lift Drag	0.03	[-]	Fuselage Length X	11	[m]
Oswold Efficiency	0.839	[-]	Fuselage Width Y	3	[m]
DeDa	0	[-]	Fuselage Height Z	2.5	[m]
Dihedral Angle	0	[deg]	Battery		
Cl0 of Airfoil	0.2	[-]	Battery Capacity	125000	[Wh]
Cm0 of Airfoil	0.18	[-]	Battery Length X	1	[m]
t/c max	0.1	[-]	Battery Width Y	1	[m]
stall min	-15	[deg]	Battery Height Z	0.5	[m]
stall max	15	[deg]	Locations		
Stab 1			Location of Battery X	3	[m]
Surface Area	9.6	[m ²]	Location of Battery Y	0	[m]
Wing Span	5	[m]	Location of Battery Z	1	[m]
SweepLE	20	[deg]	Location of Passengers X	2	[m]
Taper Ratio	0.5	[-]	Location of Passengers Y	0	[m]
Zero-Lift Drag	0.03	[-]	Location of Passengers Z	1	[m]
Oswold Efficiency	0.991	[-]	Location of Wing 1 X	10	[m]
DeDa	0.1	[-]	Location of Wing 1 Y	0	[m]
Dihedral Angle	55.44	[deg]	Location of Wing 1 Z	2.5	[m]
Offset in Y	0	[m]			
Cl0 of Airfoil	0.2	[-]			
Cm0 of Airfoil	0.18	[-]			
t/c max	0.1	[-]			
stall min	-15	[deg]			
stall max	15	[deg]			
Elevator Chord Length	0.5	[m]			

Table 3.12: Text file Input Parameters for EVE V3 (Part 1)

Input Parameter	Value	Unit	Input Parameter	Value	Unit
Location of Wing 2 X	2	[m]	Location of Forward Tf1 X	11	[m]
Location of Wing 2 Y	0	[m]	Location of Forward Tf1 Y	-6	[m]
Location of Wing 2 Z	2.5	[m]	Location of Forward Tf1 Z	2.5	[m]
Location of Stab 1 X	19	[m]	Location of Forward Tf2 X	11	[m]
Location of Stab 1 Y	0	[m]	Location of Forward Tf2 Y	6	[m]
Location of Stab 1 Z	2.5	[m]	Location of Forward Tf2 Z	2.5	[m]
Location of Stab 2 X	19	[m]	Location of Forward Tf3 X	0	[m]
Location of Stab 2 Y	0	[m]	Location of Forward Tf3 Y	0	[m]
Location of Stab 2 Z	2.5	[m]	Location of Forward Tf3 Z	0	[m]
Location of Upward T1 X	-1	[m]	Location of Forward Tf4 X	0	[m]
Location of Upward T1 Y	-7	[m]	Location of Forward Tf4 Y	0	[m]
Location of Upward T1 Z	2.5	[m]	Location of Forward Tf4 Z	0	[m]
Location of Upward T2 X	5	[m]	Location of Forward Tf5 X	0	[m]
Location of Upward T2 Y	-7	[m]	Location of Forward Tf5 Y	0	[m]
Location of Upward T2 Z	2.5	[m]	Location of Forward Tf5 Z	0	[m]
Location of Upward T3 X	-1	[m]	Location of Forward Tf6 X	0	[m]
Location of Upward T3 Y	7	[m]	Location of Forward Tf6 Y	0	[m]
Location of Upward T3 Z	2.5	[m]	Location of Forward Tf6 Z	0	[m]
Location of Upward T4 X	5	[m]	Weight		
Location of Upward T4 Y	7	[m]	Weight of Fuselage	259	[kg]
Location of Upward T4 Z	2.5	[m]	Weight of Passengers	500	[kg]
Location of Upward T5 X	7	[m]	Weight of Battery	597	[kg]
Location of Upward T5 Y	-12	[m]	Weight of Wing 1	414	[kg]
Location of Upward T5 Z	2.5	[m]	Weight of Wing 2	129	[kg]
Location of Upward T6 X	13	[m]	Weight of Stab 1	27	[kg]
Location of Upward T6 Y	-12	[m]	Weight of Stab 2	51	[kg]
Location of Upward T6 Z	2.5	[m]	Weight of an Upward Engine	24.75	[kg]
Location of Upward T7 X	7	[m]	Weight of a Forward Engine	79.625	[kg]
Location of Upward T7 Y	12	[m]			
Location of Upward T7 Z	2.5	[m]			
Location of Upward T8 X	13	[m]			
Location of Upward T8 Y	12	[m]			
Location of Upward T8 Z	2.5	[m]			
Location of Upward T9 X	0	[m]			
Location of Upward T9 Y	0	[m]			
Location of Upward T9 Z	0	[m]			
Location of Upward T10 X	0	[m]			
Location of Upward T10 Y	0	[m]			
Location of Upward T10 Z	0	[m]			
Location of Upward T11 X	0	[m]			
Location of Upward T11 Y	0	[m]			
Location of Upward T11 Z	0	[m]			
Location of Upward T12 X	0	[m]			
Location of Upward T12 Y	0	[m]			
Location of Upward T12 Z	0	[m]			

Table 3.13: Calculated Parameters

Calculation	Value	Unit
Location of Center of Gravity, X	6.22	[m]
Location of Center of Gravity, Y	0	[m]
Location of Center of Gravity, Z	1.61	[m]
Location of Neutral Point, X	7.11	[m]
Location of Neutral Point, Y	0	[m]
Location of Neutral Point, Z	2.5	[m]
Moment of Inertia, X	25783	[kg.m ²]
Moment of Inertia, Y	45396	[kg.m ²]
Moment of Inertia, Z	69302	[kg.m ²]

4

The eVTOL aircraft Model

This chapter explores the modelling of the aircraft in the MATLAB program. In section 4.1, the assumptions are stated and discussed, followed by the explanation of a typical mission profile in section 4.2. Then, the coordinate systems used by the program are discussed in section 4.3. Then, section 4.5 showcases all the forces and moments that are present on the model. In section 4.7, these forces are incorporated into the control loop that sends commands to the aircraft's engines and control surfaces.

4.1. Assumptions

It is critical for the MATLAB program to have rigorous assumptions in order for it to be representative of real life flight. Many common aerospace engineering assumptions are used, and these assumptions can be found in Table 4.1:

#	Assumptions
1	Earth is non-rotating
2	Gravity field is constant at $g = 9.81 [m/s^2]$
3	The eVTOL is a rigid body
4	The eVTOL is symmetrical around the xz-plane in the body frame
5	The aerodynamic centre is at 0.25% of the MAC
6	The Lift and Drag forces are applied on the MAC
7	Distributed forces such as Lift and Drag are modelled as point forces
8	International Standard Atmosphere, Troposphere (maximum 15 [km]) [47]
9	Wing Incidence angle is zero
10	Wing forces act on quarter chord of MAC
11	No Drag force from the side of the fuselage in Yaw
12	Sideslip is modelled as a drag force in y aircraft body axis, opposite to sideslip angle
13	Aircraft bank angle is limited to 20 [deg] due to sideslip issues at higher angle uncoordinated turns
14	No Top Drag force in conventional flight
15	Fuselage Drag does not create a pitching moment
16	Control forces only have an impact on the aircraft moments
17	In phases where control surfaces are active, the moment equations of motion are linearised
18	For the transition phases, the upward engines' intake airflow works at an optimal advance ratio, $\eta = 0.8$
19	There is no aerodynamic interference between the components of the aircraft
20	Coupling variables are ignored in the equations of motion of the 6DOF model

Table 4.1: Engine Parameters for EVE V3

Firstly, the Earth is non-rotating: this assumption implies that the Earth is considered stationary and not rotating on its axis. In other words, the effects of Earth's rotation, such as the Coriolis force, are disregarded.

Also, the gravity field is constant at $g = 9.81 [m/s^2]$: This assumption assumes that the gravitational field strength on Earth is uniform and constant. While the actual value of gravity can vary slightly depending on location and altitude, this assumption allows for simplified calculations and modelling of gravitational forces.

The eVTOL is a rigid body: This assumption considers that the eVTOL does not deform or undergo structural changes under the forces and moments experienced during its operation. This simplification allows for the application of rigid body dynamics principles to analyse the aircraft's motion and stability.

The eVTOL is symmetrical around the xz-plane in the body frame: the aircraft is assumed to be mirror-symmetric when viewed from the side (along the y-axis) in its own body frame. This simplifies the analysis by reducing the number of variables and allows for easier calculation of aerodynamic forces and moments. In addition, this eliminates the inertia variable in the xy-plane.

The aerodynamic centre is at 0.25% of the MAC and the Lift and Drag forces are applied on the MAC. This assumption simplifies the analysis by focusing the forces at a specific reference point, allowing for straightforward calculations of aerodynamic performance. To further explain this, distributed forces such as Lift and Drag are modelled as point forces.

In addition, the International Standard Atmosphere (ISA) is used, which is a reference for atmospheric conditions. The ISA model provides a standardized representation of temperature, pressure, density, and other atmospheric properties as a function of altitude.

Sideslip is modelled as a force in the y body-axis of the eVTOL, the force is opposite to the sideslip angle in order to rotate the aircraft in yaw back into the incoming airflow and to reduce the track angle to zero. Since the aircraft performs low banking turns, the sideslip angle is minimal. The aircraft always turns in uncoordinated turns, a future improvement of the program would be to coordinate the rudder angle with the ailerons in order to have zero sideslip.

Since the program is used for preliminary design, the wing Incidence angle of each wing is zero. However, this incidence can be modelled by an Increase in the zero angle of attack lift coefficient in the input text file.

Also, the drag of the fuselage is separated into a top and front drag, which are point forces on the C.G. of the aircraft. This over-simplification is due to the lack of data on current eVTOL fuselages. The user is still able to use the fuselage drag forces and tune the coefficients to match real life tests of the eVTOL.

In addition, the control surfaces' deflections do not create any extra lift, they only have an impact on the moments exerted on the eVTOL. The lift and drag of these surfaces is ignored. Also, the moment equations are linearised as the controllers for the control surfaces are not PID controllers but simple linear controllers.

During the entire flight, the aerodynamic interference effects are ignored. This includes, among others, the wing-fuselage, empennage-fuselage, upward engine-wing interactions. To add to this, the propellers only provide a thrust forces perpendicular to the propeller blades, there are no forces from the propellers in any other direction.

Moreover, during the complex transition phases of flight, the advance ratio, J , is assumed to be within the optimal efficiency range as discussed in Figure 4.6, this results in a thrust efficiency η during transition of 0.8.

At last, due to the increased complexity, it has been decided that the coupling variables are not taken into account in the equations of motion of the 6 degree of freedom model of the eVTOL. These variables could be added at a later stage as discussed in chapter 7.

4.2. Phases of Flight

Contrary to a conventional aircraft which has 3 flight phases (Climb, Cruise, Descent), an eVTOL has 7 phases of flight. The eVTOL takes off vertically, transitions, climbs, cruises, descends, transitions and then lands vertically. In the program the flight phases are being referred to as follows:

- PHASE 1: Vertical Take-Off
- PHASE 2: Transition 1
- PHASE 3: Climb
- PHASE 4: Cruise
- PHASE 5: Descent
- PHASE 6: Transition 2
- PHASE 7: Vertical Landing

In each of these phases, the control surfaces and thrusts are managed in order to obtain the wanted flight movement, this is explained in detail in section 5.7. The program switches between phases once a certain vertical or horizontal positional requirement has been met, these requirements are an input as well (section 5.2).

4.3. Coordinate System

The MATLAB program uses a conventional aeronautical body coordinate system. This means that the z-direction is pointed downwards, towards the earth. The x-direction, in line with the body of the aircraft, is positive forwards and the y-direction is pointing to the right of the aircraft, at wing level if the wings do not have any dihedral. The coordinate system during the flight loop is set around the centre of gravity as can be seen in Figure 4.1, for EVE, the C.G. has been established in section 3.9 for EVE, but the program is made to calculate the C.G. using the input parameter text file from section 5.2.

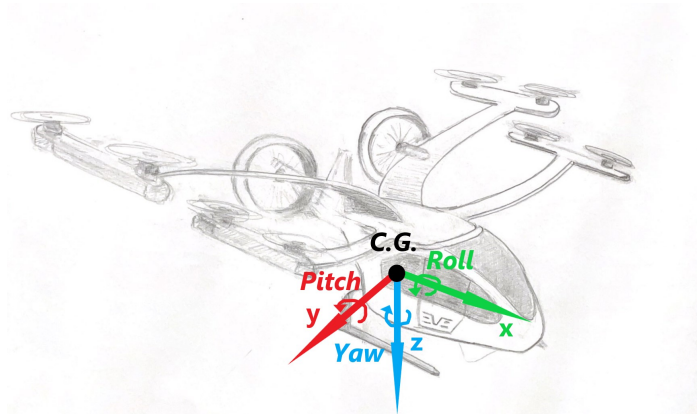


Figure 4.1: MATLAB Program Coordinate System

The pitch angle (θ) is positive for a pitch up movement of the aircraft, a banked turn to the right would be initialised by a positive roll (ψ) moment and yaw (ϕ) rotation to the right would result in positive yaw. The angle of attack (α) of the aircraft is equal to the pitch angle (θ) minus the flight path angle (γ). The flight path angle of the aircraft is determined as follows:

$$\gamma = \arctan\left(\frac{-V_z}{V_f}\right) \quad (4.1)$$

$$V_f = \sqrt{V_x^2 + V_y^2} \quad (4.2)$$

The flight path is a critical part of the transition phase for eVTOLs. This is because after Vertical Take-Off, the eVTOL has an upwards velocity, meaning the angle of attack of the wings are negative, the aircraft needs to pitch up into the flight path in order to create a positive angle of attack and this lift, see Figure 4.2.

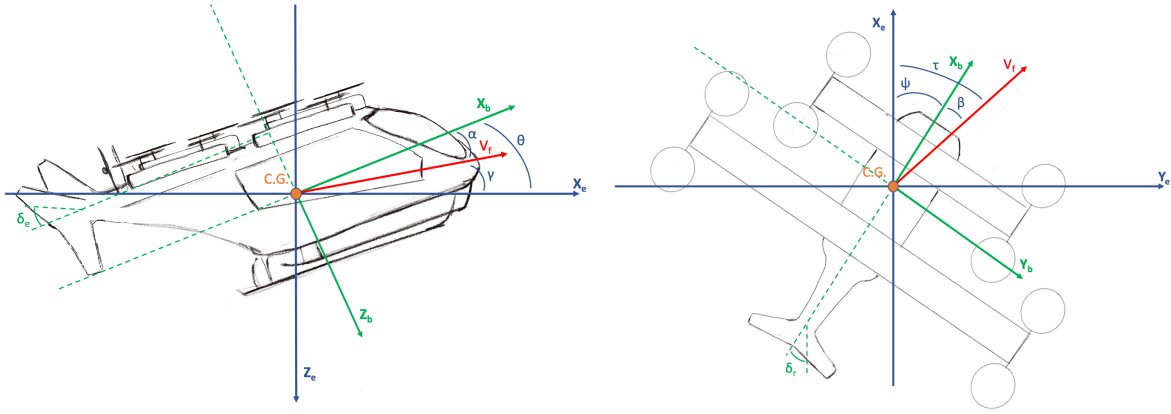


Figure 4.2: Flightpath angle and Track angle for the EVE aircraft

The track angle follows the same principle as the flightpath angle but in the x-y plane. As can be seen in Figure 4.2, the sideslip angle (β) is found by subtracting the yaw angle (ψ) to the track angle (τ). Both the angle of attack and sideslip angle are important angles used to determine the amount of lift produced by the wings and stabilizers of the aircraft, as explained in subsection 4.5.1.

In order to switch between the earth reference frame, which is the reference frame used for the output plots, and the body coordinate system, a transformation matrix is needed.

$$T_{B-E} = \begin{bmatrix} \cos \theta \cos \psi & -\cos \phi \sin \psi + \sin \phi \sin \theta \cos \psi & \sin \phi \sin \psi + \cos \phi \sin \theta \cos \psi \\ \cos \theta \sin \psi & \cos \phi \cos \psi + \sin \phi \sin \theta \sin \psi & -\sin \phi \cos \psi + \cos \phi \sin \theta \sin \psi \\ -\sin \theta & \sin \phi \cos \theta & \cos \phi \cos \theta \end{bmatrix} \quad (4.3)$$

The transformation matrix from Equation 4.3 can also be used for a transformation from the body frame to the earth frame, this is done by taking the inverse of T. An example for the use of this transformation matrix is the conversion of the Weight force from earth to body frame as all other forces of the aircraft are in the body frame.

$$\begin{aligned} \vec{F}_{G_b} &= [T] \vec{F}_{G_e} \\ &= \begin{bmatrix} \cos \theta \cos \psi & -\cos \phi \sin \psi + \sin \phi \sin \theta \cos \psi & \sin \phi \sin \psi + \cos \phi \sin \theta \cos \psi \\ \cos \theta \sin \psi & \cos \phi \cos \psi + \sin \phi \sin \theta \sin \psi & -\sin \phi \cos \psi + \cos \phi \sin \theta \sin \psi \\ -\sin \theta & \sin \phi \cos \theta & \cos \phi \cos \theta \end{bmatrix} \begin{bmatrix} 0 \\ 0 \\ mg \end{bmatrix} \\ &= \begin{bmatrix} -mg \cdot \sin \theta \\ mg \cdot \sin \phi \cos \theta \\ mg \cdot \cos \phi \cos \theta \end{bmatrix} \end{aligned} \quad (4.4)$$

4.4. Flight Conditions

The program uses an International Standard Atmosphere [47] which enables it to calculate the pressure, temperature and density for all altitude of the aircraft. The Altitude is a known variable in the flight loop, as the position of the aircraft is known. The Temperature in Kelvin is calculated as follows:

$$T = T_0 - 0.0065 * z; \quad (4.5)$$

The sea level temperature (T_0) is 288.15 [K], z is the altitude in [m]. The pressure is found with the following equation:

$$p = \left(1 - z \left(\frac{-0.0065}{T_0} \right)^{5.2561} \right) p_0; \quad (4.6)$$

The pressure at sea level (p_0) is, 101325 [Pa] and -0.0065 is the temperature gradient in the Troposphere (up to 11 000 [m]). The density, which is the most important variable as it is used in the lift, drag

and thrust equations [47], is:

$$\rho = \frac{P}{R * T} \quad (4.7)$$

R is the universal gas constant and is equal to 287 [J/kg·K]. In the flight conditions module, the time step is also updated and increases by $\Delta t = 0.1$ [s].

4.5. Forces and Moments on the Model

Before of explaining in detail how the program works, it is important to look at which forces and moments act on the aircraft at different times of flight. The forces and moments are categorised into the following: Wing forces, Control Surface forces, Thrust forces, Fuselage Forces and Other Forces.

4.5.1. Wings Forces and Moments

As discussed in section 4.1, the program can accommodate up to 2 main wings and 2 stabilisers. In a conventional configuration, the first stabiliser (Stab1) is the horizontal tail with the elevator and the second stabiliser (Stab2) is the vertical tail with the rudder for yaw control. In the case of a V-tail, only Stab1 is used, and the elevator is able to function as a rudder thanks to the stabiliser's dihedral angle [48].

Lift Forces

The Lift forces on the aircraft are the forces of the (maximum) two main wings, L_1 and L_2 , and the (maximum) two stabilisers, L_3 and L_4 . The lift equation is as follows:

$$L_x = \frac{1}{2} \rho V^2 C_{l_x} S_x \quad (4.8)$$

With the variable x being the specific wing or stabiliser. The surface area, S_x , is an input from the text file (see section 5.2) and the density (ρ) and Velocity of the aircraft (V) are variable that change during the flight. Regarding the Lift coefficient of each lifting surface, the following approximation is used:

$$C_{l_x} = \frac{AR_x * 0.11}{AR_x + 18.25 * 0.11} * (\alpha) + C_{l_{0x}} \quad (4.9)$$

This approximation comes from Prandtl's Classic Lifting-Line Theory [25] as the lift coefficient slope is dependent on the aspect ratio (AR) of the aircraft. Also, from Equation 4.9, the lift coefficient at zero angle of attack is an input in the text file (see section 5.2). The wing stall angle is an input in the text file as well as the change in downwash (ϵ) with a change in angle of attack ($\frac{\partial \epsilon}{\partial \alpha}$ typically 0.1, [27]), this means that the tailplane sees a lower angle of attack and this stalls at a later stage which is good for static stability at high angles of attack.

It is interesting to notice that the Lift of each wing goes in the negative z-direction. The Lift force acts perpendicular to the flight path of the aircraft (see section 4.6). Also, if the aircraft's wings or stabilisers have dihedral, then the Lift of the wing lift force is also multiplied by the cosine of the dihedral angle (Γ_x). The dihedral increases the stability of the aircraft in roll [49].

The lift and drag forces are applied to the aerodynamic centre at 0.25% of the mean aerodynamic chord of the aircraft. The chord length can be calculated as follows:

$$c_{MAC} = \frac{2}{3} c_{r_x} \frac{1 + \lambda_x}{1 + \lambda_x + \lambda_x^2} \quad (4.10)$$

With c_{r_x} being the root chord of the wing and λ_x being the taper ratio of the specific wing.

Drag Forces

The Drag Forces are derived from basic aerodynamics, as the drag coefficient of a wing is found using:

$$C_{d_x} = C_{d_0} + \frac{C_{l_x}^2}{e\pi AR_x} \quad (4.11)$$

With the zero lift drag coefficient (C_{d_0}) and the Oswald efficiency factor (e) being wing properties from the input file. The final Drag equation for each wing is as follows:

$$D_x = \frac{1}{2} \rho V^2 C_{d_x} S_x \quad (4.12)$$

While it may be easy to overlook the different angle at which the forces are applied, it is important to make the correct choices. The dihedral angle of the wing also has an effect on the final angle of the drag forces. [50]

Wing Moment

Due to the miss-alignment between the centre of pressure and the location where the lift force is applied, an extra wing moment has to be added for each wing of the aircraft. The equation for the wing moment is as follows:

$$M_{wing_x} = \frac{1}{2} \rho V^2 S_x c_x C m_{0_x} \quad (4.13)$$

With c_x being the mean aerodynamic chord of the specific wing of the eVTOL. $C m_{0_x}$ is an attribute of the airfoil given in the input text file. [51]

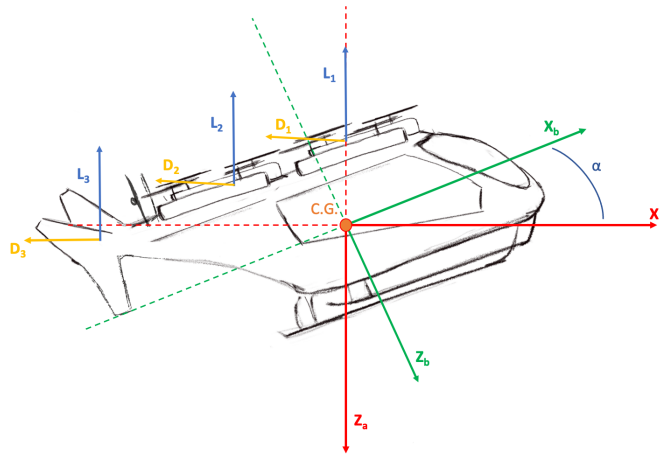


Figure 4.3: Lift and Drag diagram for the EVE aircraft

The control surfaces are one of the parameters that need to be sized by the MATLAB program. The elevators on the Stabiliser 1 change the pitch angle of the aircraft (θ), the roll (ϕ) is controlled by the ailerons on Wing 1 and the yaw angle (ψ) is controlled by the rudder placed on Stabiliser 2. In the case that the aircraft only has one stabiliser, the rudder sizing is integrated in the elevator sizing.

Elevator Control

The elevator controls the pitch of the aircraft through control surfaces that are in attack to stabiliser 1. These control surfaces are constantly active during the conventional part of flight (climb, cruise, and descent) of the aircraft in order to get the optimal angle of attack for each flight phase. In order to get the deflection angle of the elevator. The added moment is divided by the arm, the surface area and the lift slope of stabiliser 1:

$$\delta_e = \frac{M_e}{d_{(x,S1)} \rho V^2 S_e a_3 \cos(\Gamma_x)} \quad (4.14)$$

In Equation 4.14, M_e is the moment created by the elevator, $d_{(x,S1)}$ is the distance in x direction of stabiliser 1 to the C.G. and a_3 is the lift slope of Stabiliser 1. [52]

Rudder Control

The rudder is used for yaw control and is also critical in case there is an engine failure on one of the forward engines. The rudder will be sized in order to be able to provide enough yaw to stabilise the aircraft during an engine failure.

$$\delta_r = \frac{M_r}{d_{(x,S2)} \rho V^2 S_r a_4 \sin(\Gamma_x)} \quad (4.15)$$

In Equation 4.15, M_r is the moment created by the rudder, $d_{(x,S2)}$ is the distance in x direction of stabiliser 2 to the C.G. and a_4 is the lift slope of Stabiliser 2.

In case there is no second stabiliser and the aircraft has, for example, a V-Tail, the rudder deflection needed is added to the elevator deflection as the elevator and rudder will effectively be combined. Also, it is important to notice that the angle of the stabilisers is taken into account when calculating the control surface deflection.

Aileron Control

In order to provide enough roll control of the aircraft, the ailerons need to also be sized. The ailerons are positioned on Wing 1 of the aircraft, with the wing span position determined by the input text file. The chord of the aileron will be optimised.

$$\delta_{a_r} = \frac{M_a}{2d_{(y,W1)}\rho V^2 S_a a_1 \cos(\Gamma_x)} \quad (4.16)$$

The equation above is for the right aileron, a positive Roll moment means a positive right aileron deflection. Compared to the rudder and elevator, the aileron deflection is divided by 2 as both ailerons move in opposite direction to create a roll moment.

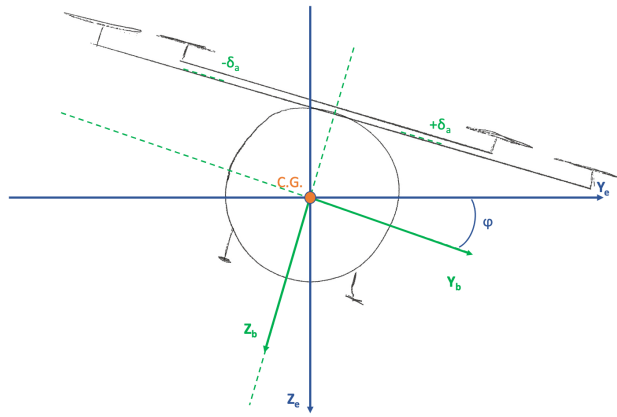


Figure 4.4: Aileron deflection angle for the EVE aircraft

4.5.2. Fuselage Forces and Moments

Since the aircraft is in the preliminary design phase, the fuselage drag forces can be resumed to a top drag force and a front drag force. The corresponding top and front drag coefficients are defined in the input file of the aircraft. During the Vertical Take-Off (Phase 1) and the Vertical Landing (Phase 2), the Top force is enabled in order for the aircraft to have a terminal velocity. The RPS of the engines is adjusted to a certain vertical climb and descent speed of the aircraft. The equation for the Top drag force is:

$$D_{top} = \frac{1}{2}\rho V_z^2 C_{d_{top}} S_{top} \quad (4.17)$$

With the top surface of the aircraft being the total surface area from a top view of the aircraft. For EVE, this value is 119 [m²].

The front fuselage area of EVE is 7.5 [m²] and the front drag coefficient is 0.245, this has been determined in subsection 3.4.3. The equation used for the front drag is:

$$D_{front} = \frac{1}{2}\rho V^2 C_{d_{front}} S_{front} \quad (4.18)$$

This front fuselage drag force is assumed to be applied to the centre of gravity of the aircraft and does not create a pitching moment.

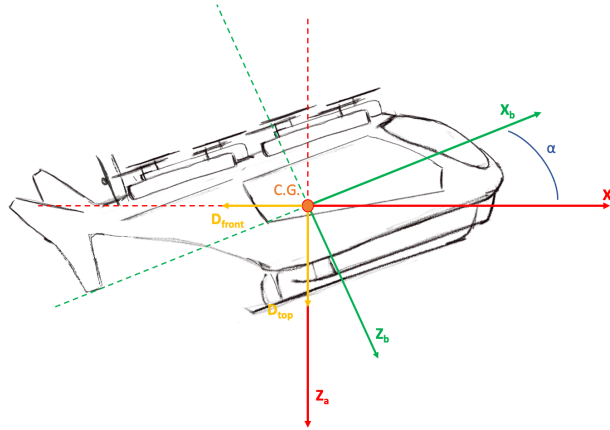


Figure 4.5: Fuselage Drag diagram angle for the EVE aircraft

4.5.3. Thrust Forces and Moments

The diameter of each engine will be optimised by the MATLAB program for each engine individually, depending on pitch and RPS constraints. The Thrust during the flight is established using the following equation:

$$T = \rho \pi r^2 RPS^2 \eta \quad (4.19)$$

The RPS varies over the course of the flight as the control loop varies it in order for the aircraft to meet its velocity and altitude targets.

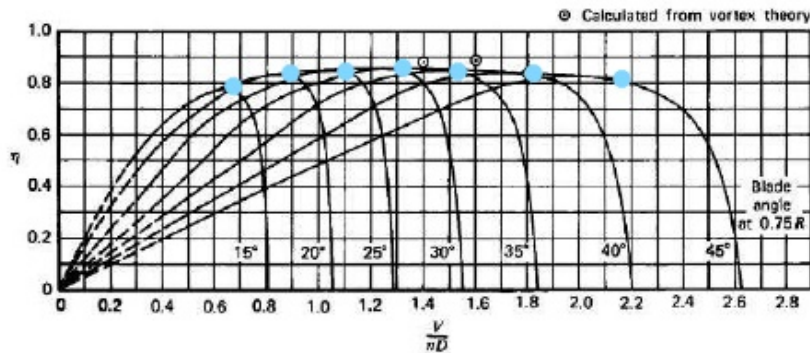


Figure 4.6: Pitch and Thrust Coefficient graph [53]

Regarding the pitch of the propeller blades, Figure 4.6 showcases the propeller efficiency as a function of the advance ratio, J :

$$J = \frac{V}{\Omega_{RPS} d_{prop}} \quad (4.20)$$

The advance ratio is non-dimensional and measures how fast the propeller is moved through the airflow. V is the free stream velocity [m/s], Ω_{RPS} is the rotational speed of the propeller [rev/s] and D is the propeller's diameter [m]. The pitch of the propeller is adapted in order to always have the maximum efficiency, which is around 0.8 (see Figure 4.6). The program automatically adjusts the pitch of the propellers during the flight in order to stay at the maximum thrust efficiency η around 0.8. The blue dots represent the data used by the program to calculate this propeller pitch.

The thrust forces propel the aircraft forward and are critical to the aircraft's capability of reaching the velocity and altitude requirements set by the user. The upwards thrust forces are always parallel to the z-axis in the body reference frame and act opposite of the z-axis which points downwards. The forward

thrust forces act parallel to the x-axis and act in the same direction as the x-axis. The user selects the number of upwards and forward engines in the input file, as well as their individual weight and location. [54]

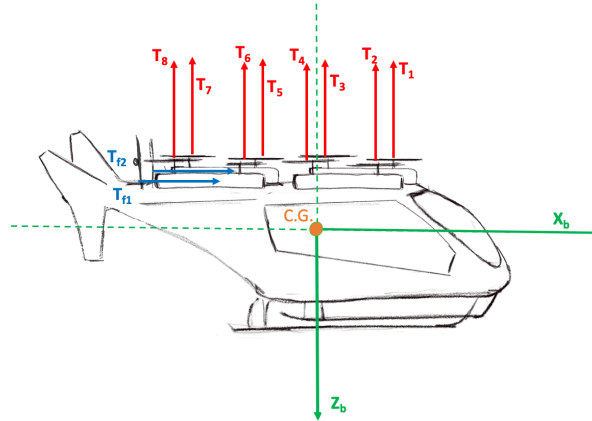


Figure 4.7: Thrust diagram for the EVE aircraft

The program is able to optimise the rotors size of the eVTOL by taking into account the maximum RPS values of the limitations text file as well as advance ratio and propeller pitch constraints as at an advance ratio higher than 2.4, the rotor efficiency (η) drops significantly (see Figure 4.6). Since the advance ratio is a function of the rotor diameter, the diameter can also be adjusted.

4.5.4. Other Forces and Moments

The last force to take into account is the weight of the aircraft, $W = mg$. The weight does not create a moment in the inertia frame, since it always points in the positive z-direction. However, in the body frame, the weight is given as:

$$W = \begin{bmatrix} W_x \\ W_y \\ W_z \end{bmatrix} = \begin{bmatrix} -mg \cdot \sin \theta \\ mg \cdot \sin \phi \cos \theta \\ mg \cdot \cos \phi \cos \theta \end{bmatrix} \quad (4.21)$$

This equation has been determined using the inertia to body frame transformation matrices from section 4.3.

4.6. Total Forces and Moments

Now that the separate forces of each component of the aircraft have been determined, they can be summed together in the body frame of the aircraft in x,y and z-direction. The Lift and Drag been transformed to the body frame as explained in subsection 4.5.1. In addition, the weight vector has been decomposed to fit the body frame as described in subsection 4.5.4.

$$F = \begin{cases} F_{body,x} = L_{1,x} + L_{2,x} + L_{3,x} + L_{4,x} + D_{1,x} + D_{2,x} + D_{3,x} + D_{4,x} + D_{f,x} \\ \quad + Tf_1 + Tf_2 + Tf_3 + Tf_4 + Tf_5 + Tf_6 + W_x \\ F_{body,y} = L_{1,y} + L_{2,y} + L_{3,y} + L_{4,y} + D_{1,y} + D_{2,y} + D_{3,y} + D_{4,y} + W_y \\ F_{body,z} = L_{1,z} + L_{2,z} + L_{3,z} + L_{4,z} + D_{1,z} + D_{2,z} + D_{3,z} + D_{4,z} + D_{f,z} + D_t \\ \quad - T_1 - T_2 - T_3 - T_4 - T_5 - T_6 - T_7 - T_8 - T_9 - T_{10} - T_{11} - T_{12} + W_z \end{cases} \quad (4.22)$$

The same is done for the moments which are summed in order to find the total moments in x,y and z-direction. The aileron, elevator, and rudder are the control surfaces that are able to change the final

value of the moment in all three different directions.

$$M = \begin{cases} M_{body,x} = M_{aileron} + M_{L1,x} + M_{L2,x} + M_{L3,x} + M_{L4,x} + M_{D1,x} + M_{D2,x} + M_{D3,x} + M_{D4,x} \\ \quad + M_{T1,x} + M_{T2,x} + M_{T3,x} + M_{T4,x} + M_{T5,x} + M_{T6,x} + M_{T7,x} + M_{T8,x} + M_{T9,x} \\ \quad + M_{T10,x} + M_{T11,x} + M_{T12,x} + M_{Tf1,x} + M_{Tf2,x} + M_{Tf3,x} + M_{Tf4,x} + M_{Tf5,x} \\ \quad + M_{Tf6,x} \\ \\ M_{body,y} = M_{elevator} + M_{W1} + M_{W2} + M_{L1,y} + M_{L2,y} + M_{L3,y} + M_{L4,y} + M_{D1,y} + M_{D2,y} \\ \quad + M_{D3,y} + M_{D4,y} + M_{T1,y} + M_{T2,y} + M_{T3,y} + M_{T4,y} + M_{T5,y} + M_{T6,y} + M_{T7,y} \\ \quad + M_{T8,y} + M_{T9,y} + M_{T10,y} + M_{T11,y} + M_{T12,y} + M_{Tf1,y} + M_{Tf2,y} + M_{Tf3,y} \\ \quad + M_{Tf4,y} + M_{Tf5,y} + M_{Tf6,y} \\ \\ M_{body,z} = M_{rudder} + M_{L1,z} + M_{L2,z} + M_{L3,z} + M_{L4,z} + M_{D1,z} + M_{D2,z} + M_{D3,z} + M_{D4,z} \\ \quad + M_{T1,z} + M_{T2,z} + M_{T3,z} + M_{T4,z} + M_{T5,z} + M_{T6,z} + M_{T7,z} + M_{T8,z} + M_{T9,z} \\ \quad + M_{T10,z} + M_{T11,z} + M_{T12,z} + M_{Tf1,z} + M_{Tf2,z} + M_{Tf3,z} + M_{Tf4,z} + M_{Tf5,z} \\ \quad + M_{Tf6,z} \end{cases} \quad (4.23)$$

As mentioned at an earlier stage, the program can accommodate up to 12 upward engines, 6 forward facing engines, 2 wings and 2 stabilisers. In the case, the aircraft uses fewer engines and/or wings, the values of the forces are simply zero, and the unused engines are not taken into account in the forces and moments calculations. The moment arms are found by using the input coordinates of the aircraft's subsystems in the input file and subtracting the location of the centre of gravity. [55][56]

4.7. Acceleration, Velocity, and Position

4.7.1. Transnational Motion

The Program uses Newton's second law of motion for the calculations of the accelerations. At each Δt increase in time, the new accelerations are calculated using the following formulas for motion [57]:

$$a(x, y, z) = \begin{cases} a_x = F_{i,x}/m \\ a_y = F_{i,y}/m \\ a_z = F_{i,z}/m \end{cases} \quad (4.24)$$

Rotations are calculated using the same method as the motion of the aircraft. At first, the angular accelerations are found using the moment equations in all three rotational directions described in section 4.6. The moment of Inertia of the aircraft has been determined in subsection 5.4.3. The following equation is used:

$$\ddot{R}(\dot{\phi}, \dot{\theta}, \dot{\psi}) = \begin{cases} \ddot{\phi} = (M_{i,x}/I_x) \frac{180}{\pi} \\ \ddot{\theta} = (M_{i,y}/I_y) \frac{180}{\pi} \\ \ddot{\psi} = (M_{i,z}/I_z) \frac{180}{\pi} \end{cases} \quad (4.25)$$

It is important to notice that these accelerations are in the body frame as the forces in x,y and z-direction on the aircraft are also calculated in the body frame. The next step is to calculate the velocities in all three directions:

$$V(x, y, z) = \begin{cases} V_x = V_{x_{old}} + a_x \Delta t \\ V_y = V_{y_{old}} + a_y \Delta t \\ V_z = V_{z_{old}} + a_z \Delta t \end{cases} \quad (4.26)$$

The angular acceleration is used in order to find the angular velocity of the aircraft. It is interesting to notice that these rotations are around the C.G. of the eVTOL in the body frame. The angular velocity is found using:

$$\dot{R}(\dot{\phi}, \dot{\theta}, \dot{\psi}) = \begin{cases} \dot{\phi} = \dot{\phi}_{old} + \ddot{\phi} \Delta t \\ \dot{\theta} = \dot{\theta}_{old} + \ddot{\theta} \Delta t \\ \dot{\psi} = \dot{\psi}_{old} + \ddot{\psi} \Delta t \end{cases} \quad (4.27)$$

At last, the new position of the aircraft can be determined using the newly found velocities:

$$P(x, y, z) = \begin{cases} x = x_{old} + V_x \Delta t \\ y = y_{old} + V_y \Delta t \\ z = z_{old} + V_z \Delta t \end{cases} \quad (4.28)$$

At last, the new angular positions are determined for the aircraft:

$$R(\phi, \theta, \psi) = \begin{cases} \phi = \phi_{old} + \dot{\phi} \Delta t \\ \theta = \theta_{old} + \dot{\theta} \Delta t \\ \psi = \psi_{old} + \dot{\psi} \Delta t \end{cases} \quad (4.29)$$

The aircraft will act differently based on the flight phase as certain engines will either be on or off. This impact is calculated in the forces and affects the aircraft's acceleration, velocity, and position. The angles of roll, pitch, and yaw (ϕ , θ , ψ) are used to position the aircraft in earth frame through body to earth transformation matrices. Moreover, these angles are to calculate the alpha of attack (α) and the sideslip angle (β). The later are used in the lift and drag equation of all lifting surfaces.

5

The Flight Dynamics Loop

In this chapter, the flight loop is covered in detail. In section 5.1, the steps taken by the flight loop are thoroughly explained. In the first step of the loop, in section 5.2, the inputs and outputs of the program are discussed. Then, the initialisation sequence is explained in section 5.3 and the text file checks are explained in section 5.4.

5.1. Total Program Overview

Before providing a detailed explanation of the MATLAB program, Figure 5.1 has been created to give a simplified overview of the program.

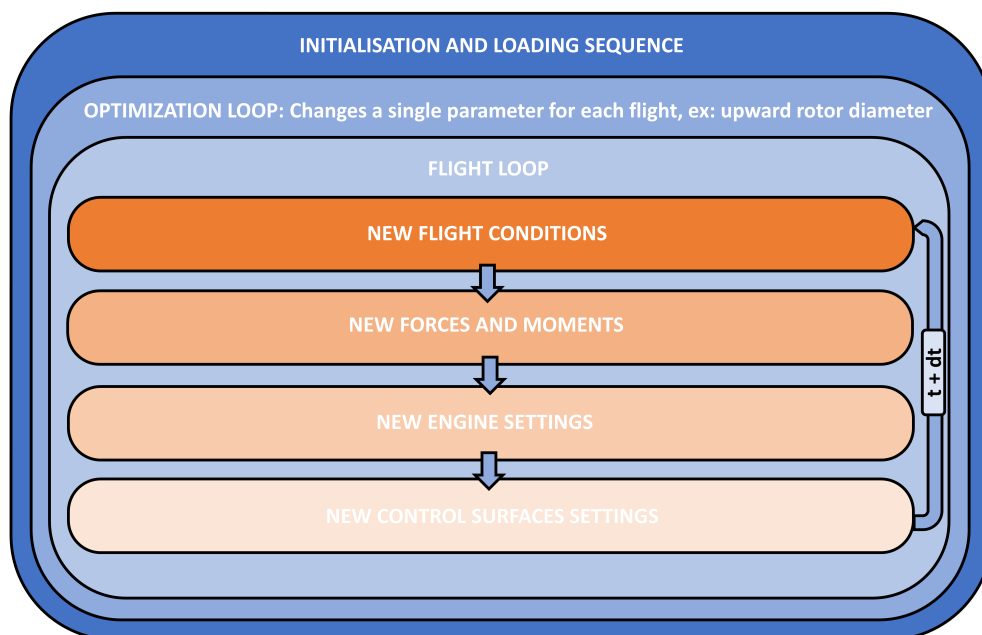


Figure 5.1: MATLAB Program Overview

The program takes the following steps, at first, the plane parameters are loaded, preliminary calculations are done, and the flight loop is started. In this flight loop, for each time step, new flight conditions like the air pressure, density, and temperature are calculated. Then follows the calculation of the forces and moments like the lift, drag, and thrust of the aircraft. All calculations are done in the body frame of the aircraft (see section 4.3). Using these new forces and moments, the thrust settings and control surface setting can be found for the next iteration of the flight loop. This loop repeats until the final

destination of the aircraft is reached. At the end, the outputs of the program are shown as explained in section 5.2.

5.2. Inputs and Outputs

The Inputs and Outputs of the program are established in this section. The following diagram gives an overview of the input and output files of the MATLAB program. The first step in operating the program is to modify the input file in order to have right flight requirements and airplane parameters.

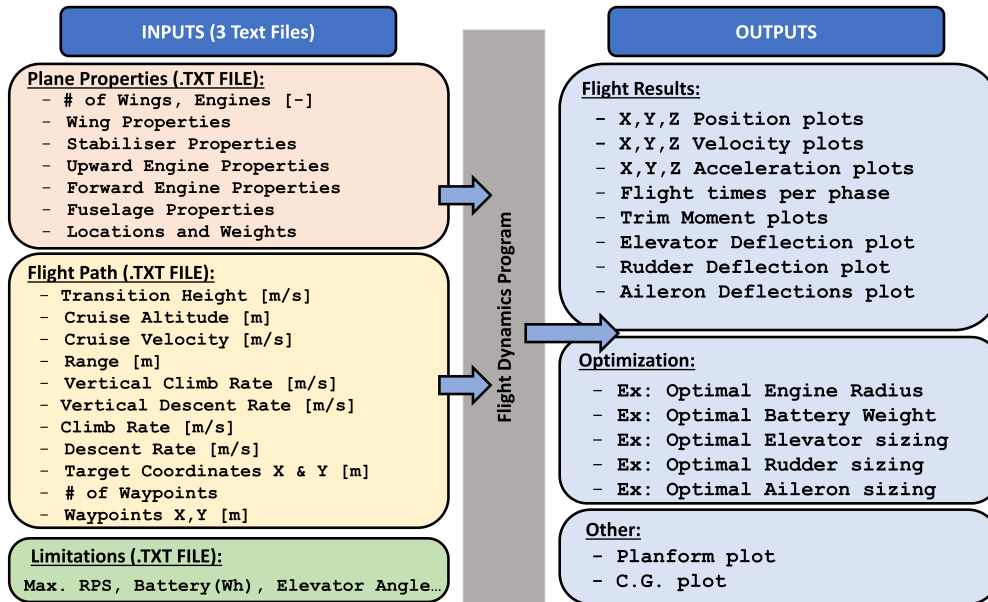


Figure 5.2: MATLAB Program Inputs and Outputs

When running the program, the user needs to prepare three .txt files (see templates in Appendix A). One text file is for the geometry of the aircraft, it outlines the size of the wings, engines, and fuselage as well and the positions and weights of each component of the eVTOL. Another text file is the Limitations text file which highlights the limitation of certain aspects of the aircraft, this file is used for the optimization output of the simulation as the MATLAB program will be aware of the limitations like the maximum RPM of the engines for example. At last, the Flightpath text file is used to tell the program what the target location, velocity, and angle of attack is for each phase of flight. This file also gives information about the waypoints that will size the aileron of the eVTOL, which is explained in detail at a later stage). The input file structure of the MATLAB program is as follows:

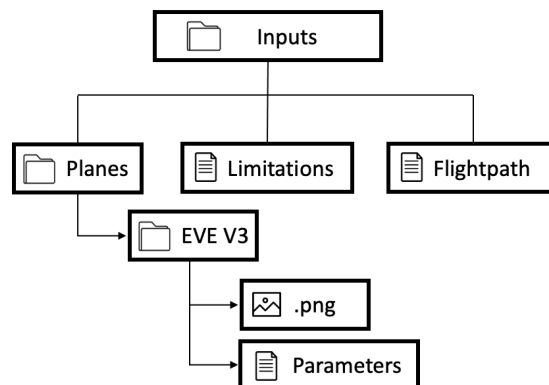


Figure 5.3: MATLAB Program Inputs

VTOL Parameters test file

As can be seen in Figure 5.2, the Plane properties text file includes all the needed properties for the eVTOL to fly. This includes basic information about the eVTOL: mass (m), Design Cruise Velocity (V_{cruise}), Design Range (R_d), number of passengers, wings, and stabilisers. Please note that the Design Velocity and Range are not requirements set for the flight but merely an indication of the specific aircraft's capabilities.

The next step is to establish the Wing and Stabiliser properties for all the lifting surfaces (denoted x), which includes the Surface Area (S_x), Wing Span (b_x), Sweep at the leading edge (Λ_x), Taper Ratio (λ_x), Zero-Lift Drag coefficient ($C_{D_{0,x}}$), Oswald Efficiency Factor (e_x) and Dihedral Angle (Γ_x). This part also includes the specific control surfaces sizes for the elevator, rudder, and aileron (please refer to Figure 4.5.1 for more details). The ailerons are placed on Wing 1, The elevators on Stab 1 and the rudder on Stab 2. In case the aircraft only has a stabiliser (Stab 1) with, for example, a V-tail, then the elevator and rudder surfaces are combined. It is also possible to add an Offset in the y-direction to the stabilisers so that they are directly onto the fuselage, like for the AIR AIR ONE aircraft for example [11]. In addition, the user can select the size of the cylindrical empennage connection that connect the fuselage the to the stabilisers.

Then, the number of upward engines is specified (n), with the diameter of the engines (D) and the thrust efficiency (η). The same is defined for the forward engines with the number of engines denoted (n_f), the diameter (D_f) and the thrust coefficient ($C_{t,f}$). The next part of the text file define the width height and length of the fuselage (w_f, h_f, l_f) as well as the fuselage top ($C_{d,top}$) and front drag coefficients ($C_{d,front}$). Then, the battery dimensions are established (w_b, h_b, l_b) and its corresponding battery capacity (B_c). All units are specified in the text file template. In addition, the location in X,Y,Z of all the subcomponents is established as well as the mass of each of the subcomponents (m_x).

VTOL Limitations text file

The limitations text file shown in Appendix B is explained in this part. The engine and control surfaces need minimum and maximum values in order to be optimised by the MATLAB program. As a result, the engines have a maximum RPS setting (for EVE V3 this is 80 RPS for both the upwards and forwards engines). In addition, the control surfaces' deflections are limited by a maximum and minimum deflection. For EVE V3, the elevators have a minimum deflection of $-20 [deg]$ and a maximum deflection of $25 [deg]$. The ailerons have a minimum deflection of $-10 [deg]$ and a maximum deflection of $10 [deg]$. At last, the rudder has a minimum deflection of $-20 [deg]$ and a maximum deflection of $20 [deg]$. The maximum energy density in $[Wh/kg]$ is also defined in order to be able to size the battery of the eVTOL.

VTOL Flightpath text file

The flightpath text file highlighted in Appendix C is used by the MATLAB program in order to find the optimal flight path for the specific flight coordinates. The file specifies the target X and Y locations in $[m]$ as well as velocity and altitude requirements for each phase of the flight. The following requirements are used for the EVE V3 eVTOL:

Table 5.1: Program System requirements

Identification	Requirement	Value (EVE V3)	Unit
MAT-ALL-01	Maximum Passenger G force	1.3	$[G]$
MAT-PH1-01	Vertical Take-Off Climb Rate	10	$[m/s]$
MAT-PH2-01	Transition height	300	$[m]$
MAT-PH2-02	Transition angle of attack	0	$[deg]$
MAT-PH3-01	Climb Rate (V_z)	8	$[m/s]$
MAT-PH3-02	Climb Velocity (V_{cl})	55.67	$[m/s]$
MAT-PH4-01	Cruise Altitude	2000	$[m]$
MAT-PH4-02	Cruise Velocity (V_c)	55.67	$[m/s]$
MAT-PH7-01	Vertical Descent Rate	-2	$[m/s]$

At first, the Vertical Take-Off Velocity in $[m/s]$ is specified for the phase 1 of flight. Then, for phase 2, the Vertical Transition Height in $[m]$ is set as well as the Transition Angle of Attack in $[deg]$. In phase

3, the Climb Rate (V_z) in $[m/s]$ and Climb Velocity (V_{cl}) in $[m/s]$ are defined. Then, for phase 4, the Cruise Altitude in $[m]$ and Cruise Velocity (V_c) in $[m/s]$ are established. At last, the Vertical Descent Velocity in $[m/s]$ is defined for the phase 7, the last phase of the flight.

The user can also specify waypoints. Up to 6 waypoints can be specified by coordinates in X,Y. The aircraft will fly to each waypoint in order before landing at the target destination. An example of a Limitations text file is found in Appendix B and the Flightpath text file is found in Appendix C.

5.3. Initialisation Sequence

The initialisation sequence encompasses the necessary steps that need to be taken in order to have a functioning aircraft that is ready to fly in the MATLAB program. The following steps are taken, all starting values are set to zero, this includes, the accelerations, velocities, and positions. Then, the aircraft parameters are loading into the program using the input text file.

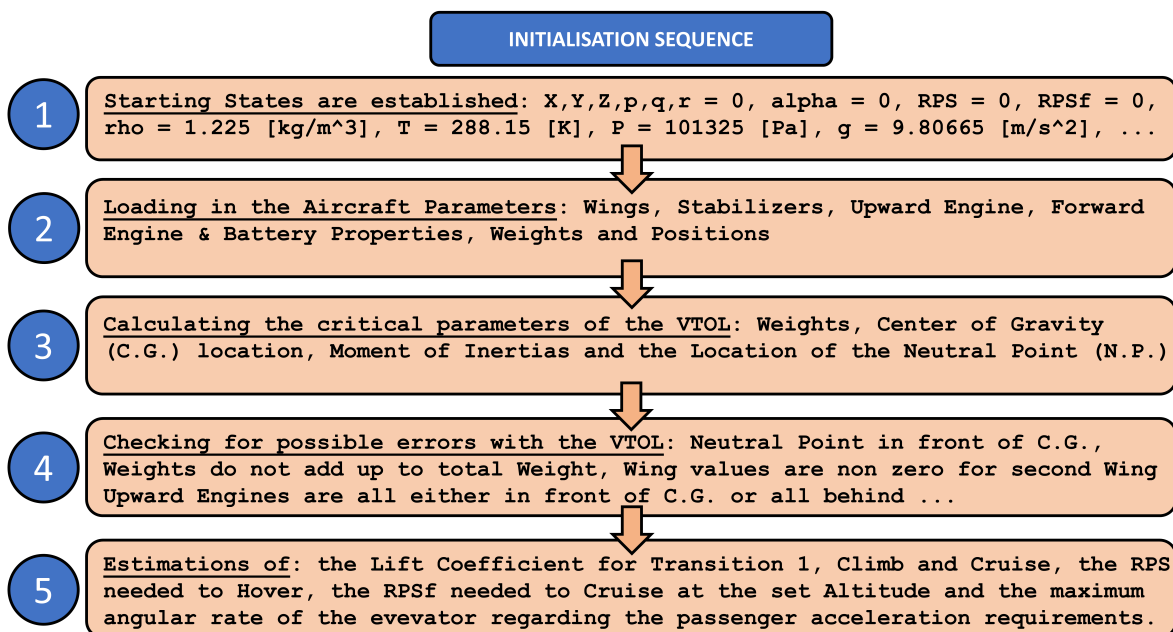


Figure 5.4: MATLAB Program Initialisation

These parameters from the text file are checked so that the aircraft does not crash in flight because of an input error. At last, the necessary RPS settings and velocities for flight are calculated. Then, the parameters are manipulated in order to get certain critical aspects for flight including the centre of gravity location, the neutral point location and the moment of inertia for example.

5.3.1. Initialise Variables

The program needs starting values. All Thrust RPS settings of the upward and forward engines are set to zero. Also, the position (x,y,z) of the aircraft is set to zero along with the rotational positions (ϕ, θ, ψ) . The flight data matrices are created, which each simulated flight representing one row of the matrix, with the columns representing a time step increase (see section 6.2). The atmospheric conditions at sea level are given as follows:

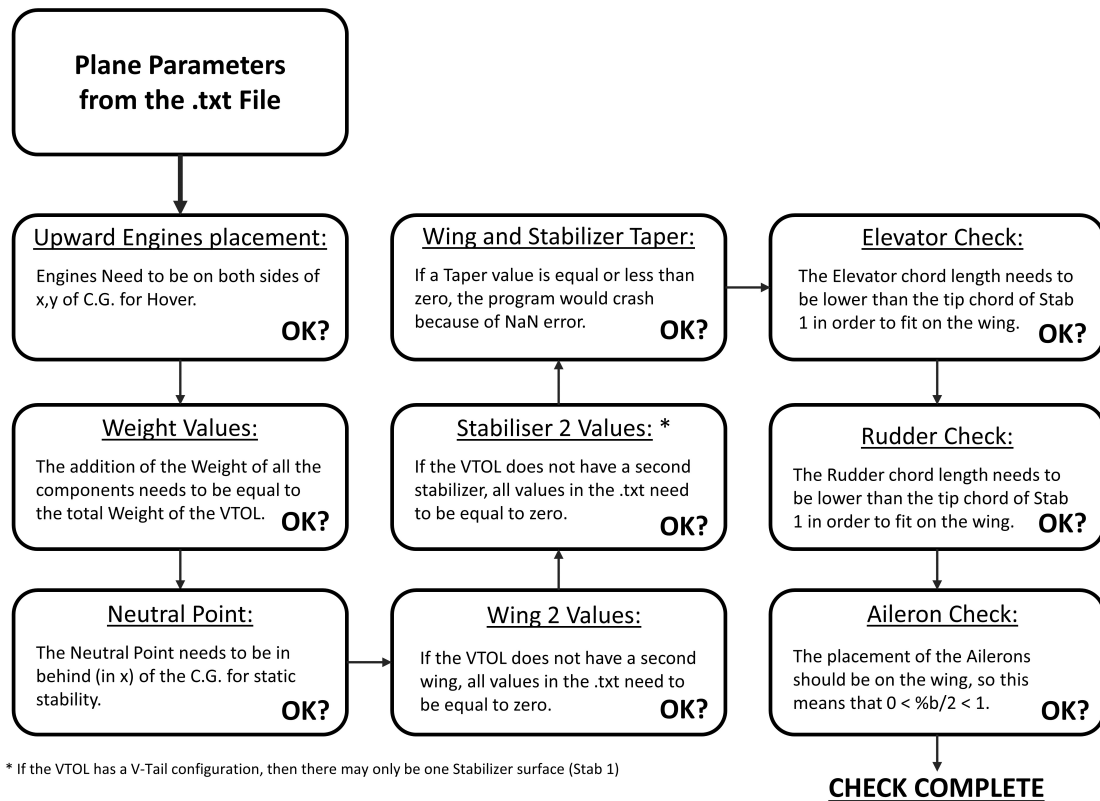
Table 5.2: General Parameters for EVE V3

Parameter	Symbol	Value	Unit
Grav. Constant	g	9.80665	$[m/s^2]$
Sea Level Density	ρ_0	1.225	$[kg/m^3]$
Sea Level Pressure	p_0	101325	$[Pa]$
Sea Level Temperature	T_0	288.15	$[K]$

The next step is to load the aircraft parameter text file that was explained in section 5.2 and check is the text file does not contain any errors that could prevent the aircraft from flying.

5.3.2. Check Parameters

The check phase is critical for the flight's success, as many things could be inputted wrong in the text file. The checks include the checks for the wings, stabilisers, and control surfaces.

**Figure 5.5:** MATLAB Program Parameter Check

The next step is to calculate the important values needed for flight which includes the location of the centre of gravity, the location of the neutral point and the moment of inertia in all three directions of the aircraft.

5.4. Plane Preliminary Calculations

When the plane data is loaded into the program, the program proceeds with the calculations of different aspects of the aircraft.

5.4.1. Center of Gravity (C.G.)

The centre of gravity is calculated by simple multiplication of the positions of the point masses multiplied by the masses of each component. This process is done for each new flight and the same equations

are used as with the EVE V3 Case study in chapter 3. For EVE, the C.G is located at **6.22** meters from the front of the aircraft.

5.4.2. Neutral Point (N.P)

The neutral point is an important aspect of longitudinal stability. The full calculation of the location of the neutral is highlighted in section 3.10. The neutral point was found using [58][59], solving for $X_{N.P.}$:

$$(\mathbf{X}_{N.P.} - l_1)\zeta(\alpha_1) + (\mathbf{X}_{N.P.} - l_2)\zeta(\alpha_2) - (\mathbf{X}_{N.P.} - l_3)\zeta(\alpha_3) - (\mathbf{X}_{N.P.} - l_4)\zeta(\alpha_4) = 0 \quad (5.1)$$

This equation is modular for up to two wings and two stabilizers just like the limitation of the program itself, the equation of ζ is explained in section 3.10. For EVE, the location of the C.G. is in front of the neutral point, so the aircraft is statically stable. [60]

5.4.3. Moment of Inertia

The moment of Inertia is calculated by multiplying the mass of each subcomponent by their position relative to the C.G. of the aircraft squared. Using Equation 5.2 and Equation 5.3, the inertia matrix can be established.

$$I = \begin{bmatrix} I_{xx} & 0 & -I_{xz} \\ 0 & I_{yy} & 0 \\ -I_{xz} & 0 & I_{zz} \end{bmatrix} \quad (5.2)$$

$$\begin{aligned} I_{xx} &= \sum (m_i \cdot z_i^2 + m_i \cdot y_i^2) \\ I_{yy} &= \sum (m_i \cdot x_i^2 + m_i \cdot z_i^2) \\ I_{zz} &= \sum (m_i \cdot x_i^2 + m_i \cdot y_i^2) \\ I_{xz} &= \sum (m_i \cdot x_i \cdot z_i) \end{aligned} \quad (5.3)$$

The next step is to find the principal inertia axis as outlined in section 3.11. The inertia value is used at the moment calculations for rotations in roll, pitch and yaw around all three axis highlighted in section 4.6.

5.4.4. Heading in Flight

The heading of the aircraft in flight is controlled by a module that measures the difference between the direction of the aircraft and the heading of the waypoint. If this delta is positive, then the ailerons deflect upwards on the left side of the aircraft and downwards on the right side, the aircraft will turn right until the delta is zero again. The same principle applies for a turn to the left side when the delta is negative, the control surfaces will move in the opposite direction. While this is calculated at every time step in the flight loop, which will be explained in chapter 5, the first heading calculation is done in the initialisation phase as the aircraft will align its heading with the first waypoint heading.

5.5. Program Capabilities

This section highlights the limits to the program. While giving the preliminary design engineers enough freedom to play around with their models, the program has to stay simple and usable for the end user. As a result, these are the program's maximum inputs:

Table 5.3: General Parameters for EVE V3

Parameter	Max Number
Wings	2
Stabilisers	2
Upward Engines	12
Forward Engines	6
Battery	1
Waypoints	6

5.6. The Flight Loop

The flight loop is the main part of the MATLAB program. In this loop, all the flight calculations are done until the aircraft has reached its final destination coordinates from the Flightpath text file.

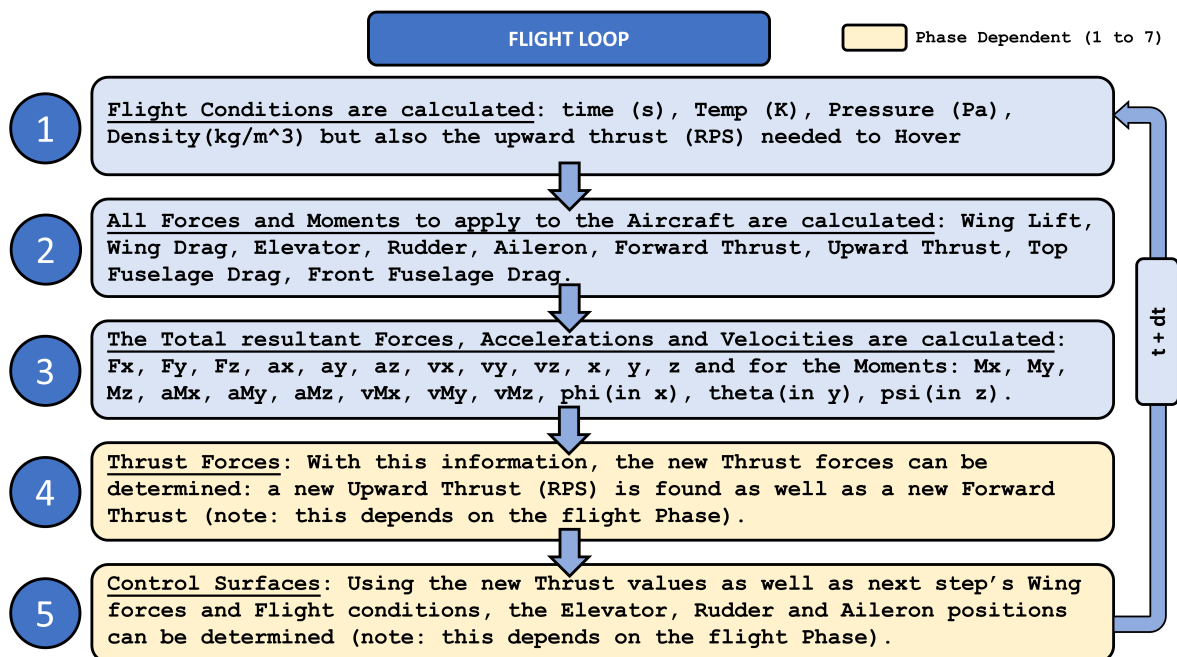


Figure 5.6: MATLAB Program Flight Loop

As can be seen in Figure 5.6, the Flight Dynamics MATLAB program works as a for loop with increasing step in time (Δt). For each iteration of the loop, the same calculations are done. Firstly, the flight conditions are updated. This means that the program calculates the temperature, density, and pressure for its current altitude as well as the required thrust for the eVTOL to hover. Secondly, the forces and moments are calculated individually. For example, the lift and drag change with angle of attack while the thrust is a function of the RPS of the engine which is set by the previous loop (during module 4 in Figure 5.6). The third module calculates the total forces and moments, then the accelerations, then the velocities and finally the new positions and angular positions of the aircraft. In this module the flight path angle is also calculated as it is equal to the inverse tangent of the velocity in the minus z-direction divided by the velocity in the x-direction. It is important to notice that the conventional aeronautical axis system is used, which means that z is pointed downward, towards the earth in normal flight. Module 4 is phase dependent, this means that the thrust force calculations are not the same for all phases of flight. There are 7 flight phases for an eVTOL: Vertical Take-Off (1), Transition 1 (2), Climb (3), Cruise (4), Descent (5), Transition 2 (6) and Vertical Landing (7). During phase 1 and 7, the aircraft moves like a multicopter, this means that the wings do not provide any lift force as the aircraft is moving in a vertical direction (in the z-direction for take-off for example). Also, the forward facing engines are turned off, so only the upward engines are active during these phases. During transitions (phases 2 and 6), the aircraft's upward thrust is changed to wing lift and vice versa, the forward engines are turned also on and the upward engines turn off as a result of the increasing lift. At last, in phases 3,4 and 5, the aircraft acts like a conventional aircraft and has sufficient velocity to use the control surfaces with are controlled in module 5 of the loop (Figure 5.6). After this module, the time step increases and the loop starts over again.

In order to change in between the phases of flight, certain altitudes and positions have to be obtained by the eVTOL in the program. For example, in order to move from phase 1 to 2, the eVTOL has to climb to the transition altitude which is an input which is a requirement (see Figure 5.2) set by the user.

5.7. Control Loops

This section elaborates on the control loops of the MATLAB program. The engines have different commands during each phase of flight. In addition, the control surfaces also need to be commanded for the aircraft to follow its intended flight path.

5.7.1. Control Overview

For the control of the eVTOL, the aircraft uses conventional control surfaces during climb, cruise and descend and uses differential RPM in order to manoeuvre in all other phases of flight which include the Vertical Take-Off, Transition 1, Transition 2 and the Vertical Descent.

Phase	DOF	Symbol	Control
Vertical Flight + Transitions	Roll	ϕ	$\Delta\Omega$ of the left and right rotors
	Pitch	θ	$\Delta\Omega$ of the front and rear rotors
	Yaw	ψ	$\Delta\Omega$ of rotors with different rotational directions
Conventional Flight	Roll	ϕ	Aileron deflection δ_a
	Pitch	θ	Elevator deflection, δ_e
	Yaw	ψ	Rudder deflection, δ_r

Table 5.4: Control Options for each phase of flight

5.7.2. Phase 1: Vertical Take-Off

The first step in the flight loop is for the aircraft to take-off vertically. The eVTOL's upward engines turn on to create an upwards force. The z position (z axis direction is negative for an upward movement, see section 4.3) of the aircraft can not be positive, so the loop has a safety net that prevents the aircraft from going into the ground as the engines slowly turn on. When the engines are turned on to their vertical climb speed, the program has already calculated at what height, the engines need to slow down to hover RPS (rotations per second) in order to hover exactly at the transition altitude.

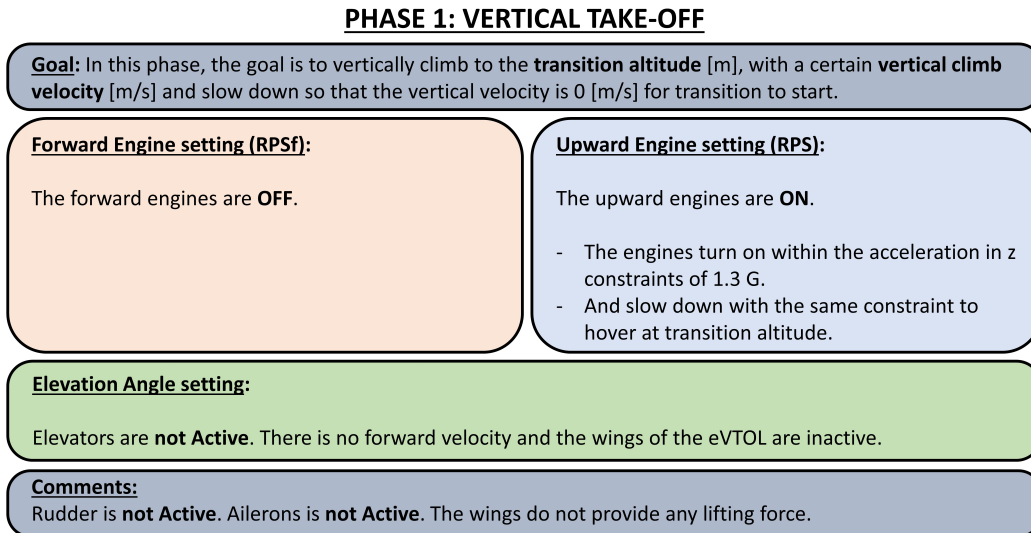


Figure 5.7: Phase 1 Flight Loop Diagram

To clarify, all engine RPS changes are done so that the G-force exerted on the passengers does not exceed the maximum of 1.3 G. In order for the eVTOL to remain balanced in pitch, the upward engines use differential RPS. The program knows which engines are in front of the C.G. and which engines are behind the C.G. and balances the RPS of the engines accordingly using the following equations:

$$\sum_{n_B} p_{T_B}(n_B) \text{ and } \sum_{n_A} p_{T_A}(n_A) \quad (5.4)$$

The average position of the engines before and after the C.G. is found using Equation 5.4. p_{T_B} and p_{T_A} are the individual positions of each of the engines and n_B and n_A are the number of engines before and after the C.G. respectively. The equation for the differential RPM is derived from the moment equilibrium and is:

$$R_B = \sqrt{\frac{|n * p_{T_A}|}{n_B * p_{T_B} + n_B * p_{T_A}}} \text{ and } R_A = \sqrt{\frac{|n * p_{T_B}|}{n_A * p_{T_A} + n_A * p_{T_B}}} \quad (5.5)$$

R_B and R_A and the ratios of differential RPS that the RPS for a fully symmetric eVTOL has to be multiplied by. This equation works for any amount of upward engines as long as there is at least one engine before the C.G. and one engine after the C.G, this is checked in the initialisation phase explained in subsection 5.3.2.

5.7.3. Phase 2: Transition 1

During the transition period, the lifting force from the upward engines is converted into the lifting force of the wings of the aircraft. In order to achieve this transition, the aircraft needs to accelerate forward using its forward engines within the acceleration constraints for the passengers.

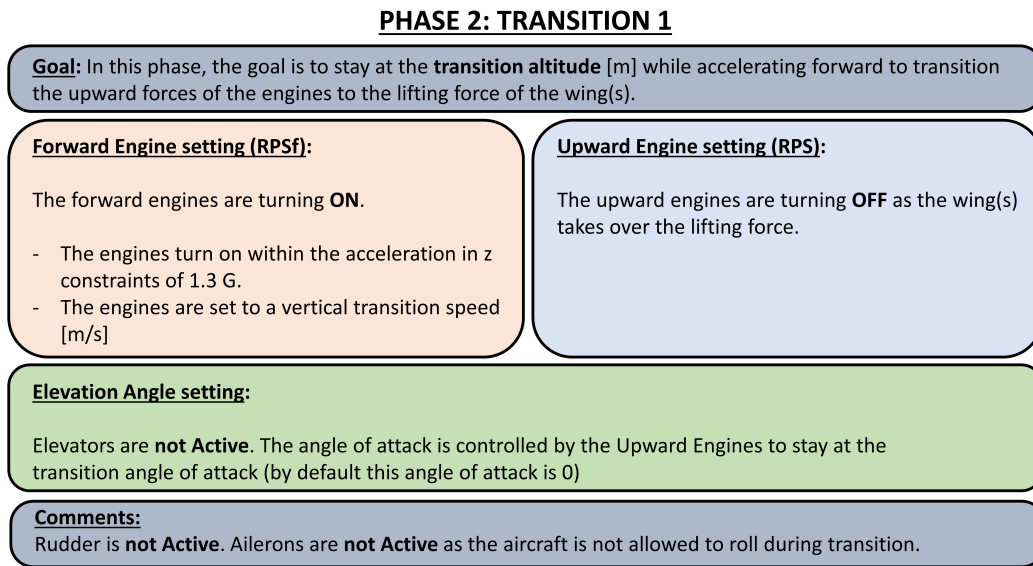


Figure 5.8: Phase 2 Flight Loop Diagram

The wings of the eVTOL need to generate enough lift to support the weight of the eVTOL without the help of the upward engines. As a result, the velocity needed to achieve this can simply be derived from the condition that the Lift of the eVTOL equals the Weight ($L = W$). This gives the following equation for the transition velocity at zero angle of attack:

$$V_t = \sqrt{\frac{mg}{\frac{1}{2}\rho_t(\cos \Gamma_1 Cl_{0_1} S_1 + \cos \Gamma_2 Cl_{0_2} S_2 + \cos \Gamma_3 Cl_{0_3} S_3 + \cos \Gamma_4 Cl_{0_4} S_4)}} \quad (5.6)$$

With Cl_{0_x} being the specific wing's zero angle of attack lift coefficient, ρ_t is the density at transition height, the angle Γ_x is the wing's dihedral angle and S_x is the wing surface area. If the eVTOL has less than four wings (or stabilisers), the equation is still valid, as the unused wings' surface area is zero. The drag coefficient for the transition phase needs to be calculated, as the forward thrust needs to be equal to the drag at the transition velocity V_t . In transition conditions, the drag coefficient is:

$$C_{d_{x,t}} = C_{d_0} + \frac{Cl_{0_x}}{e_x \pi A R_x} \quad (5.7)$$

The RPSf (forward rotations per second) of each engine is calculated for transition using the following

equation:

$$RPSf_t = \sqrt{\frac{\frac{1}{2}\rho_t V_t^2 (C_{d_{1,t}} S_1 + C_{d_{2,t}} S_2 + C_{d_{3,t}} S_3 + C_{d_{4,t}} S_4 + C_{d_{front}} S_f)}{n_f \rho_t A_f C_{t_f}}} \quad (5.8)$$

With this forward thrust setting, the aircraft will be able to transition without climbing until the upward engines are completely turned off, the output graph of the transition 1 phase can be found in section 6.2.

5.7.4. Phase 3: Climb

The first phase of conventional flight is the climb phase. In this phase, the angle of attack and thrust are set to that the aircraft has a specific climb rate from the requirements [61].

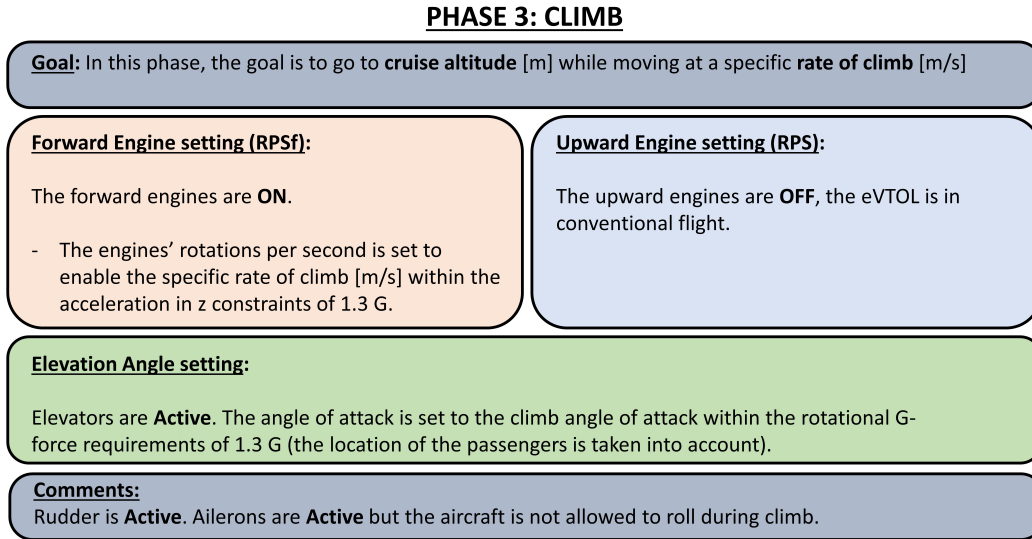


Figure 5.9: Phase 3 Flight Loop Diagram

For the climb phase, The climb rate and climb velocity are a user input from the requirements.

Parameter	Symbol	Value	Unit
Angle of Attack	α	Variable	[deg]
Thrust	T_{cl}	Variable	[N]
Climb Rate	$V_{z_{cl}}$	Requirements	[m/s]
Climb Velocity	V_{cl}	Requirements	[m/s]

Table 5.5: Values in Equation 5.7.4 and Equation 5.7.4

Using these input values, the flightpath angle (γ) can be calculated:

$$\gamma = \arctan\left(\frac{V_{z_c}}{\sqrt{V_c^2 - V_{z_c}^2}}\right) \quad (5.9)$$

In order to obtain the angle of attack and thrust setting for the forward engines, two equations of motion of the eVTOL have to be solved. The first equation is the sum of force equal to zero in the z-direction and the second equation is the sum of force equal to zero in the x-direction:

$$\begin{aligned} \sum F_x = 0 : & -\sin(\gamma) * [L_1(\alpha) + L_2(\alpha) + L_3(\alpha) + L_4(\alpha)] \\ & -\cos(\gamma) * [D_1(\alpha) + D_2(\alpha) + D_3(\alpha) + D_4(\alpha) + D_f(\alpha)] + T_c \cos(\alpha + \gamma) = 0 \end{aligned} \quad (5.10)$$

$$\sum F_z = 0 : -\cos(\gamma) * [L_1(\alpha) + L_2(\alpha) + L_3(\alpha) + L_4(\alpha)] + \sin(\gamma) * [D_1(\alpha) + D_2(\alpha) + D_3(\alpha) + D_4(\alpha) + D_f(\alpha)] - T_c \sin(\alpha + \gamma) + W = 0 \tag{5.11}$$

The RPS of the forward engines can be found using the thrust equation and the thrust value found in Equation 5.7.4. The set of solutions for EVE V3 are a climb angle of attack: $\alpha_{cl} = 0.42 [deg]$ and an RPS setting of $RPS_{cl} = 91.4 [RPS]$.

5.7.5. Phase 4: Cruise

The cruise phase is the most energy intensive phase. Also, it is the most complex phase for the control surfaces, as the aircraft has to navigate the waypoints while keeping the cruise altitude.

Parameter	Symbol	Value	Unit
Angle of Attack	α	Variable	[deg]
Thrust	T_c	Variable	[N]
Cruise Rate	V_{z_c}	Requirements	[m/s]
Cruise Velocity	V_c	Requirements	[m/s]

Table 5.6: Values in Equation 5.7.4 and Equation 5.7.4

During the cruise phase, the same equations (Equation 5.7.4 and Equation 5.7.4) are resolved as in the climb phase, only this time the velocity is replaced by the cruise velocity (V_c) and the flight path angle (γ) is zero as the plane is in level flight. The set of solutions for EVE V3 are a cruise angle of attack: $\alpha_c = 0.44 [deg]$ and an RPS setting of $RPS_c = 75.9 [RPS]$.

PHASE 4: CRUISE

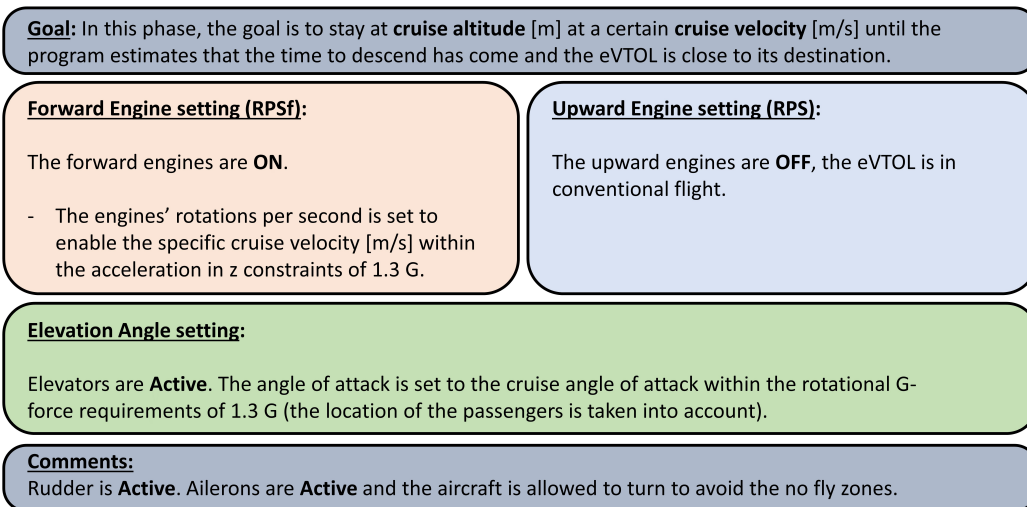


Figure 5.10: Phase 4 Flight Loop Diagram

The elevators control the pitch of the aircraft so that it stays at the requirement cruise altitude. In addition, the high speed ailerons enable the aircraft to fly towards each of its waypoints before landing at its target coordinates in X and Y.

5.7.6. Phase 5: Descent

During the descend phase, the aircraft glides down at a maximum Lift over Drag ratio, this ensures that the aircraft able to move forward as efficiently as possible. This ratio is found in the MATLAB program and displayed as an output as seen in section 6.2.

PHASE 5: DESCENT

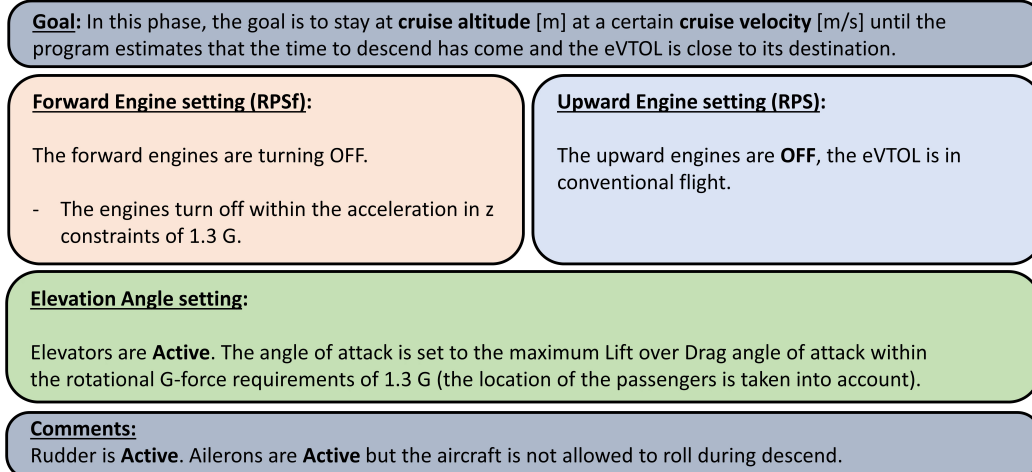


Figure 5.11: Phase 5 Flight Loop Diagram

During this phase, the elevators have to maintain this optimal Lift over Drag angle of attack angle. The aircraft does not use any battery as all engines are off. In the future, it is believed that this phase could even regenerate the battery has the potential energy could charge the batteries through the turning of the forward and upward propellers by the airflow.

5.7.7. Phase 6: Transition 2

During the second transition phase of the flight, the opposite happens to the first transition, as this time the lift of the wings is transferred to the lift force of the upward engines.

PHASE 6: TRANSITION 2

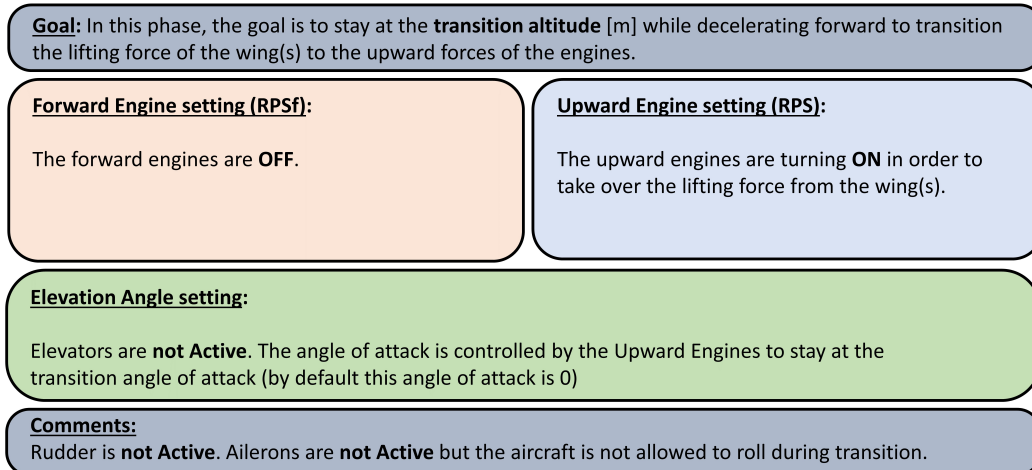


Figure 5.12: Phase 6 Flight Loop Diagram

Differential RPM is used to level the aircraft in order for it to land vertically, as explained in the first transition. When the aircraft's forward speed is zero, then the aircraft is able to start reducing its upward engines RPS in order to descend in a controlled manner.

5.7.8. Phase 7: Vertical Landing

This is the last phase of flight and the aircraft descends with a certain descent velocity requirement (which is equal to $-2 [m]$ for the EVE V3 mission).

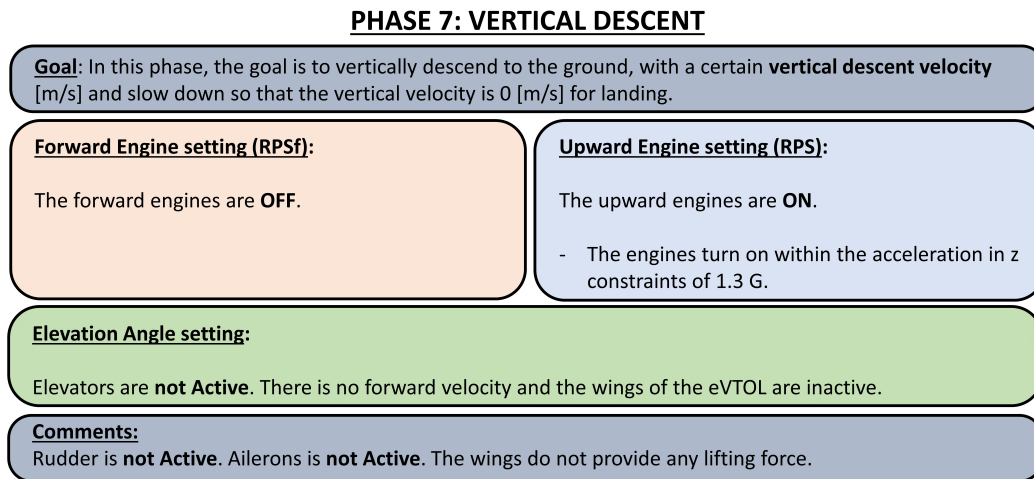


Figure 5.13: Phase 7 Flight Loop Diagram

During the vertical landing phase, the aircraft's pitch is kept at zero and the aircraft lands on the target location which are requirements in the flightpath file set by the user of the MATLAB program.

All aspects of the MATLAB program have been discussed, and the next step is to showcase the output plots that are made by the program and to show the optimised version of the EVE V3 aircraft.

6

Optimisation of the VTOL and Output

This chapter covers the performance and the optimisation plots of the MATLAB program. In section 6.1, the performance plots are outlined such as the planform, the forces, and moment plots and the trim plots. In section 6.2, the optimisation plots are found. This includes the mass plot, the dimensions plot, the control surface plots and the battery plot.

6.1. General Output Graphs

The program outputs general performance graphs for each flight. This is not connected to the optimisation part of the MATLAB program, and these plots are performance plots of the aircraft. These plots include a planform plot, the stability plots, forces, and moment plots and propeller pitch plot.

The most important plot is the trajectory plot, as the user is able to see the aircraft move in the X,Y coordinate system. The aircraft clearly goes through all waypoints before landing at the target coordinates. All seven phases of flight can clearly be identified, and the aircraft stays in cruise for the longest period.

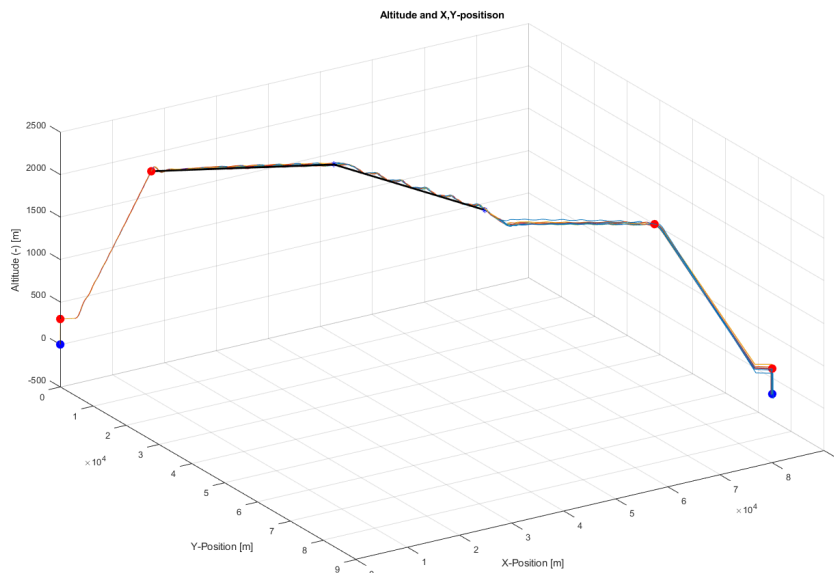


Figure 6.1: Trajectory of EVE V3

During that period, some oscillation can be identified, this is due to the fact the program uses linear

control surface deflections which creates these oscillations. However, this is not a critical program as the important value for the control surface deflection sizing is the minimum or maximum value of the deflection, thus these cruise oscillations have zero influence on the sizing of the elevator surfaces.

6.1.1. Planform

From the input text file, the MATLAB program is able to create a 3D plot for the user to visualise the aircraft. This plot is very useful when designing and modifying the input text file and this plot can be created merely by loading the text file and the entire flight loop does not need to run.

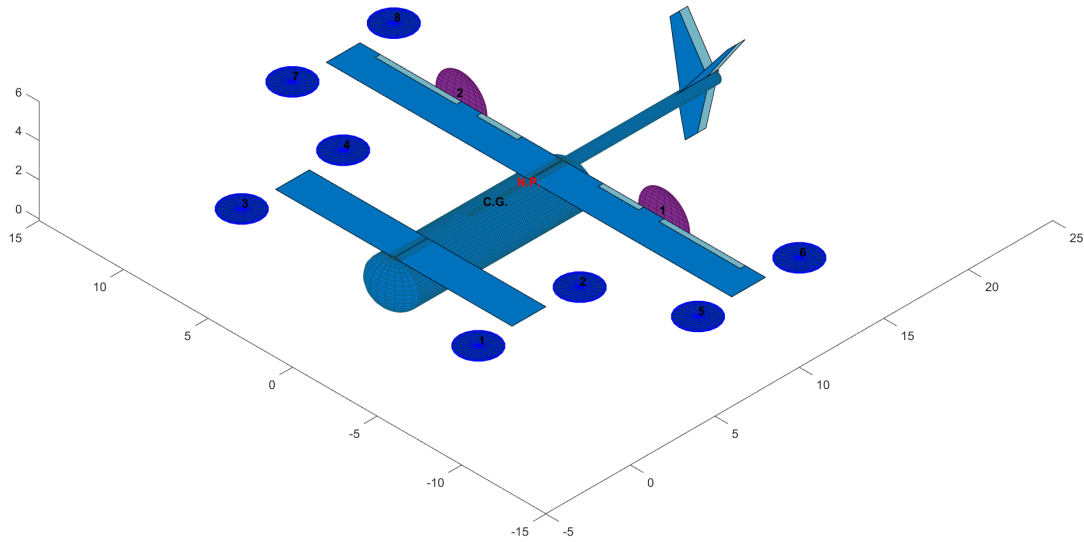


Figure 6.2: Planform of EVE V3

This is a planform plot of EVE V3 which clearly showcases its eight upward engines, two forward engines, two wings and two stabilisers (a V-tail and a rudder).

6.1.2. Forces and Phases Panel

For each flight, all forces are also plotted against time. This can be useful in order to see the performance of the eVTOL for each phase of flight. Some interesting force changes include Transition 1 where it can clearly be seen that the lift from the upward engines is transferred to the lifting surfaces (many force plots are found in Appendix D):

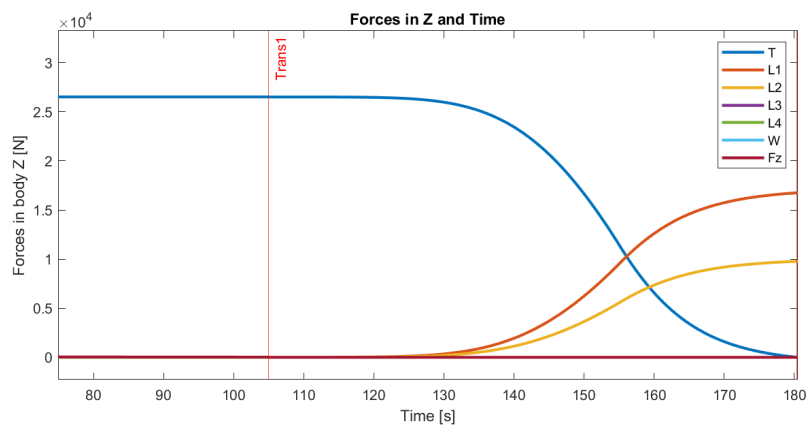


Figure 6.3: Transition 1 forces in Z of EVE V3

During the transition phase, the lift of Wing 1 and Wing 2 increases while the upward engine thrust decreases. This happens without any force in the z-direction, and the aircraft accelerates in the forward direction while staying level. It is also interesting to notice that the third lifting surface (the V-tail) does not produce any lift as its zero angle of attack lift coefficient is 0 and for this flight, the transition happens at an angle of attack of zero. Regarding the forces in the x-direction, as seen in Figure 6.4, the aircraft accelerates until the forward thrust is equal to the aircraft's drag:

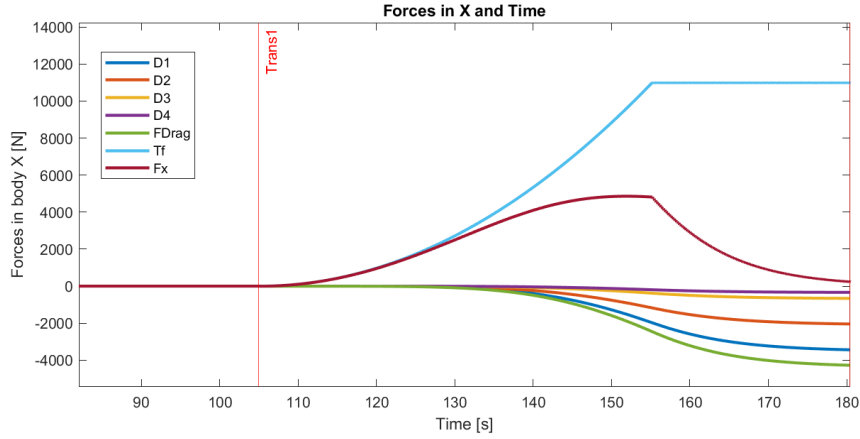


Figure 6.4: Transition 1 forces in X of EVE V3

6.1.3. Stability Panel

The stability panel is an interesting panel when looking at the stability of the aircraft as well as the trim angle of attacks. In this panel, the Lift of Drag plot is present which is used during the descent phase of flight at which the eVTOL flies at L/D_{max} .

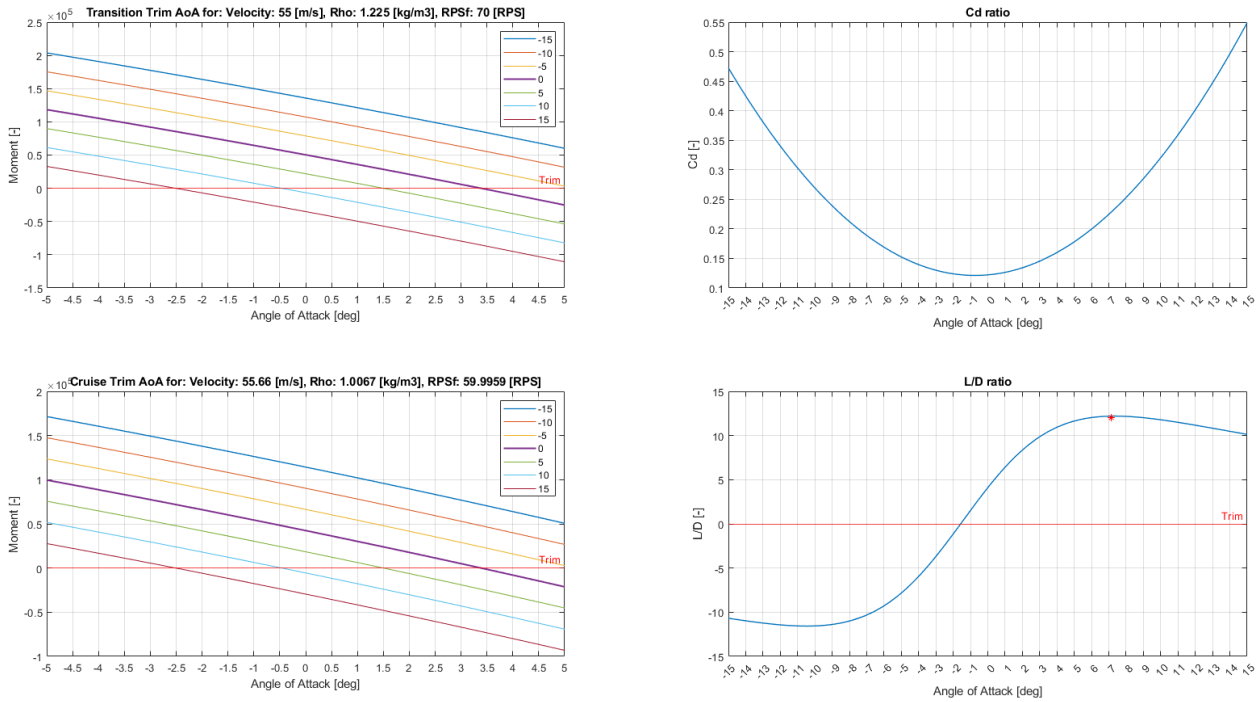


Figure 6.5: Trim Panel of EVE V3

In addition, the elevator deflection needed for certain angle of attacks can be found in the moment trim plot. For example, in cruise conditions, to obtain the trim angle of $0.44 [deg]$ mentioned in section 5.7, the elevator deflection will be approximately $7 [deg]$. Also, as can be seen from Figure 6.5, the maximum Lift over Drag ratio of EVE V3 is obtained at an angle of attack of $7.1 [deg]$ and the value of the L/D ratio is 12.35.

6.1.4. Moment in X

Another interesting view of the transition is the moment plot in around the x-axis, this plot clearly shows the use of differential RPM in order for the aircraft to not roll (ϕ). The same happens in the moments around the y-axis, as the aircraft should not pitch (θ) in purely vertical flight.

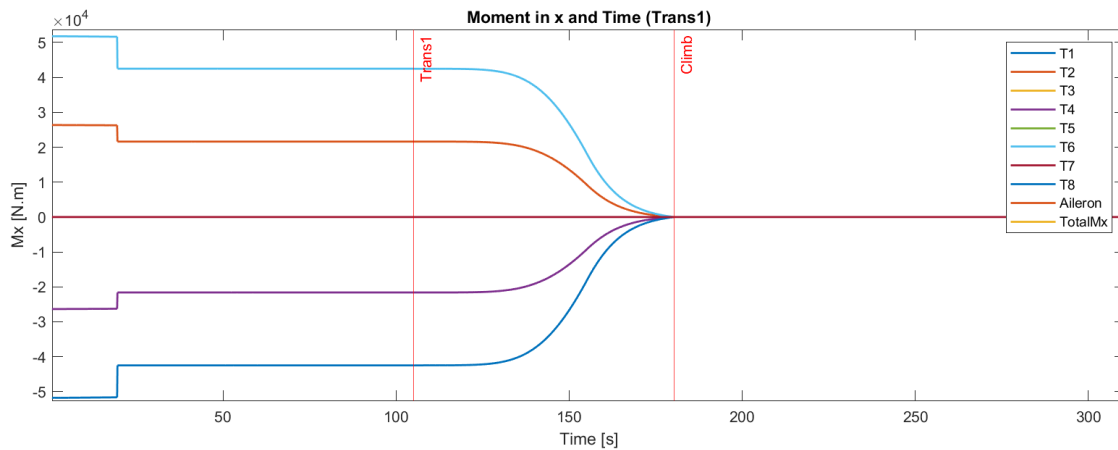


Figure 6.6: Transition 1 moments in X of EVE V3

While EVE V3 has eight upward engines, only four lines can be seen on the moment plot since the engines are on the tip of the wings, this results in the engines having the same moment arm and thrust force.

6.1.5. Propeller Pitch

The propeller pitch plots showcase the pitch of the propellers for each phase of flight for both the upward and forward propellers. This is critical to ensure that the propellers work at their maximum efficiency. To showcase this plot, the forward propeller pitch is shown in climb, cruise and descend:

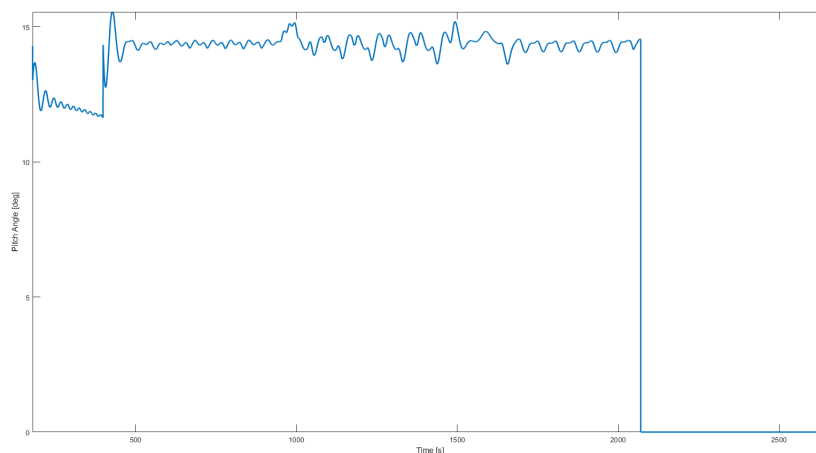


Figure 6.7: Pitch of the forward propeller of EVE V3

The pitch of the propeller varies because of the velocity variations due to the turns performed by the

aircraft. It hovers around a pitch of $14.1 [deg]$. The pitch is controlled automatically during the entire flight in order to ensure that the propellers works at an optimal thrust efficiency.

6.2. Optimisation

The optimisation of the eVTOL aircraft is done starting a new flight loop until convergence is achieved for the variables that need to be optimised. These variables include the propeller diameter of all engines, the control surface areas, the masses of the subcomponents of the aircraft and the battery capacity.

6.2.1. Concept Explanation

Sizing and Optimising the eVTOL is an iterative process as its mass change with each flight due to the Class II weight estimation. In order to effectively size the aircraft, the program has to run many flights. This is computationally expensive, but there is no other way, as many variables change during each iteration. An explanation on the program iterations can be found in subsection 6.3.7.

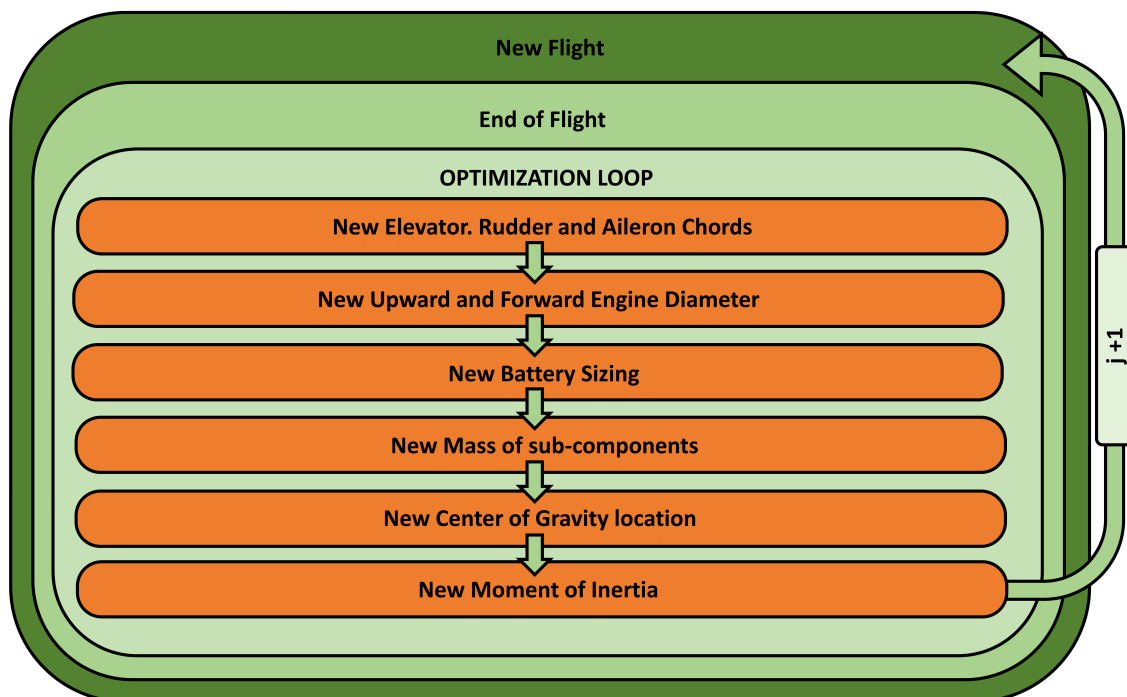


Figure 6.8: Optimization loop

In the optimization loop, the control surfaces are sized to their limit from the limitations file first, followed by the engine diameters. Then, the new masses are calculated using a Class II weight estimation, which results in a new centre of gravity location and different moments of inertia.

6.3. Flightpath and Limitations files

The more complex part of the output plots are the optimisation plots. The aircraft is constantly modified for each different flight. For each flight, the aircraft may be different, but the requirements and limitations stay the same during the entire optimisation process. The input text files for the flightpath and the limitations for the EVE V3 flight are as follows:

The optimised aspects of the eVTOL are the masses of each of the subcomponents: the Fuselage, the Battery, the Wings, Stabilisers, Upward Engines, Forward Engines. With the exceptions of the passenger mass, which stay constant at each flight. In addition, the control surfaces chord length changes

and the diameter of the engines.

Table 6.1: Flightpath Text File Values

Name	Value	Unit
Target Coordinates		
End of flight Coordinates X	85000	[m]
End of flight Coordinates Y	85000	[m]
Flight Requirements		
P1 Vertical Take-Off Velocity	10	[m/s]
P2 Vertical Transition Height	300	[m]
P2 Transition Angle of Attack	0	[deg]
P3 Climb Rate (V_z)	8	[m/s]
P3 Climb Velocity (V_{cl})	55.66	[m/s]
P4 Cruise Altitude	2000	[m]
P4 Cruise Velocity (V_c)	55.66	[m/s]
P7 Vertical Descent Velocity	-2	[m/s]
Waypoints		
Number of Waypoints	2	-
Waypoint 1 location X	40000	[m]
Waypoint 1 location Y	20000	[m]
Waypoint 2 location X	50000	[m]
Waypoint 2 location Y	50000	[m]

Table 6.2: Limitations Text File Values

Name	Value	Unit
Upward Engines		
Up. Engines Max RPS	60	[RPS]
Up. Engine Same Radius	0	[-]
Up. Engine Power Margin	50	[%]
Forward Engines		
Fr. Engines Max RPS	60	[RPS]
Fr. Engines Power Margin	50	[%]
Control Surfaces		
Aileron Min deflection	-5	[deg]
Aileron Max deflection	5	[deg]
Aircraft Roll Rate	20	[deg/s]
Elevator Min deflection	-20	[deg]
Elevator Max deflection	25	[deg]
Rudder Min deflection	-20	[deg]
Rudder Max deflection	20	[deg]
Battery		
Battery Max Energy Density	500	[$\frac{Wh}{kg}$]
Battery Efficiency	85	[%]
State of Charge	20	[%]

6.3.1. Class II Weight Estimation

The Class II weight estimation is an iterative process, leading to a slightly altered version of EVE V3 for each flight. With a different mass, centre of gravity and moment of inertia, each flight is different. Also, the mass of the battery is calculated by considering the energy that was needed by the previous flight, as explained in section 3.6. The mass of the battery is therefore a direct result of the distance travelled by the aircraft. The limitation of the battery is a maximum energy density of 500 [Wh/kg], an efficiency of 85 [%] and a state of charge of 20 [%]. The flight used for the plots in the report is a flight with two waypoints that account for a total horizontal distance of 127 [km] due to the waypoints. This is slightly higher than the design range of the aircraft of 100 [km]. As can be seen in Table 6.4, the new mass values of EVE V3 are found after 20 iterations of the MATLAB program are:

Table 6.3: Input Mass Values

Component	Value	Unit
Fuselage	258.8	[kg]
Battery	597.9	[kg]
Passengers	500	[kg]
Wing 1	414.63	[kg]
Wing 2	128.39	[kg]
Stab 1 (V-tail)	50.86	[kg]
Stab 2 (Rudder)	26.80	[kg]
Upward Engines	8×29.05	[kg]
Forward Engines	2×104.40	[kg]
Total	2418	[kg]

Table 6.4: Optimised Mass Values

Component	Value	Unit
Fuselage	264.30	[kg]
Battery	739.617	[kg]
Passengers	500	[kg]
Wing 1	439.61	[kg]
Wing 2	143.90	[kg]
Stab 1 (V-tail)	45.84	[kg]
Stab 2 (Rudder)	14.14	[kg]
Upward Engines A	4×22.12	[kg]
Upward Engines B	4×19.08	[kg]
Forward Engines	2×189.99	[kg]
Total	2704	[kg]

The main difference in mass comes from the battery mass, which is a result of the flight being slightly

longer than the 100 [km] design range as the aircraft has to navigate the waypoints. The new total mass of EVE V3 for this specific mission is, **2704 [kg]**. The strength of this program is that with other requirements or limitations, this weight will be different. The aircraft performance team could therefore run many simulations and apply the needed safety factors to the values found by the program.

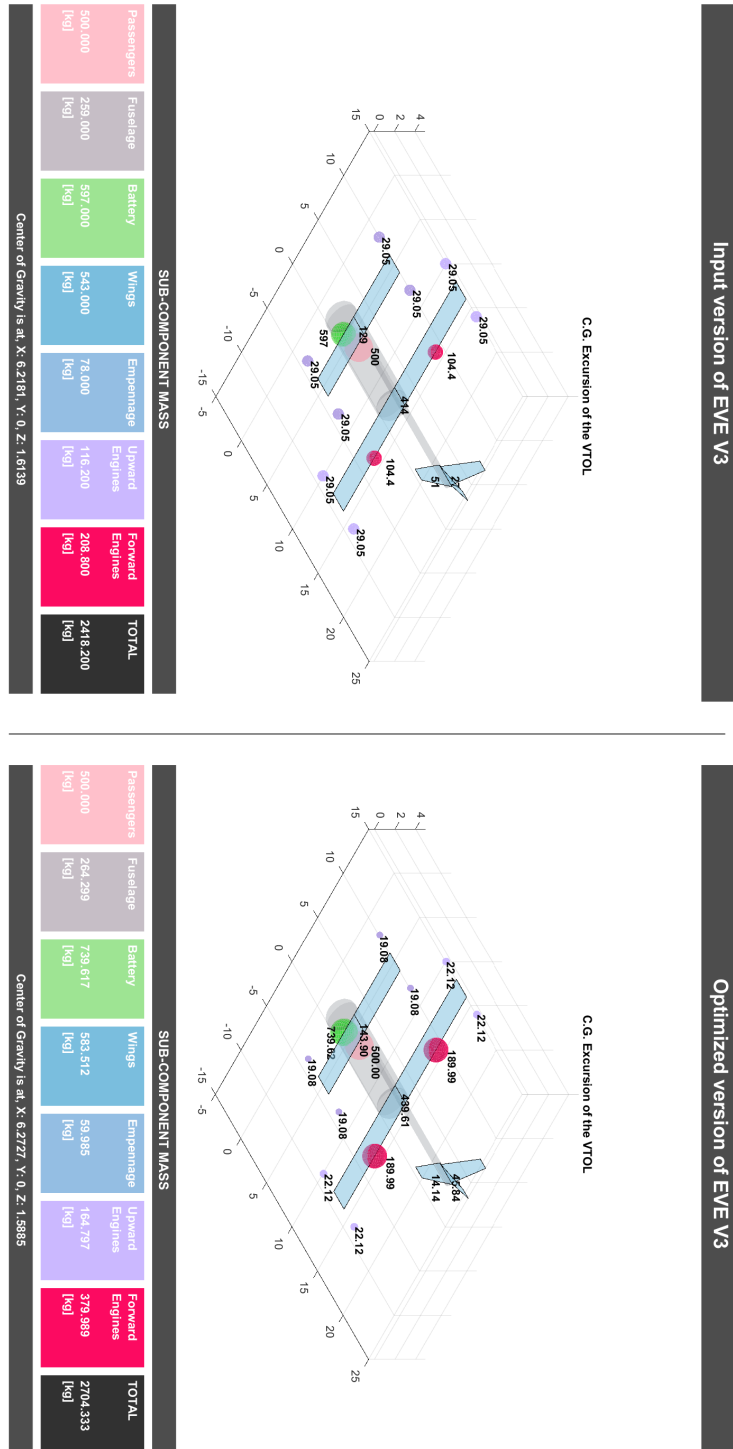


Figure 6.9: Optimum Mass of EVE V3

6.3.2. Parameter Dimensions

In parallel to the mass estimation, the parameters such as the upward and forward engines, the elevator, the rudder, and the ailerons' chord are sized. The program considers the limits of the limitations text file. As mentioned, the limits used for this flight are a maximum engines RPS of 60 (3600 RPM) for both the upward and forward engines. The minimum elevator deflection is $-20 [deg]$ and the maximum deflection is $25 [deg]$. For the rudder, the minimum is $-20 [deg]$ and the maximum is $20 [deg]$. At last, the ailerons have a $-5/5 [deg]$ limit.

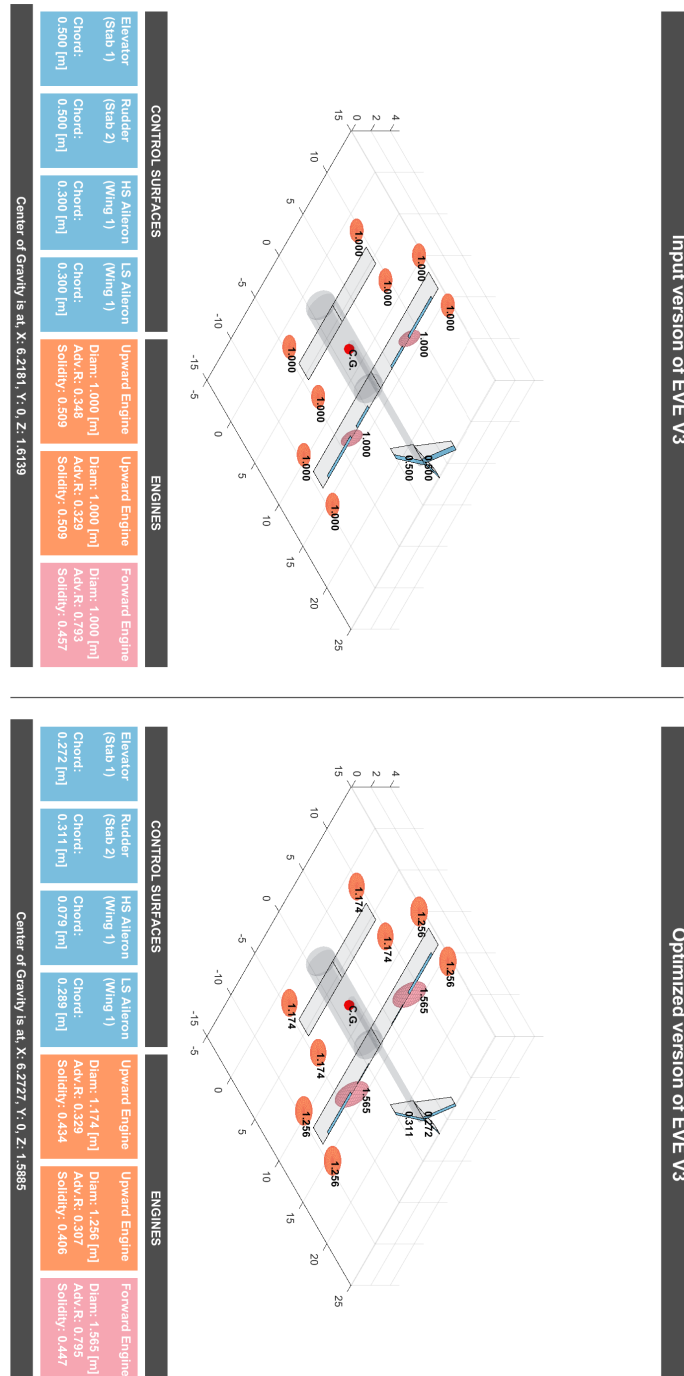


Figure 6.10: Optimum Mass of EVE V3

As can be seen in Figure 6.10, EVE V3 is optimised for the specific flight. The centre of Gravity has shifted backwards to $6.27 [m]$ in x-direction. In addition to the dimensions plot, the MATLAB program outputs plots for each subcomponent that has been optimised.

6.3.3. Empennage Control Surfaces

The program optimises the chord length of the elevator and rudder of the aircraft. This is done by increasing the chord length of the control surfaces to a size for which the deflections during the entire flight are within the minimum and maximum deflection limits of each of the control surfaces.

Regarding the sizing of the rudder, it is sized for a one engine out condition. This means that the aircraft is still able to control its motion in yaw (ψ) at every point of flight, even with one engine failure. For this calculation, the most outer placed forward engine is taken as the failing engine. In the case of EVE V3, with only two forward engines, the program just takes the first forward engine. Taking the second forward engine would result in an opposite rudder deflection of the same magnitude.

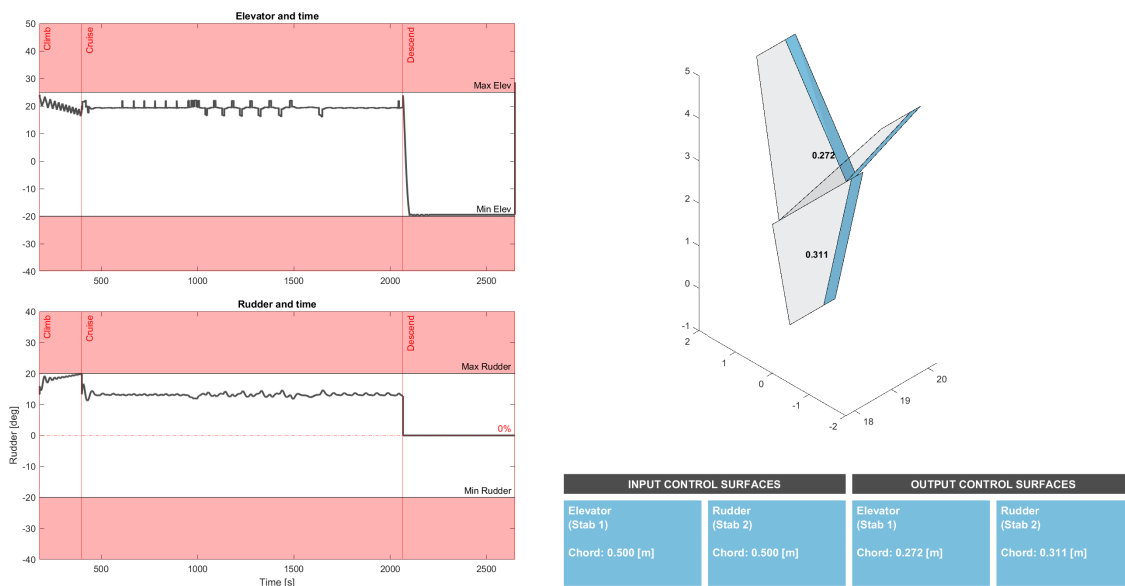


Figure 6.11: Optimum Empennage Control Surfaces of EVE V3

For EVE V3, in this given flight, the chord of the elevator is $0.266 [m]$ and the chord for the rudder is $0.311 [m]$. Regarding the elevator, the limitation point is the descent phase where the elevator deflects $-20 [deg]$ and for the rudder the maximum deflection would be at the end of the climb phase with a deflection of $20 [deg]$ if a forward engine fails on EVE V3.

6.3.4. Wing Control Surfaces

The program is able to size two ailerons surfaces, one for low speed flight and the other for high speed flight. The low Speed Ailerons are used after transition and the high speed ailerons are for use during cruise. These ailerons are sized using the roll rate limit in the limitations text file. For EVE V3, the roll rate is $20 [deg/s]$, this results in a high speed aileron chord of $0.079 [m]$ and a low speed aileron chord of $0.289 [m]$. The start and stop positions of the ailerons are specified in the input parameters text file.

Figure 6.12: Values for Transition Conditions

Transition Conditions		
Time	105-181	[s]
Phase	Transition	[-]
Velocity	0-63.15	[m/s]
Density (ρ)	1.1903	[kg/m ³]

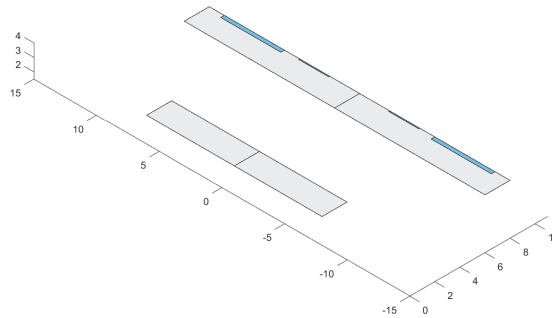


Figure 6.13: Values for Cruise Conditions

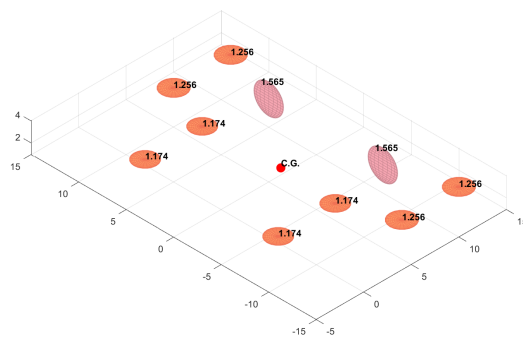
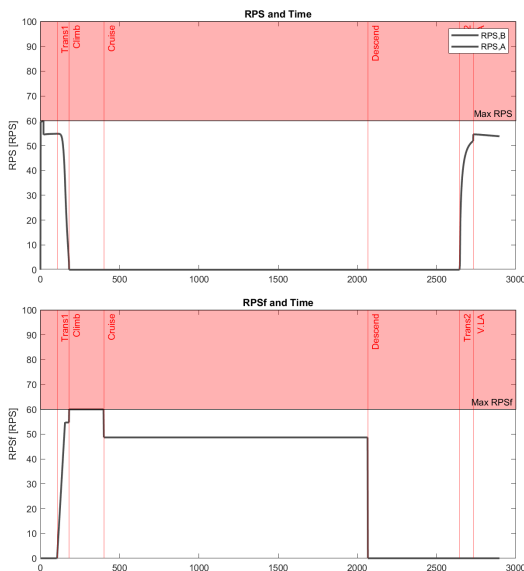
Cruise Conditions		
Time	400-2000	[s]
Phase	Cruise	[-]
Velocity	55.67	[m/s]
Density (ρ)	1.0067	[kg/m ³]

INPUT CONTROL SURFACES		OUTPUT CONTROL SURFACES	
HS Aileron (Wing 1)	LS Aileron (Wing 1)	HS Aileron (Wing 1)	LS Aileron (Wing 1)
Chord: 0.300 [m]	Chord: 0.300 [m]	Chord: 0.079 [m]	Chord: 0.289 [m]

Figure 6.14: Optimum Wing Control Surfaces of EVE V3

6.3.5. Optimised Engines

The main constraint to the engine's sizing is the RPS as the pitch can be changed in order to obtain the best advance ratio using Figure 4.6. As can be seen in Figure 6.15, the engine is sized in order for the RPS to be lower than the limit RPS of 60 RPS. The program split the upward engines in two groups, the engines before the C.G. (in x-direction) or after the C.G. This results in the groups of upward engines having different propeller radii. However, in the limitations file, this option can be disabled using the binary variable: "Upward Engine Same Radius, 0, -".



INPUT ENGINES			INPUT ENGINES		
Upward Engine	Upward Engine	Forward Engine	Upward Engine	Upward Engine	Forward Engine
Diam: 1.000 [m]	Diam: 1.000 [m]	Diam: 1.000 [m]	Diam: 1.174 [m]	Diam: 1.256 [m]	Diam: 1.565 [m]
Adv.R: 0.348	Adv.R: 0.329	Adv.R: 0.793	Adv.R: 0.329	Adv.R: 0.307	Adv.R: 0.795
Solidity: 0.509	Solidity: 0.509	Solidity: 0.457	Solidity: 0.434	Solidity: 0.406	Solidity: 0.447

Figure 6.15: Optimum Engines of EVE V3

The optimisation results in a diameter of 1.174 [m] for the Upward Engine situated before the C.G. and a diameter of 1.256 [m] for the Upward Engine situated after the C.G. In addition, the Forward Engine has a diameter of 1.565 [m].

Regarding the engines, the program also outputs the solidity and advance ratios of each engine. The solidity of a VTOL is a measure of the amount of blade area relative to the total area swept by the rotor. This value is typically expressed as a percentage, and it is an important factor in the design and performance of a VTOL's rotor system.

$$\sigma = \frac{N * c}{\pi * R} \quad (6.1)$$

The Solidity is impacted by the number of blades N , the chord of each blade c and the radius of the propeller, R . A rotor with a high solidity will have more blade area relative to the total area swept by the rotor, while a rotor with a low solidity will have less blade area. In general, a high-solidity rotor will generate more lift, but it will also be less efficient and more susceptible to blade flutter, a potentially dangerous oscillation of the blades. The solidity of the propellers is around 0.45 which is a reasonable value for propellers.

The Advance Ratio is dependent on the true airspeed V_{TAS} , the RPS, Ω , and the radius of the propeller R . During a flight, EVE's propellers pitch constantly adjusts in order to fly at the optimal Advance Ratio. The Advance Ratio is relatively low for the Upward Engines in this case around 0.35 which is mainly due to the low take-off speed of 10 [m/s] and the high number of engines which reduces the RPS of each of the individual engines. The forward engines have a higher advance ratio of 0.795 which reinforces the fact that they are able to operate efficiently throughout the entire flight as highlighted in subsection 6.1.5.

6.3.6. Optimised Battery

The Battery mass is optimised as a result of its maximum energy density, the flight distance and power consumed during the flight. While the battery is drained to zero when optimised for the flight, there is a 20 [%] reserve that is specified in the state of charge line in the limitations text file. This is accounted for in the mass calculation of the battery.

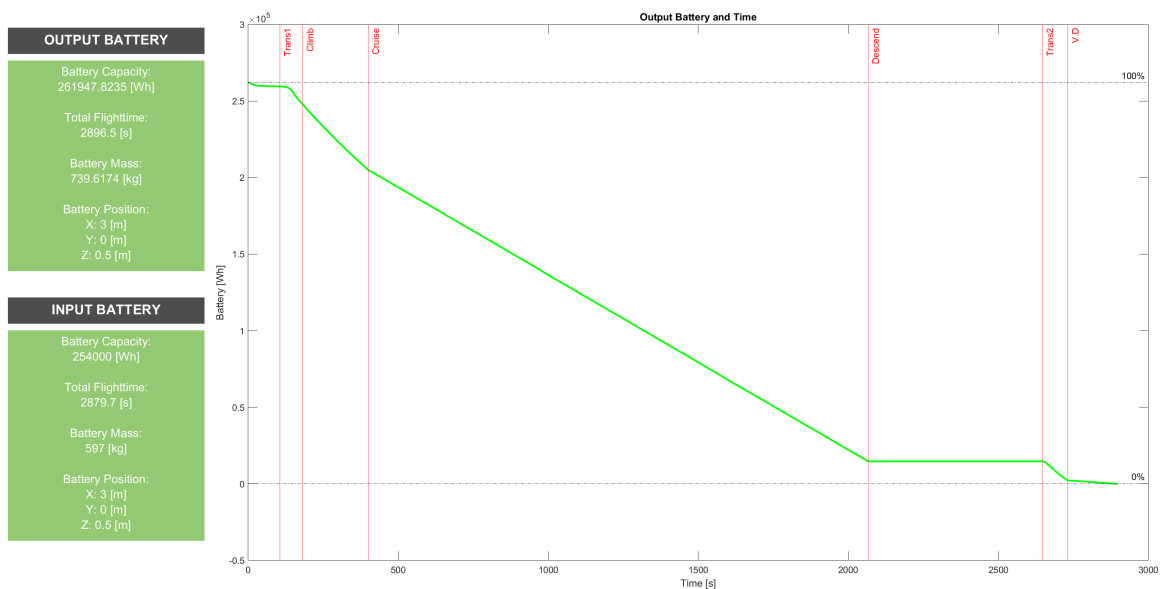


Figure 6.16: Optimum Battery of EVE V3

The final battery for this flight has a mass of 739.62 [kg] and a capacity of 262 [kWh]. This capacity excludes the reserve capacity, so the total capacity of the engine is 314 [kWh] for this specific flight.

6.3.7. Convergence Plots

The convergence plots are interesting as they show the variables changing for each loop. This confirms that the program is able to optimise the aircraft for the given flight parameters, and it was found that 20 iterations would be sufficient for convergence, as each variable would change under 1% from the previous loop.

The program has been tested with many starting mass values and converges every-time. The diameter of the engines is the values that changes the least amount from each iteration.

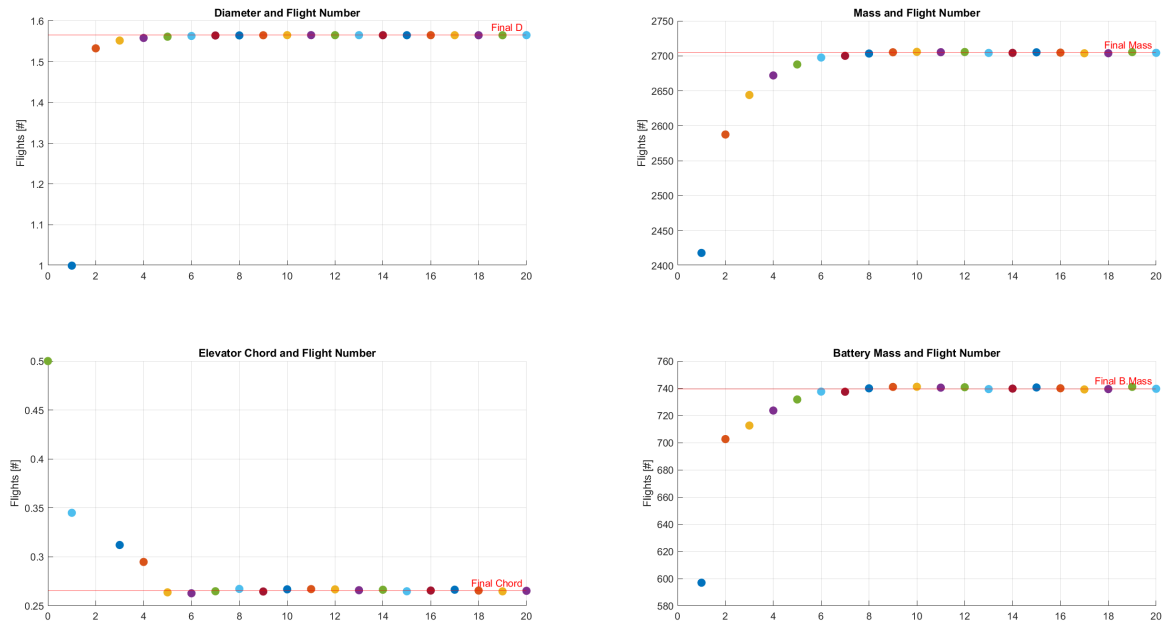


Figure 6.17: Optimum Convergence of EVE V3

Many other variables that are not shown in the convergence plot vary each for each new flight. This includes, the masses of the subcomponents, the centre of gravity location, the moments of inertia among others. The converged values for EVE V3 can be summarised in the following table:

Table 6.5: Final Values for EVE V3, 1

Name	Value	Unit
Center of Gravity		
Location of C.G., X	6.27	[m]
Location of C.G., Y	0	[m]
Location of C.G., Z	1.59	[m]
Moment of Inertia		
Moment of Inertia, X	25783	[kg.m ²]
Moment of Inertia, Y	45396	[kg.m ²]
Moment of Inertia, Z	69302	[kg.m ²]
Control Surfaces		
Elevator Chord	0.272	[m]
Rudder Chord	0.311	[m]
HS Aileron Chord	0.079	[m]
LS Aileron Chord	0.289	[m]

Table 6.6: Final Values for EVE V3, 2

Name	Value	Unit
Engines		
Upward Engine Diameter A	1.174	[m]
Upward Engine Diameter B	1.256	[m]
Forward Engine Diameter A	1.565	[m]
Battery		
Battery Capacity	314	[kWh]

6.4. Range Effects

When comparing the data of multiple different optimised flights with different ranges, it is apparent that the mass of the aircraft increase with increasing range. This is due to the fact that the battery needs to be bigger in order to have enough capacity to power the aircraft through the entire flight. This increase in battery mass also increases the mass of each component in the Class II weight estimation, as the wings and stabilisers for example have a mass term in their respective equations. Also, the engines need to be bigger to accommodate the extra weight of the aircraft. They are sized through the maximum power in the flight, which is also increased with a longer flight as the aircraft is heavier and consequently needs more thrust.

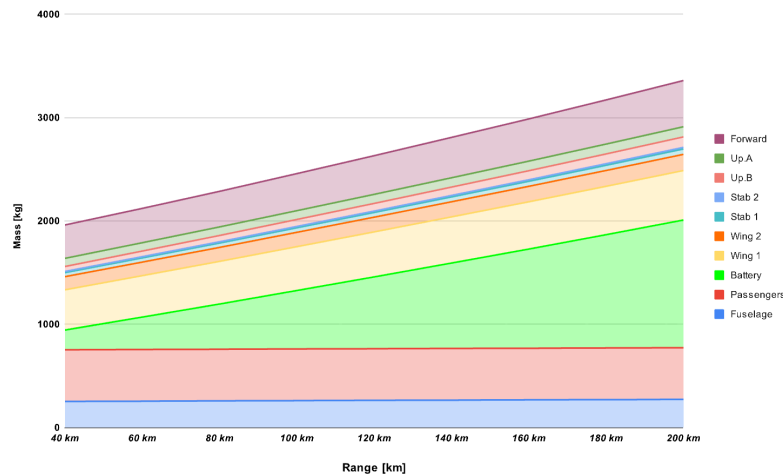


Figure 6.18: Mass and Range of EVE V3

It is also interesting to notice that the before and after upward engines masses change in different ways as the centre of gravity shifts forward due to the heavier battery with increasing flight range. As a result, the moment arm of the before C.G. upward engines is reduced, leading to an increase in the diameter of those engines. Consequently, this diameter increases faster than the diameter of the after C.G. upward engines. This table highlights the changes in mass with different flight ranges for the EVE V3 aircraft.

Table 6.7: Mass values for different flight ranges

Parameters	100km	140km	% Change	180km	% Change
Fuselage	260.948	265.858	1.88%	270.431	3.63%
Passengers	500	500	0.00%	500	0.00%
Battery	565.56	826.551	46.15%	1096.481	93.88%
Wing 1	424.42	446.8	5.27%	468.31	10.34%
Wing 2	138.92	146.25	5.28%	153.29	10.34%
Stab 1	43.6	46.92	7.61%	50.18	15.09%
Stab 2	13.45	14.47	7.58%	15.48	15.09%
Up 1	16.83	20.18	19.90%	23.59	40.17%
Up 2	16.83	20.18	19.90%	23.59	40.17%
Up 3	16.83	20.18	19.90%	23.59	40.17%
Up 4	16.83	20.18	19.90%	23.59	40.17%
Up 5	21.28	22.55	5.97%	23.89	12.27%
Up 6	21.28	22.55	5.97%	23.89	12.27%
Up 7	21.28	22.55	5.97%	23.89	12.27%
Up 8	21.28	22.55	5.97%	23.89	12.27%
For 1	179.41	195.48	8.96%	213.64	19.08%
For 2	179.41	195.48	8.96%	213.64	19.08%
TOTAL	2458.158	2808.729	14.26%	3171.372	29.01%

It can be concluded that the main components that increase in mass are the battery and the engines as the aircraft flies further. The program does not change the wing parameters, so its mass only increases slightly. In the future, the program could modify and optimise the wing parameters such as wing span, surface area and taper ratio for example, this is discussed in chapter 7.

Regarding the Engine diameters, they increase with increasing range as the area of the engines needs to increase in order to move the heavier aircraft. Since the RPS of the engines is bounded, the only way to produce more thrust is by increasing the engine size (see Appendix D for all range values).

7

Conclusion

To conclude, this thesis consists in making a flight dynamics model for Lift + Cruise aircraft in MATLAB. This is done by taking as example the EVE V3 aircraft made by Embraer. This VTOL is of the Lift + Cruise type and has 8 upwards engines and 2 forward engines. Its range is 100 [km] and it has a cruise speed of 200 [km/h]. The aircraft has an operational empty weight of 1500 [kg] and can transport 4 passengers and 1 pilot.

This study successfully demonstrates the capability to assess various flight scenarios and conduct a full eVTOL flight that includes Vertical Take-Off, Transition, Climb, Cruise, Descent, Transition 2 and Vertical Descent. The program is heavily modifiable, a gives the preliminary design engineers enough room to modify and improve the eVTOL. In addition, the program is also a good basis for further modification to the flight model that will increase its accuracy.

In this thesis, the program is able to optimise any Lift + Cruise eVTOL input aircraft, given it is within the design limits of the program. The program is able to accommodate up to 12 upward facing engines, 6 forward engines, 2 wings and 2 stabilisers. Regarding the flight dynamics, the program is able to fly to up to 6 waypoints before landing at its target destination. After each flight, the optimisation of the aircraft is done in which new masses, engine diameter and control surfaces are determined for the next flight. After iteration, the program outputs the optimal aircraft for the specific requirement inputs. These inputs are in the form of three text files: one for the parameters of the aircraft, one for the determination of the flightpath which includes the target coordinates and the waypoint coordinates and one file for the limitations of the control surfaces deflections and the engine limitations. These limits are used by the program to optimise the aircraft after each flight. In addition, this thesis enables the user to estimate the correct battery capacity and mass for the given aircraft and flight scenario. This program is heavily modifiable and many aircraft and flights can be tested.

Furthermore, the simulation-based approach has significantly reduced the need for costly and time-consuming physical prototyping and testing, making it a cost-effective and efficient tool for the early stages of eVTOL aircraft development. By allowing for rapid iteration and optimization of the design, flight dynamics simulation will accelerate the design process and will ultimately contribute to the realization of more advanced and capable eVTOL aircraft.

In conclusion, this flight dynamics simulation and optimisation in MATLAB has proven to be a key tool for the preliminary design of Lift + Cruise eVTOL aircraft. Its ability to simulate and analyse complex aerodynamic behaviour, optimize design parameters and speed up the design process makes it an indispensable asset for engineers and designers seeking efficient, safe and high-performance eVTOL aircraft. As the field of electric aviation continues to grow, flight dynamics simulation will undoubtedly play an even more important role in shaping the future of eVTOL technology.

Recommendations

This part of the report covers the recommendations and future improvements that will improve the accuracy of the MATLAB model.

Matlab Structure

For any new user that wants to improve the flight dynamics program, it is important to know how the MATLAB program is structured. The runfile is the master file of the program and is also the only file that is run in order to launch an optimisation. The Input folder is the folder used by the user to select the settings of the flight. This input folder holds two text files: the Limitations text file used by the optimisation part of the MATLAB code and the Flightpath text file used by the program to simulate the entire flight. In addition to these two text files there is a "Plane" folder in which there are many different eVTOL aircraft. When creating a new aircraft that needs to be run by the program, the user can simply copy a text file from another aircraft and modify it. The name needs to be added to the index text file in order for MATLAB to recognise the new text file.

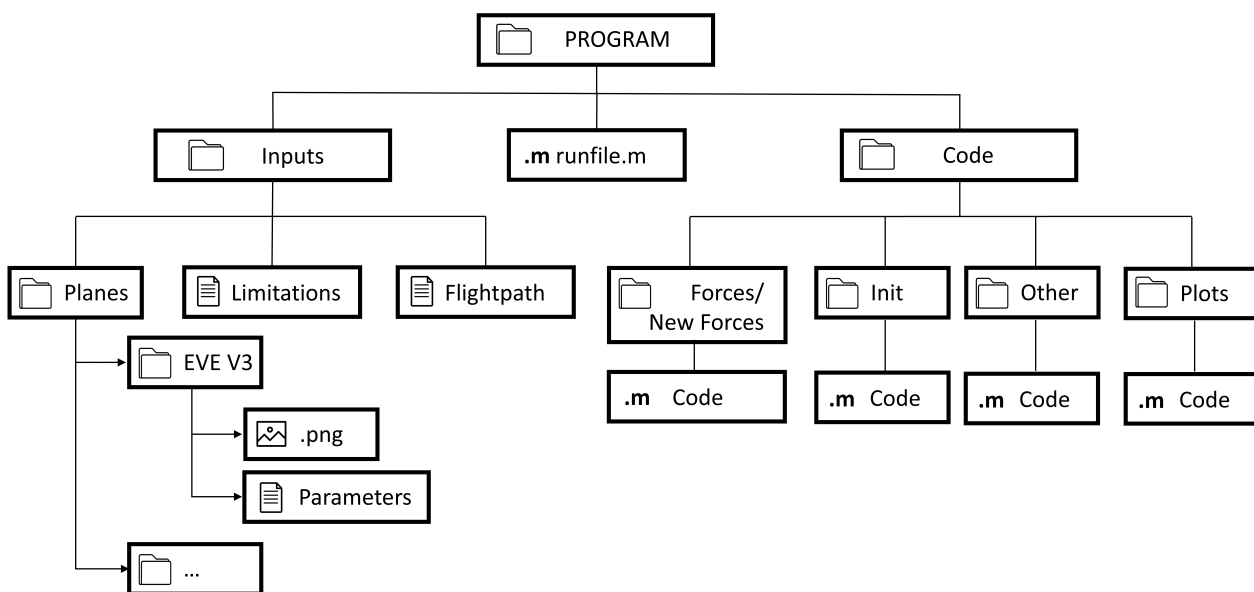


Figure 7.1: MATLAB program file structure

Regarding the "Code" folder in which the entire code is placed, the code is organised in multiple categories. The "Plot" folder holds all the plot code and the "Init" folder holds the initialisation part, checks part, and the preliminary calculations code of the MATLAB program. An important MATLAB code file is the "loading.m" file which is located in the "Init" folder, this file loads all the aircraft parameters in MATLAB and also loads the limitations and flightpath text file. Also, the "Other" folder is used for smaller scripts that track data, or perform some extra optional calculations for the MATLAB program. At last, the "Forces" and "New Forces" folders hold the flight loop force calculations for the: Flight Conditions ("flightconditions.m"), Lift and Drag of the lifting surfaces ("wingforces.m"), the Fuselage Drag ("fuselageforces.m"), the Upward Engine forces ("upwardforces.m") and the Forward Engine forces ("forwardforces.m"). The same applies for the "New Forces" folder which is used by the control surface module of the program.

The "Output" folder is the folder in which the plots (performance and optimization plots) are stored. There is also a command window log text file in which all the accelerations, velocities, and positions of

the aircraft at each phase are listed.

The runfile itself is structured in the following order. For each new flight the j variable increases by one until it reaches, j_{max} which is a variable at the top of the code that the user can change in order to change the number of total flight the program performs for the optimization. In addition, the variable i is the time step counter in the flight loop. This counter is reset for each new flight and the time step in this MATLAB program is $\Delta t = 0.1$ [s]. This time step value is the variable dt which is found in the "init.m" file.

Future Improvements

The MATLAB program is a solid basis for the preliminary design of a Lift + Cruise eVTOL aircraft. However, it does have some limitations due to the relatively limited time spent on such a big project. Here are a few recommendations for further improvement of both the accuracy and the scalability of the MATLAB program:

- **Modelling of the incoming flow for the Engines:** Using Blade Element Theory, the program's accuracy in the engine section could be improved. For now, the pitch of the propellers change in order to have the best engine efficiency possible. However, during transitions, the assumption is made that the advance ratio still gives optimal efficiency while that is not the case since the aircraft is moving forwards only. Regarding the forward engines, they operate at optimal advance ratio (with adaptive pitch) throughout the entire flight.
- **Improvements to Sideslip model:** More accurate sideslip forces and coefficients can be introduced to the program. This would include a Lift force from the sideslip angle and a different angle of attack for each side of the wing during roll. Each side of each lifting surface is an independent force in the program, so this could easily be implemented.
- **More freedom in the amount of parameters:** The program could be upgraded in order to allow more engines and even more wings and stabilisers. In addition to lifting surfaces, the empennage connection's drag could also be modelled, as well as any other non-wing surface of the aircraft.
- **Non-Linear control systems:** PID controllers could be used in order to more accurately model the turns and pitch manoeuvres. This would also increase the accuracy of the sizing of the control surfaces. As of now, since the control loop is relatively simple, the moment equations are linearised.
- **Pitch, Yaw and Roll control in Vertical Flight:** In the current version of the MATLAB program, the aircraft is only able to move in the z-direction during Vertical Take-Off and Vertical Descent. The program could be improved in order for then aircraft to be able to pitch and roll during these phases and navigate to a safer and better place for the start of Transition 1.
- **Wind modelling:** Wind forces in x,y,z can be added during the flight in order to model the effect of headwind and tailwind and what the impact is on the battery size of the aircraft as well as on the overall mass of the eVTOL. The Wind could be modelled as a constant wind force or as random gusts that occur during the flight.
- **Improved Turning and Bank angles:** As of now, the aircraft uses the moment of inertia around the x-axis in order to be able to bank the aircraft for the turn to the next waypoints in uncoordinated turns. However, this bank angle is currently limited to 20 degrees, as the sideslip becomes too large after that in an uncoordinated turn. The ailerons could be sized more accurately with a new roll controller, that works with the rudder in order to have zero sideslip during turns. At last, the waypoints could be replaced by no-fly zones that are in the shape of circles in the sky that the aircraft automatically avoids in order to get to its destination.
- **Fuselage drag forces:** The Fuselage drag coefficients' accuracy could be improved with real-life data or other data sources. In addition, the location where the forces are applied could change as a function of the flightpath, creating a moment due to the fuselage drag.
- **Incidence angle for the Wing:** In order to give the eVTOL designer more freedom, an incidence angle for each wing and stabiliser could be introduced. For now, this incidence angle could artificially be added with a different zero angle of attack lift coefficient. Also, the lift slope can be more detailed in the future as the program moves away from the Prandtl's Classic Lifting-Line Theory [25].

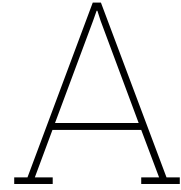
- **Possibility to change the angle of Forward and Upward engines:** For now, the forward engines' propellers are perpendicular to the fuselage and the upward engines' propellers are parallel. The aircraft input text file can be modified in the future in order to be able to introduce certain engines at different angles. For example, the Airbus NextGEN's forward propellers are slightly pitched up, this is not modelled in the current MATLAB program.
- **Expansion to other eVTOL categories:** At last, the program could be upgraded in order to accommodate all eVTOLs and the program would be able to make Multicopters fly as well as Vectored Thrust aircraft. The transitions of the latter category will be more difficult, but with the possibility to pitch in vertical flight and to model the incoming airflow angles to the propellers, the accuracy of the transitions could greatly be improved.
- **Optimization of Wing Parameters:** Wing parameters could be modified from flight to flight in order to accommodate the changes in mass of the aircraft. While not the focus of this thesis, the wings and stabilisers surfaces are a critical part of the eVTOL as they are active in five out of seven phases of flight. The program could, in the future, optimise the wing span, surface area and taper ratio for example.

References

- [1] Department of Economic United Nations and Social Affairs. "2022 revision of the World Urbanization Prospects". In: *United Nations 1.1* (2022), pp. -.
- [2] Lockheed Martin. *F-35 Lightning II*. 2022. URL: <https://www.lockheedmartin.com/en-us/products/f-35/f-35-about.html> (visited on 11/27/2022).
- [3] Boeing. *V-22 Osprey*. 2022. URL: <https://www.boeing.com/defense/v-22-osprey/> (visited on 11/27/2022).
- [4] BusinessWire. *Global Electric VTOL Aircraft Market Report 2022: Increasing Road Traffic Congestion in Urban Areas Driving Growth*. 2022. URL: <https://www.businesswire.com/news/home/20221104005427/en/Global-Electric-VTOL-Aircraft-Market-Report-2022-Increasing-Road-Traffic-Congestion-in-Urban-Areas-Driving-Growth---ResearchAndMarkets.com> (visited on 01/06/2023).
- [5] Saba Al-Rubaye, Antonios Tsourdos, and Kamesh Namuduri. "Advanced Air Mobility Operation and Infrastructure for Sustainable Connected eVTOL Vehicle". In: *Drones 7.5* (2023). ISSN: 2504-446X. DOI: 10.3390/drones7050319. URL: <https://www.mdpi.com/2504-446X/7/5/319>.
- [6] NASA. *WHAT IS AAM?* 2020. URL: https://www.nasa.gov/sites/default/files/atoms/files/what-is-aam-student-guide_0.pdf (visited on 11/27/2022).
- [7] *Volocopter 2X's aircraft specifications from the EVTOL journal*. URL: <https://evtol.news/volocopter-2x>.
- [8] *Hoversurf Scorpion 3's aircraft specifications from the EVTOL journal*. URL: <https://evtol.news/hoversurf-scorpion>.
- [9] *Joby S4's aircraft specifications from the EVTOL journal*. URL: <https://evtol.news/joby-s4>.
- [10] *AIR AIR ONE's aircraft specifications from the EVTOL journal*. URL: <https://evtol.news/air-one>.
- [11] AIR AIR ONE. *AIR AIR ONE information website*. 2021. URL: <https://www.airev.aero/air-one> (visited on 11/24/2022).
- [12] *Hover test AIR AIR ONE*. URL: <https://www.youtube.com/watch?v=2IdgzSnsW0Y&t=8s>.
- [13] *Airbus CityAirbus Nextgen's aircraft specifications from the EVTOL journal*. URL: <https://evtol.news/airbus-cityairbus-nextgen>.
- [14] Future Flight. *AIRBUS BUILDS TEST CENTER TO WORK ON CITYAIRBUS NEXTGEN EVTOL AIRCRAFT*. 2022. URL: <https://www.futureflight.aero/news-article/2022-07-28/airbus-builds-test-center-work-cityairbus-nextgen-evtol-aircraft> (visited on 11/28/2022).
- [15] *VoloRegion's aircraft specifications from the EVTOL journal*. URL: <https://evtol.news/volocopter-voloconnect>.
- [16] Mundo Geo. *VoloConnect: Volocopter's 4-Seater eVTOL Takes Maiden Flight*. 2022. URL: <https://www.jobyaviation.com/news/joby-revolutionary-low-noise-footprint-nasa-testing/> (visited on 11/27/2022).
- [17] VFS Staff. <https://evtol.news/news/supporting-the-electric-vtol-revolution>. 2020. URL: <https://evtol.news/news/supporting-the-electric-vtol-revolution> (visited on 03/16/2023).
- [18] *Airbus CityAirbus's aircraft specifications from the EVTOL journal*. URL: <https://evtol.news/airbus-helicopters>.
- [19] *Midnight's aircraft specifications from the EVTOL journal*. URL: <https://evtol.news/archer/>.
- [20] *VX-4's aircraft specifications from the EVTOL journal*. URL: <https://evtol.news/vertical-aerospace-va-1x>.

- [21] *Eve V3's aircraft specifications from the EVTOL journal*. URL: <https://evtol.news/embraer/>.
- [22] Stan Hall. *How Big The Tail*. 1th ed. Technical Advisor, Engineering, EAA Chapter 62: EAA, 2000.
- [23] A.I. Kibzun et al. "Statistical Analysis Module for Weight Design of Aircraft Elements". In: 13 (Jan. 2020), pp. 29–42. DOI: 10.14529/mmp200303.
- [24] D. Scholtz. "Empennage sizing with the tail volume complemented with a method for dorsal fin layout". In: *Hamburg University of Applied Sciences 1* (Oct. 2009), p. 13.
- [25] W. Phillips and Deryl Snyder. "Modern Adaptation of Prandtl's Classic Lifting-Line Theory". In: *Journal of Aircraft - J AIRCRAFT 37* (July 2000), pp. 662–670. DOI: 10.2514/2.2649.
- [26] Nicholas Landell-Mills. "Calculation of the downwash generated by a wing." In: *Journal of Aeronautics Aerospace Engineering 06* (Jan. 2017). DOI: 10.4172/2168-9792.1000204.
- [27] Mohammed Abdulla. "Prediction of Wing Downwash Using CFD". In: *INCAS Bulletin 7* (June 2015), pp. 6–07. DOI: 10.13111/2066-8201.2015.7.2.10.
- [28] Kenneth D. Korkan, Jose Camba, and Patrick M. Morris. "Aerodynamic data banks for Clark-Y, NACA 4-digit and NACA 16-series airfoil families". In: 1986.
- [29] Daniel Raymer. *Aircraft Design: A Conceptual Approach, Sixth Edition*. Sept. 2018. ISBN: 978-1-62410-490-9. DOI: 10.2514/4.104909.
- [30] M. Niță and D. Scholz. *Estimating the Oswald Factor from Basic Aircraft Geometrical Parameters*. Deutsche Gesellschaft für Luft- und Raumfahrt - Lilienthal-Oberth e.V., 2012. URL: <https://books.google.jo/books?id=229fuwECAAJ>.
- [31] Marinlena Pavel. *Helicopter Master course*. 2021. URL: www.brightspace.com (visited on 01/13/2023).
- [32] Matthew Warren et al. "Effects of Range Requirements and Battery Technology on Electric VTOL Sizing and Operational Performance". In: Jan. 2019. DOI: 10.2514/6.2019-0527.
- [33] Yu Miao et al. "Current Li-Ion Battery Technologies in Electric Vehicles and Opportunities for Advancements". In: *Energies 12.6* (2019). ISSN: 1996-1073. DOI: 10.3390/en12061074. URL: <https://www.mdpi.com/1996-1073/12/6/1074>.
- [34] The Economist. *The growth of lithium-ion battery power*. 2017. URL: <https://www.economist.com/graphic-detail/2017/08/14/the-growth-of-lithium-ion-battery-power> (visited on 01/25/2023).
- [35] Ole Bergmann et al. "Comparison and evaluation of blade element methods against RANS simulations and test data". In: *CEAS Aeronautical Journal 13.2* (Apr. 2022), pp. 535–557. ISSN: 1869-5590. DOI: 10.1007/s13272-022-00579-1. URL: <https://doi.org/10.1007/s13272-022-00579-1>.
- [36] Osita Ugwueze et al. "An Efficient and Robust Sizing Method for eVTOL Aircraft Configurations in Conceptual Design". In: *Aerospace 10.3* (2023). ISSN: 2226-4310. DOI: 10.3390/aerospace10030311. URL: <https://www.mdpi.com/2226-4310/10/3/311>.
- [37] EMRAX. *EMRAX Electric Motors/Generators*. 2023. URL: <https://emrax.com/e-motors/> (visited on 04/25/2023).
- [38] MAGicALL. *Industry-Leading Electric Propulsion Systems*. 2023. URL: <https://www.magnix.aero/services> (visited on 04/25/2023).
- [39] Siemens eAircraft. *Disrupting the Way You Will Fly!* 2023. URL: <https://www.ie-net.be/sites/default/files/Siemens%5C%20%20eAircraft%5C%20-%5C%20Disrupting%5C%20Aircraft%5C%20Propulsion%5C%20-%5C%2000%5C%20JH%5C%20TH0%5C%20-%5C%20180427.cleaned.pdf> (visited on 04/25/2023).
- [40] Jan Roskam. *Airplane Design—Part V: Component Weight Estimation; Design, Analysis and Research*. Sept. 1997, p. 201. ISBN: 978-1-62410-490-9. DOI: 10.2514/4.104909.
- [41] Egbert Torenbeek. *Synthesis of Subsonic Airplane Design: First Edition*. Sept. 1982, p. 201. ISBN: 978-1-62410-490-9. DOI: 10.2514/4.104909.
- [42] Zhongyun Fan, Zhou Zhou, and Xiaoping Zhu. "Development and Analysis of Variable Pitch Propeller with Aerodynamic Stable Blades". In: *Journal of Aircraft 58.2* (2021), pp. 216–227. DOI: 10.2514/1.C035832.

- [43] Xinglu Xia et al. "Blade Shape Optimization and Analysis of a Propeller for VTOL Based on an Inverse Method". In: *Applied Sciences* 12 (Apr. 2022), p. 3694. DOI: 10.3390/app12073694.
- [44] Dr. Jan Roskam. *Airplane Design Part V: Component Weight Estimation*. 5th ed. DAR Corporation, 2020.
- [45] JSBSim Open Source Flight Dynamics Model. *Moment of Inertia Metrics for various aircraft*. 2021. URL: <https://jsbsim.sourceforge.net/MassProps.html> (visited on 03/18/2023).
- [46] Deepak Paul Tirkey. *Helicopter Moment of Inertia estimation*. 2021. URL: <https://www.slideshare.net/deepakpaultirkey/helicopter-moment-of-inertia> (visited on 03/17/2023).
- [47] Mustafa Cavcar. "The International Standard Atmosphere (ISA)". In: *School of Civil Aviation 7* (Jan. 2000), pp. 6–07.
- [48] Federal Aviation Administration. *FAA-H-8083-25A Pilot's Handbook of Aeronautical Knowledge*. 1st ed. Washington, DC: U.S. Department of Transportation, 2008.
- [49] Antonio Kieling. "The Study and Analysis of Using Wing Dihedral on the Side of an Aircraft's Static Stability". In: *Proceedings of the World Congress on Engineering 2015 Volume II* (July 2015), p. 1296.
- [50] Michael V. Cook. "Chapter 13 - Aerodynamic Stability and Control Derivatives". In: *Flight Dynamics Principles (Third Edition)*. Ed. by Michael V. Cook. Third Edition. Butterworth-Heinemann, 2013, pp. 371–439. ISBN: 978-0-08-098242-7. DOI: <https://doi.org/10.1016/B978-0-08-098242-7.00013-4>. URL: <https://www.sciencedirect.com/science/article/pii/B9780080982427000134>.
- [51] Snorri Gudmundsson. "Chapter 9 - The Anatomy of the Wing". In: *General Aviation Aircraft Design*. Ed. by Snorri Gudmundsson. Boston: Butterworth-Heinemann, 2014, pp. 299–399. ISBN: 978-0-12-397308-5. DOI: <https://doi.org/10.1016/B978-0-12-397308-5.00009-X>. URL: <https://www.sciencedirect.com/science/article/pii/B978012397308500009X>.
- [52] Omran al-shamma, Rashid Ali, and Haitham Hasan. "An instructive algorithm for aircraft elevator sizing to be used in preliminary aircraft design software". In: *Istrazivanja i projektovanja za privredu* 15 (Jan. 2017), pp. 489–494. DOI: 10.5937/jaes15-14829.
- [53] Jiawei Yu et al. "Study of Propeller Vortex Characteristics under Loading Conditions". In: *Symmetry* 15.2 (2023). ISSN: 2073-8994. DOI: 10.3390/sym15020445. URL: <https://www.mdpi.com/2073-8994/15/2/445>.
- [54] Nicholas Landell-Mills. *Propeller thrust explained by Newtonian physics*. Apr. 2021.
- [55] Robert Stengel. *Aircraft Equations of Motion: Flight Path Computation*. 2021. URL: <http://www.stengel.mycpanel.princeton.edu/MAE331Lecture11.pdf> (visited on 03/17/2023).
- [56] Ir. Paul Roling (Dr.Ir. Mark Voskuil). *AE2230-I Flight Orbital Mechanics, Handout 1: Stability*. 2021. URL: www.brightspace.com (visited on 03/18/2023).
- [57] Michael A. Konyak (Federal Aviation Administration) Mark Peters. *The Engineering Analysis and Design of the Aircraft Dynamics Model For the FAA Target Generation Facility*. 1st ed. Atlantic City, NJ: U.S. Department of Transportation, 2012.
- [58] James D. Phillips. "Approximate neutral point of a subsonic canard aircraft". In: 1985.
- [59] Illinois Institute of Technology Matthew M. Peet. *Spacecraft and Aircraft Dynamics, Lecture 6*. 2021. URL: <http://control.asu.edu/Classes/MMAE441/Aircraft/441Lecture6.pdf> (visited on 03/20/2023).
- [60] F.G. IRVING. "CHAPTER 7 - Flight Tests to Measure Static Stability". In: *An Introduction to the Longitudinal Static Stability of Low-Speed Aircraft*. Ed. by F.G. IRVING. Pergamon, 1966, pp. 71–81. ISBN: 978-1-4832-0019-4. DOI: <https://doi.org/10.1016/B978-1-4832-0019-4.50011-9>. URL: <https://www.sciencedirect.com/science/article/pii/B9781483200194500119>.
- [61] National Aeronautics and Space Administration. *Forces in a Climb (Conventional aircraft)*. 2001. URL: <https://www.grc.nasa.gov/www/k-12/VirtualAero/BottleRocket/airplane/climb.html> (visited on 03/17/2023).



EVE V3 Parameter text file

```
Parameter, Value, Unit
#-----
# Notes: The Coordinate system is centered at 0,0,0 on the front, at the
bottom and in the middle of the fuselage. If the rotors of the aircraft
can rotate please use the upwards engines and not the forward engines.
If there is a V-Tail, use Stabilizer 1.
#-----
# General Data
#-----
Mass, 2337, kg
Design Cruise Velocity, 200, km/h
Design Range, 100, km
Number of Passengers, 5, -
Number of Wings, 2, -
Number of Stabilizers, 2, -

Wing 1 Surface Area, 48, m2
Wing 1 Wing Span, 24, m
Wing 1 SweepLE, 0, deg
Wing 1 Taper Ratio, 1, -
Wing 1 Zero-Lift Drag Coefficient, 0.03, -
Wing 1 Oswald Efficiency factor, 0.75, -
Wing 1 DeDa, 0, -
Wing 1 Dihedral Angle, 0, deg
Wing 1 Cl0 of Airfoil, 0.15, -
Wing 1 Cm0 of Airfoil, 0.18, -
Wing 1 t/c max, 0.1, %
Wing 1 stall min, -15, deg
Wing 1 stall max, 15, deg
LS Aileron Chord Length, 0.3, m
LS Aileron Start %b/2, 0.5, %
LS Aileron Stop %b/2, 0.9, %
HS Aileron Chord Length, 0.3, m
HS Aileron Start %b/2, 0.2, %
HS Aileron Stop %b/2, 0.4, %

Wing 2 Surface Area, 28, m2
Wing 2 Wing Span, 14, m
Wing 2 SweepLE, 0, deg
Wing 2 Taper Ratio, 1, -
```

Wing 2 Zero-Lift Drag Coefficient, 0.03, -
Wing 2 Oswald Efficiency factor, 0.75, -
Wing 2 DeDa, 0, -
Wing 2 Dihedral Angle, 0, deg
Wing 2 Cl0 of Airfoil, 0.15, -
Wing 2 Cm0 of Airfoil, 0.18, -
Wing 2 t/c max, 0.1, %
Wing 2 stall min, -15, deg
Wing 2 stall max, 15, deg

Stab 1 Surface Area, 9.46, m²
Stab 1 Wing Span, 6, m
Stab 1 SweepLE, 20, deg
Stab 1 Taper Ratio, 0.5, -
Stab 1 Zero-Lift Drag Coefficient, 0.03, -
Stab 1 Oswald Efficiency factor, 0.75, -
Stab 1 DeDa, 0.1, -
Stab 1 Dihedral Angle, 55.44, deg
Stab 1 Offset in Y, 0, m
Stab 1 Cl0 of Airfoil, 0, -
Stab 1 Cm0 of Airfoil, 0.18, -
Stab 1 t/c max, 0.1, %
Stab 1 stall min, -15, deg
Stab 1 stall max, 15, deg
Elevator Chord Length, 0.5, m

Stab 2 Surface Area, 4.8, m²
Stab 2 Wing Span, 2.6, m
Stab 2 SweepLE, 20, deg
Stab 2 Taper Ratio, 0.5, -
Stab 2 Zero-Lift Drag Coefficient, 0.03, -
Stab 2 Oswald Efficiency factor, 0.75, -
Stab 2 DeDa, 0.1, -
Stab 2 Dihedral Angle, -90, deg
Stab 2 Offset in Y, 0, m
Stab 2 Cl0 of Airfoil, 0, -
Stab 2 Cm0 of Airfoil, 0, -
Stab 2 t/c max, 0.1, %
Stab 2 stall min, -15, deg
Stab 2 stall max, 15, deg
Rudder Chord Length, 0.5, m

Empennage Connection Width, 0.6, m
Empennage Connection Height, 0.6, m

Number of Upward Engines, 8, -
Diameter Upward Engines, 1, m
Thrust Coefficient Upward Engines, 0.8, -
Number of Blades Upward Engines, 5, -
Average Blade Chord Upward Engines, 0.16, m

Number of Forward Engines, 2, -
Diameter Forward Engines, 1, m
Thrust Coefficient Forward Engines, 0.8, -
Number of Blades Forward Engines, 5, -
Average Blade Chord Forward Engines, 0.22, m

Fuselage Upward Drag Coefficient, 0.8, -
Fuselage Forward Drag Coefficient, 0.245, -
Fuselage Length X, 11, m
Fuselage Width Y, 3, m
Fuselage Height Z, 2.5, m

Battery, 254000, Wh
Battery Length X, 1, m
Battery Width Y, 1, m
Battery Height Z, 0.5, m

Location of Battery X, 3, m
Location of Battery Y, 0, m
Location of Battery Z, 0.5, m

Location of Passengers X, 4.5, m
Location of Passengers Y, 0, m
Location of Passengers Z, 1.25, m

Location of Wing 1 X, 10, m
Location of Wing 1 Y, 0, m
Location of Wing 1 Z, 2.5, m

Location of Wing 2 X, 2, m
Location of Wing 2 Y, 0, m
Location of Wing 2 Z, 2.5, m

Location of Stab 1 X, 19, m
Location of Stab 1 Y, 0, m
Location of Stab 1 Z, 2.5, m

Location of Stab 2 X, 19, m
Location of Stab 2 Y, 0, m
Location of Stab 2 Z, 2.5, m

Location of Upward T1 X, -1, m
Location of Upward T1 Y, -7, m
Location of Upward T1 Z, 2.5, m

Location of Upward T2 X, 5, m
Location of Upward T2 Y, -7, m
Location of Upward T2 Z, 2.5, m

Location of Upward T3 X, -1, m
Location of Upward T3 Y, 7, m
Location of Upward T3 Z, 2.5, m

Location of Upward T4 X, 5, m
Location of Upward T4 Y, 7, m
Location of Upward T4 Z, 2.5, m

Location of Upward T5 X, 7, m
Location of Upward T5 Y, -12, m
Location of Upward T5 Z, 2.5, m

Location of Upward T6 X, 13, m
Location of Upward T6 Y, -12, m
Location of Upward T6 Z, 2.5, m

Location of Upward T7 X, 7, m
Location of Upward T7 Y, 12, m
Location of Upward T7 Z, 2.5, m

Location of Upward T8 X, 13, m
Location of Upward T8 Y, 12, m
Location of Upward T8 Z, 2.5, m

Location of Upward T9 X, 0, m
Location of Upward T9 Y, 0, m
Location of Upward T9 Z, 0, m

Location of Upward T10 X, 0, m
Location of Upward T10 Y, 0, m
Location of Upward T10 Z, 0, m

Location of Upward T11 X, 0, m
Location of Upward T11 Y, 0, m
Location of Upward T11 Z, 0, m

Location of Upward T12 X, 0, m
Location of Upward T12 Y, 0, m
Location of Upward T12 Z, 0, m

Location of Forward Tf1 X, 11, m
Location of Forward Tf1 Y, -6, m
Location of Forward Tf1 Z, 2.5, m

Location of Forward Tf2 X, 11, m
Location of Forward Tf2 Y, 6, m
Location of Forward Tf2 Z, 2.5, m

Location of Forward Tf3 X, 0, m
Location of Forward Tf3 Y, 0, m
Location of Forward Tf3 Z, 0, m

Location of Forward Tf4 X, 0, m
Location of Forward Tf4 Y, 0, m
Location of Forward Tf4 Z, 0, m

Location of Forward Tf5 X, 0, m
Location of Forward Tf5 Y, 0, m
Location of Forward Tf5 Z, 0, m

Location of Forward Tf6 X, 0, m
Location of Forward Tf6 Y, 0, m
Location of Forward Tf6 Z, 0, m

Weight of Fuselage, 259, kg
Weight of Passengers, 500, kg
Weight of Battery, 597, kg
Weight of Wing 1, 414, kg

Weight of Wing 2, 129, kg

Weight of Stab 1, 27, kg

Weight of Stab 2, 51, kg

Weight of an Upward Engine, 29.05, kg

Weight of a Forward Engine, 104.40, kg

B

Limitations text file

```
Parameter, Value, Unit
#-----
# This is the limitations file for the flight dynamics MATLAB program.
#-----
# Limitations
#-----
Upward Engines maximum RPS, 60, RPS
Upward Engine Same Radius, 0, -
Upward Engine Power Margin, 50, %

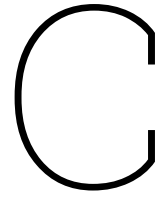
Forward Engines maximum RPS, 60, RPS
Forward Engines Power Margin, 50, %

Aileron minimum deflection, -5, deg
Aileron maximum deflection, 5, deg
Aircraft Roll Rate, 20, deg/s

Elevator minimum deflection, -20, deg
Elevator maximum deflection, 25, deg

Rudder minimum deflection, -20, deg
Rudder maximum deflection, 20, deg

Battery Maximum Energy Density, 500, Wh/kg
Battery Efficiency, 85, %
State of Charge, 20, %
```



Flightpath text file

```
Parameter, Value, Unit
#-----
# Flight Path
#-----
End of flight Coordinates X, 100000, m
End of flight Coordinates Y, 100000, m
#-----
PHASE 1 Vertical Take-Off Velocity, 10, m/s

PHASE 2 Vertical Transition Height, 300, m
PHASE 2 Transition Angle of Attack, 0, deg

PHASE 3 Climb Rate (Vz), 8, m/s
PHASE 3 Climb Velocity (V), 55.66, m/s

PHASE 4 Cruise Altitude, 2000, m
PHASE 4 Cruise Velocity (V), 55.66, m/s

PHASE 7 Vertical Descent Velocity, -2, m/s
#-----
Number of Waypoints, 3, -

Waypoint 1 location X, 40000, m
Waypoint 1 location Y, 20000, m

Waypoint 2 location X, 50000, m
Waypoint 2 location Y, 50000, m

Waypoint 3 location X, 80000, m
Waypoint 3 location Y, 60000, m

Waypoint 4 location X, 0, m
Waypoint 4 location Y, 0, m

Waypoint 5 location X, 0, m
Waypoint 5 location Y, 0, m

Waypoint 6 location X, 0, m
Waypoint 6 location Y, 0, m
```

D

EVE V3 Data

Requirements for the flight of EVE V3: Cruise Altitude of 2000 [m] | Cruise Velocity of 200.376 [km/h] | Range of 127274.4526 [m] | Transition height of 300 [m]

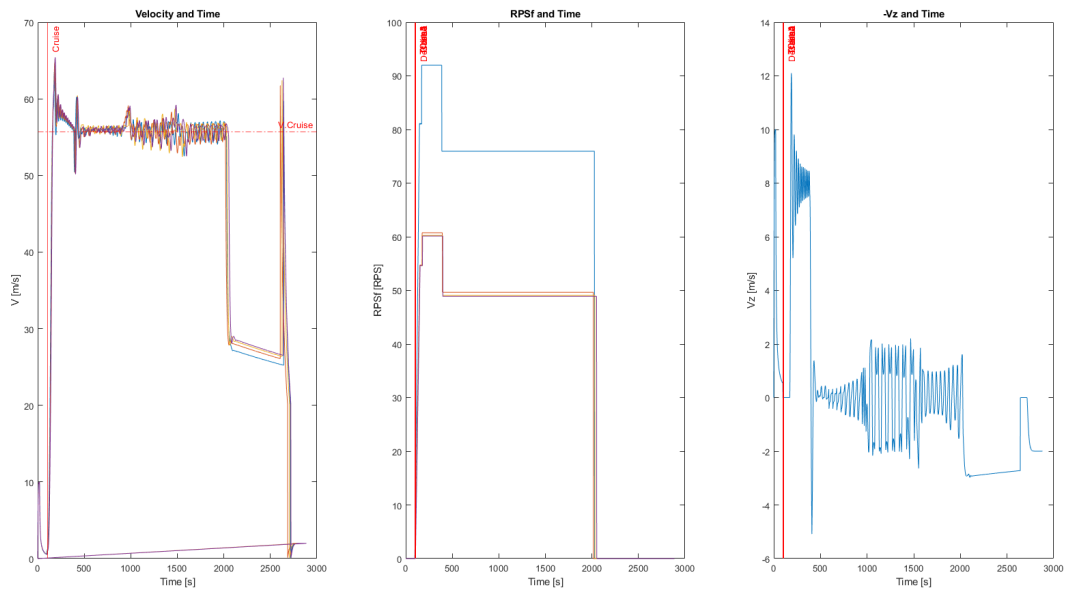


Figure D.1: Velocities/RPS for EVE V3

Table D.2: Engine values for different flight ranges

Engines	100km	140km	% Change	180km	% Change
Up.A	1.108	1.204	8.66%	1.294	16.79%
Up.B	1.234	1.267	2.67%	1.301	5.43%
Front	1.539	1.578	2.53%	1.617	5.07%

Table D.3: Battery values for different flight ranges

Battery	100km	140km	% Change	180km	% Change
Capacity	203000	293736	44.70%	388337	91.30%

Table D.1: Range and Mass Values for EVE V3

Parameters	100km	120km	% Change	140km	% Change	160km	% Change	180km	% Change	200km	% Change
Fuselage	260.948	263.447	0.96%	265.858	1.88%	268.165	2.77%	270.431	3.63%	272.625	4.47%
Passengers	500	500	0.00%	500	0.00%	500	0.00%	500	0.00%	500	0.00%
Battery	565.56	694.742	22.84%	826.551	46.15%	959.556	69.66%	1096.481	93.88%	1236.346	118.61%
Wing 1	424.42	435.72	2.66%	446.8	5.27%	457.57	7.81%	468.31	10.34%	478.86	12.83%
Wing 2	138.92	142.62	2.66%	146.25	5.28%	149.78	7.82%	153.29	10.34%	156.74	12.83%
Stab 1	43.6	45.27	3.83%	46.92	7.61%	48.54	11.33%	50.18	15.09%	51.8	18.81%
Stab 2	13.45	13.96	3.79%	14.47	7.58%	14.97	11.30%	15.48	15.09%	15.98	18.81%
Up 1	16.83	18.49	9.86%	20.18	19.90%	21.87	29.95%	23.59	40.17%	25.31	50.39%
Up 2	16.83	18.49	9.86%	20.18	19.90%	21.87	29.95%	23.59	40.17%	25.31	50.39%
Up 3	16.83	18.49	9.86%	20.18	19.90%	21.87	29.95%	23.59	40.17%	25.31	50.39%
Up 4	16.83	18.49	9.86%	20.18	19.90%	21.87	29.95%	23.59	40.17%	25.31	50.39%
Up 5	21.28	21.9	2.91%	22.55	5.97%	23.21	9.07%	23.89	12.27%	24.57	15.46%
Up 6	21.28	21.9	2.91%	22.55	5.97%	23.21	9.07%	23.89	12.27%	24.57	15.46%
Up 7	21.28	21.9	2.91%	22.55	5.97%	23.21	9.07%	23.89	12.27%	24.57	15.46%
Up 8	21.28	21.9	2.91%	22.55	5.97%	23.21	9.07%	23.89	12.27%	24.57	15.46%
For 1	179.41	187.16	4.32%	195.48	8.96%	204.23	13.83%	213.64	19.08%	223.57	24.61%
For 2	179.41	187.16	4.32%	195.48	8.96%	204.23	13.83%	213.64	19.08%	223.57	24.61%
TOTAL	2458.158	2631.639	7.06%	2808.729	14.26%	2987.361	21.53%	3171.372	29.01%	3359.011	36.65%

E

Other eVTOLS

E.1. Airbus NextGen

E.1.1. Input Parameter File

Parameter, Value, Unit

```
#-----  
# Notes: The Coordinate system is centered at 0,0,0 on the bottom middle  
of the fuselage. If the rotors of the aircraft can rotate please use the  
upwards engines and not the forward engines. If there is a V-Tail, use  
Stabilizer 1.  
#-----  
# General Data  
#-----  
Mass, 3000, kg  
Design Cruise Velocity, 249, km/h  
Range, 160, km  
Number of Passengers, 5, -  
Number of Wings, 1, -  
Number of Stabilizers, 2, -  
  
Wing 1 Surface Area, 55, m2  
Wing 1 Wing Span, 25, m  
Wing 1 SweepLE, 5, deg  
Wing 1 Taper Ratio, 0.6, -  
Wing 1 Zero-Lift Drag Coefficient, 0.03, -  
Wing 1 Oswald Efficiency factor, 0.75, -  
Wing 1 DeDa, 0, -  
Wing 1 Dihedral Angle, 8, deg  
Cl0 of Airfoil 1, 0.2, -  
Cm0 of Airfoil 1, 0.18, -  
Wing 1 t/c max, 0.1, %  
Wing 1 stall min, -15, deg  
Wing 1 stall max, 15, deg  
LS Aileron Chord Length, 0.3, m  
LS Aileron Start %b/2, 0.5, %  
LS Aileron Stop %b/2, 0.9, %  
HS Aileron Chord Length, 0.3, m  
HS Aileron Start %b/2, 0.2, %  
HS Aileron Stop %b/2, 0.4, %  
  
Wing 2 Surface Area, 0, m2
```

Wing 2 Wing Span, 0, m
Wing 2 SweepLE, 0, deg
Wing 2 Taper Ratio, 0, -
Wing 2 Zero-Lift Drag Coefficient, 0, -
Wing 2 Oswald Efficiency factor, 0, -
Wing 2 DeDa, 0, -
Wing 2 Dihedral Angle, 0, deg
Wing 2 Cl0 of Airfoil, 0, -
Wing 2 Cm0 of Airfoil, 0, -
Wing 2 t/c max, 0, %
Wing 2 stall min, 0, deg
Wing 2 stall max, 0, deg

Stab 1 Surface Area, 8, m²
Stab 1 Wing Span, 6, m
Stab 1 SweepLE, 0, deg
Stab 1 Taper Ratio, 0.9, -
Stab 1 Zero-Lift Drag Coefficient, 0.03, -
Stab 1 Oswald Efficiency factor, 0.75, -
Stab 1 DeDa, 0.1, -
Stab 1 Dihedral Angle, 0, deg
Stab 1 Offset in Y, 0, m
Stab 1 Cl0 of Airfoil, 0.2, -
Stab 1 Cm0 of Airfoil, 0.18, -
Stab 1 t/c max, 0.1, %
Stab 1 stall min, -15, deg
Stab 1 stall max, 15, deg
Elevator Chord Length, 0.5, m

Stab 2 Surface Area, 12, m²
Stab 2 Wing Span, 6, m
Stab 2 SweepLE, 50, deg
Stab 2 Taper Ratio, 0.6, -
Stab 2 Zero-Lift Drag Coefficient, 0.03, -
Stab 2 Oswald Efficiency factor, 0.75, -
Stab 2 DeDa, 0.1, -
Stab 2 Dihedral Angle, 38, deg
Stab 2 Offset in Y, 0, m
Stab 2 Cl0 of Airfoil, 0.2, -
Stab 2 Cm0 of Airfoil, 0.18, -
Stab 2 t/c max, 0.1, %
Stab 2 stall min, -15, deg
Stab 2 stall max, 15, deg
Rudder Chord Length, 0.5, m

Empennage Connection Width, 0, m
Empennage Connection Height, 0, m

Number of Upward Engines, 6, -
Diameter Upward Engines, 1, m
Thrust Coefficient Upward Engines, 0.8, -
Number of Blades Upward Engines, 5, -
Average Blade Chord Upward Engines, 0.3, m

Number of Forward Engines, 2, -
Diameter Forward Engines, 1, m

Thrust Coefficient Forward Engines, 0.8, -
Number of Blades Forward Engines, 5, -
Average Blade Chord Forward Engines, 0.3, m

Fuselage Upward Drag Coefficient, 0.8, -
Fuselage Forward Drag Coefficient, 0.245, -
Fuselage Length X, 7.3, m
Fuselage Width Y, 2.8, m
Fuselage Height Z, 2.8, m

Battery, 250000, Wh
Battery Length X, 1, m
Battery Width Y, 1, m
Battery Height Z, 1, m

Location of Battery X, 0, m
Location of Battery Y, 0, m
Location of Battery Z, 1, m

Location of Passengers X, 2, m
Location of Passengers Y, 0, m
Location of Passengers Z, 1, m

Location of Wing 1 X, 4.5, m
Location of Wing 1 Y, 0, m
Location of Wing 1 Z, 2.8, m

Location of Wing 2 X, 0, m
Location of Wing 2 Y, 0, m
Location of Wing 2 Z, 0, m

Location of Stab 1 X, 11.3, m
Location of Stab 1 Y, 0, m
Location of Stab 1 Z, 4.72, m

Location of Stab 2 X, 8, m
Location of Stab 2 Y, 0, m
Location of Stab 2 Z, 2.8, m

Location of Upward T1 X, 5, m
Location of Upward T1 Y, 14, m
Location of Upward T1 Z, 4.6, m

Location of Upward T2 X, 5, m
Location of Upward T2 Y, -14, m
Location of Upward T2 Z, 4.6, m

Location of Upward T3 X, 8, m
Location of Upward T3 Y, 7, m
Location of Upward T3 Z, 4.2, m

Location of Upward T4 X, 8, m
Location of Upward T4 Y, -7, m
Location of Upward T4 Z, 4.2, m

Location of Upward T5 X, 2, m

Location of Upward T5 Y, 7, m
Location of Upward T5 Z, 4.2, m

Location of Upward T6 X, 2, m
Location of Upward T6 Y, -7, m
Location of Upward T6 Z, 4.2, m

Location of Upward T7 X, 0, m
Location of Upward T7 Y, 0, m
Location of Upward T7 Z, 0, m

Location of Upward T8 X, 0, m
Location of Upward T8 Y, 0, m
Location of Upward T8 Z, 0, m

Location of Upward T9 X, 0, m
Location of Upward T9 Y, 0, m
Location of Upward T9 Z, 0, m

Location of Upward T10 X, 0, m
Location of Upward T10 Y, 0, m
Location of Upward T10 Z, 0, m

Location of Upward T11 X, 0, m
Location of Upward T11 Y, 0, m
Location of Upward T11 Z, 0, m

Location of Upward T12 X, 0, m
Location of Upward T12 Y, 0, m
Location of Upward T12 Z, 0, m

Location of Forward Tf1 X, 12, m
Location of Forward Tf1 Y, -3, m
Location of Forward Tf1 Z, 4, m

Location of Forward Tf2 X, 12, m
Location of Forward Tf2 Y, 3, m
Location of Forward Tf2 Z, 4, m

Location of Forward Tf3 X, 0, m
Location of Forward Tf3 Y, 0, m
Location of Forward Tf3 Z, 0, m

Location of Forward Tf4 X, 0, m
Location of Forward Tf4 Y, 0, m
Location of Forward Tf4 Z, 0, m

Location of Forward Tf5 X, 0, m
Location of Forward Tf5 Y, 0, m
Location of Forward Tf5 Z, 0, m

Location of Forward Tf6 X, 0, m
Location of Forward Tf6 Y, 0, m
Location of Forward Tf6 Z, 0, m

Weight of Fuselage, 800, kg

Weight of Passengers, 400, kg
Weight of Battery, 700, kg
Weight of Wing 1, 400, kg
Weight of Wing 2, 0, kg
Weight of Stab 1, 140, kg
Weight of Stab 2, 0, kg
Weight of an Upward Engine, 30, kg
Weight of a Forward Engine, 30, kg

E.1.2. Output Plots

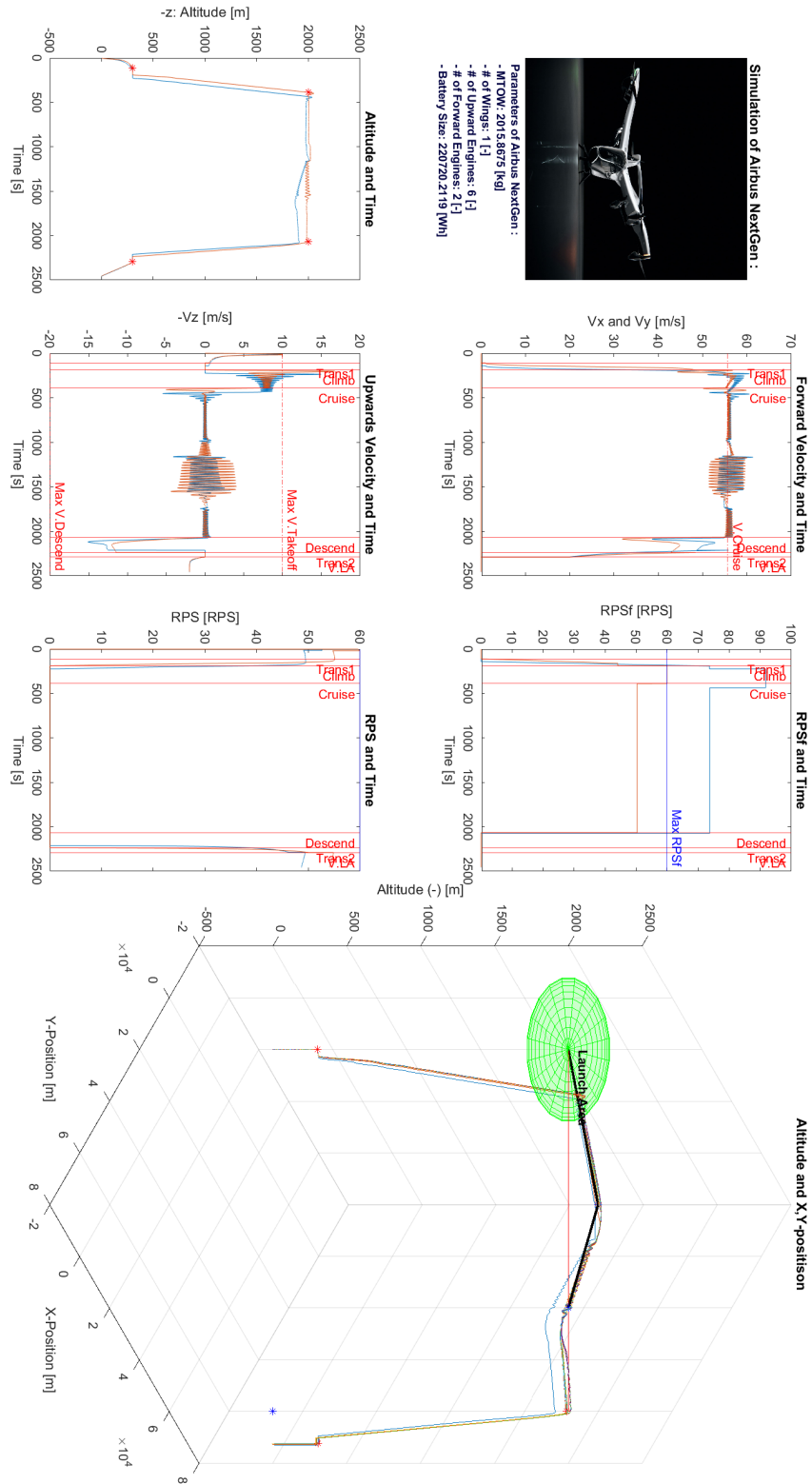


Figure E.1: Optimum Path of Airbus NextGEN

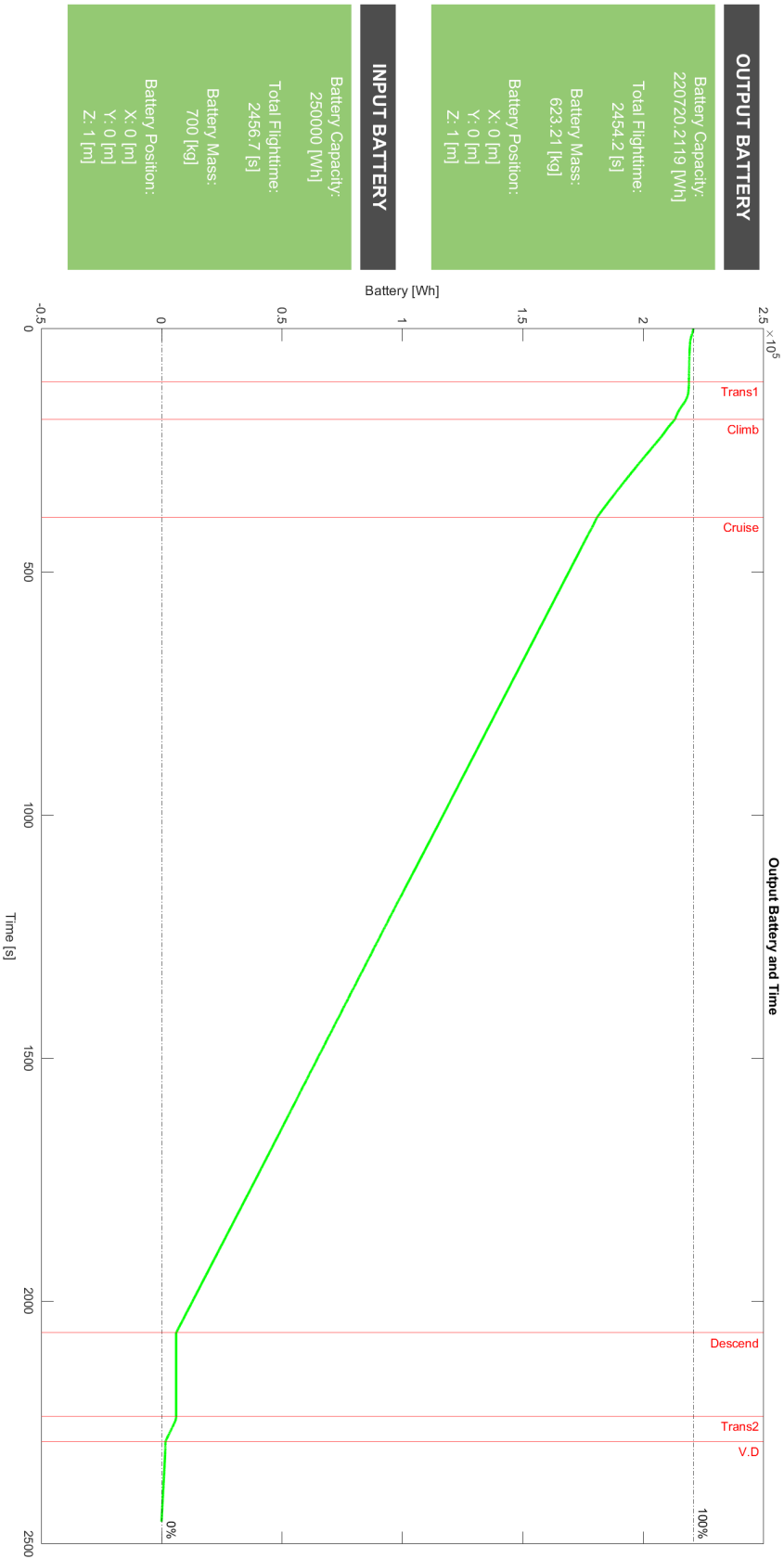


Figure E.2: Optimum Battery of Airbus NextGEN

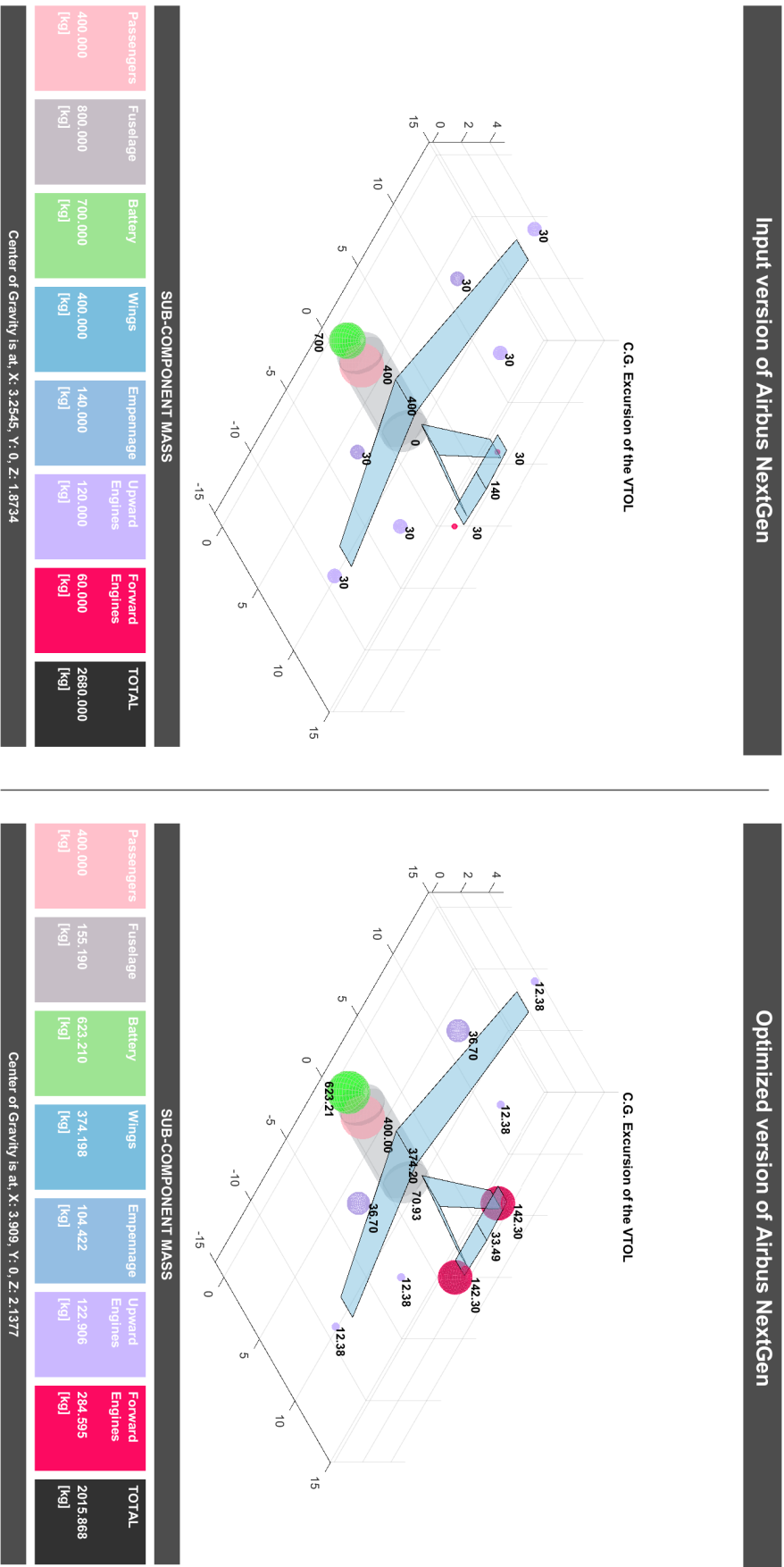
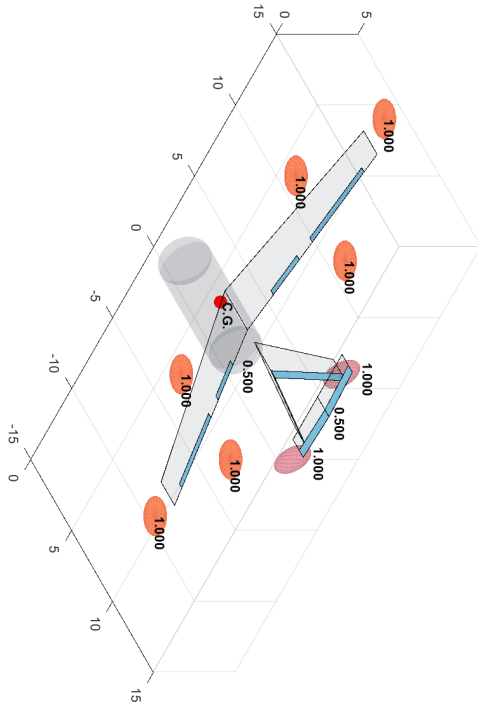


Figure E.3: Optimum Masses of Airbus NextGEN

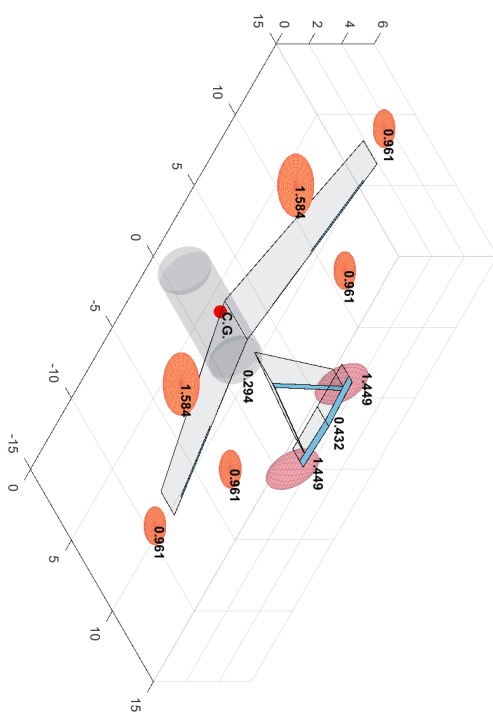
Input version of Airbus NextGen



CONTROL SURFACES				ENGINES		
Elevator (Stab 1)	Rudder (Stab 2)	HS Aileron (Wing 1)	LS Aileron (Wing 1)	Upward Engine	Upward Engine	Forward Engine
Chord: 0,500 [m]	Chord: 0,500 [m]	Chord: 0,300 [m]	Chord: 0,300 [m]	Diam: 1,000 [m] Adv.R: 0,191 Solidity: 0,955	Diam: 1,000 [m] Adv.R: 0,434 Solidity: 0,955	Diam: 1,000 [m] Adv.R: 0,832 Solidity: 0,625

Center of Gravity is at: X: 3,2545, Y: 0, Z: 1,8734

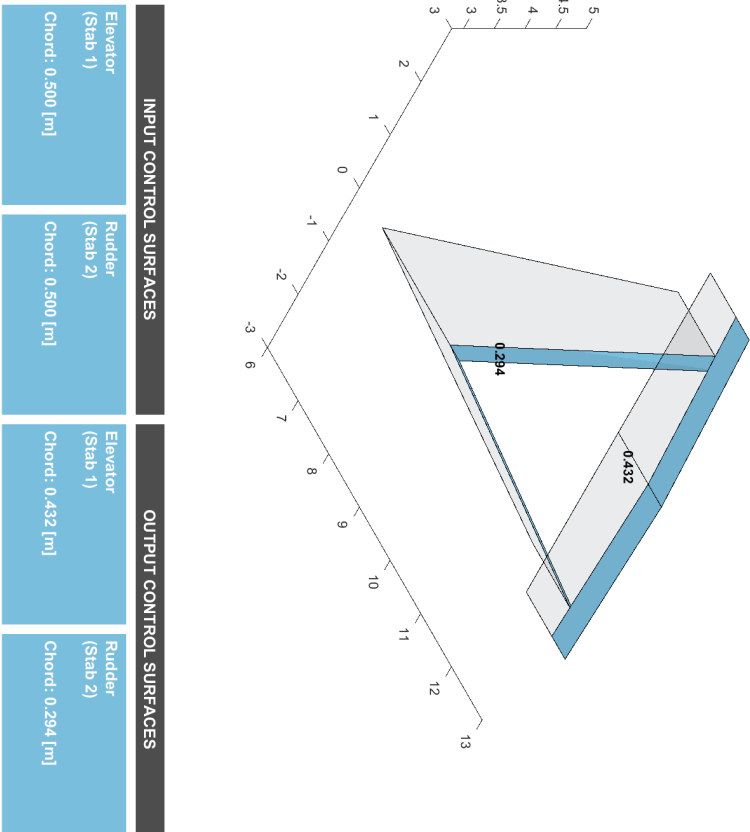
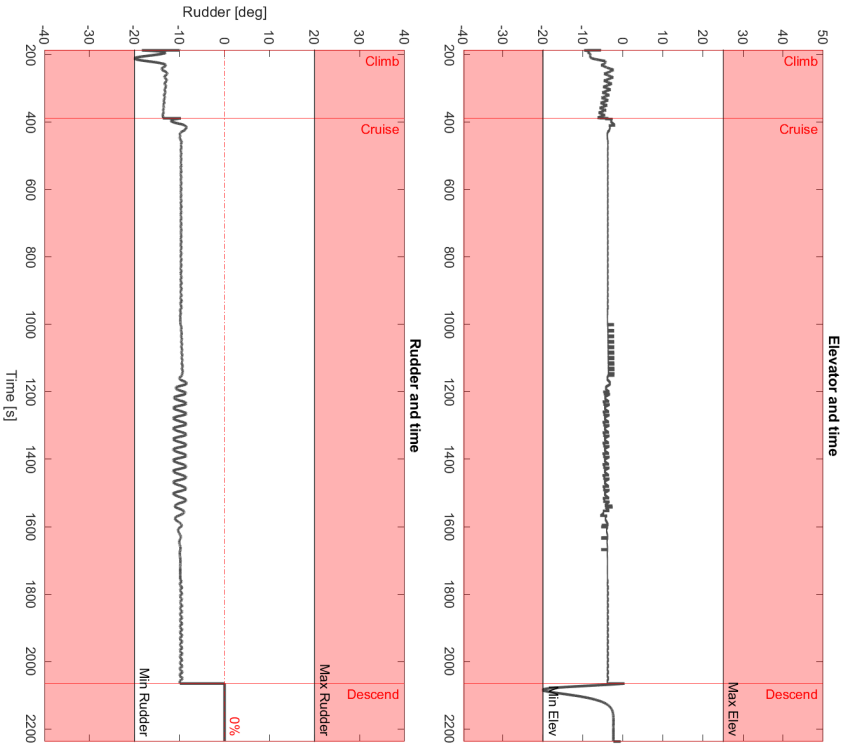
Optimized version of Airbus NextGen



CONTROL SURFACES				ENGINES		
Elevator (Stab 1)	Rudder (Stab 2)	HS Aileron (Wing 1)	LS Aileron (Wing 1)	Upward Engine	Upward Engine	Forward Engine
Chord: 0,432 [m]	Chord: 0,294 [m]	Chord: 0,015 [m]	Chord: 0,093 [m]	Diam: 1,584 [m] Adv.R: 0,253 Solidity: 0,603	Diam: 0,961 [m] Adv.R: 0,416 Solidity: 0,993	Diam: 1,449 [m] Adv.R: 0,823 Solidity: 0,659

Center of Gravity is at: X: 3,909, Y: 0, Z: 2,1377

Figure E.4: Optimum Dimensions of Airbus NextGEN



INPUT CONTROL SURFACES		OUTPUT CONTROL SURFACES	
Elevator (Stab 1)	Rudder (Stab 2)	Elevator (Stab 1)	Rudder (Stab 2)
Chord: 0.500 [m]	Chord: 0.500 [m]	Chord: 0.432 [m]	Chord: 0.294 [m]

Figure E.5: Optimum Stabiliser of Airbus NextGEN

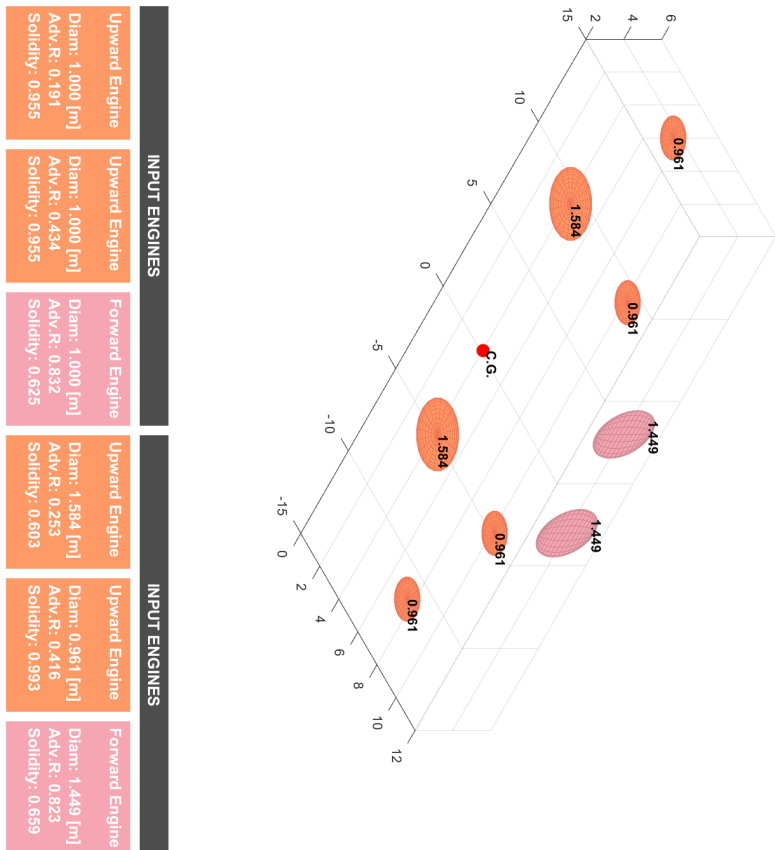
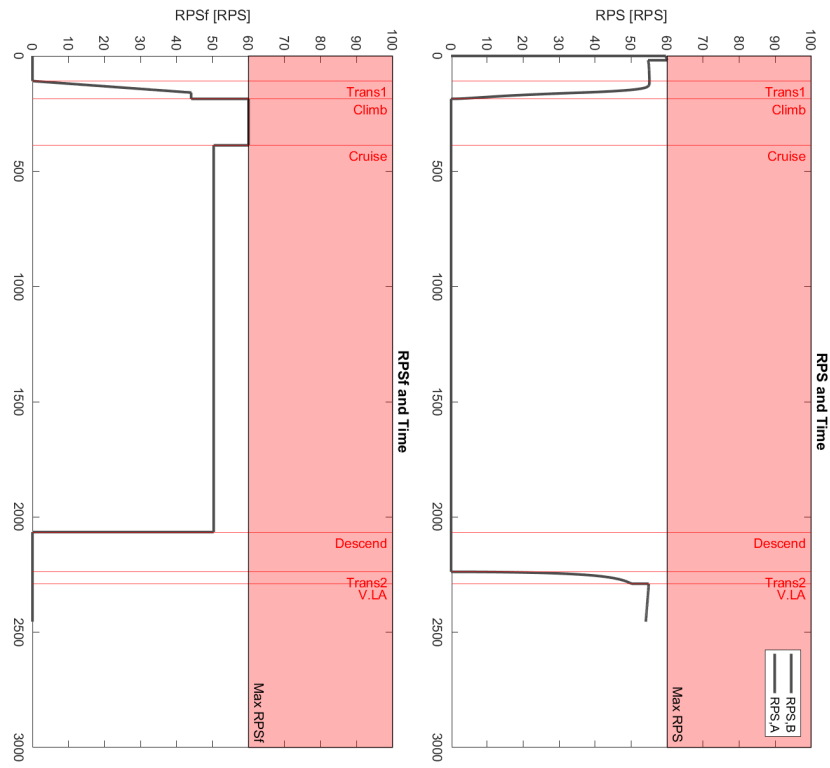


Figure E.6: Optimum Engines of Airbus NextGEN

E.2. Korean KUS

E.2.1. Input Parameter File

Parameter, Value, Unit

```
#-----
# Notes: The Coordinate system is centered at 0,0,0 on the front, at the
# bottom and in the middle of the fuselage. If the rotors of the aircraft
# can rotate please use the upwards engines and not the forward engines.
# If there is a V-Tail, use Stabilizer 1.
#-----
# General Data
#-----
Mass, 2337, kg
Design Cruise Velocity, 200, km/h
Design Range, 100, km
Number of Passengers, 0, -
Number of Wings, 1, -
Number of Stabilizers, 2, -

Wing 1 Surface Area, 32, m2
Wing 1 Wing Span, 20, m
Wing 1 SweepLE, -2, deg
Wing 1 Taper Ratio, 0.8, -
Wing 1 Zero-Lift Drag Coefficient, 0.03, -
Wing 1 Oswald Efficiency factor, 0.80, -
Wing 1 DeDa, 0, -
Wing 1 Dihedral Angle, 0, deg
Wing 1 Cl0 of Airfoil, 0.15, -
Wing 1 Cm0 of Airfoil, 0.18, -
Wing 1 t/c max, 0.1, %
Wing 1 stall min, -15, deg
Wing 1 stall max, 15, deg
LS Aileron Chord Length, 0.3, m
LS Aileron Start %b/2, 0.5, %
LS Aileron Stop %b/2, 0.9, %
HS Aileron Chord Length, 0.3, m
HS Aileron Start %b/2, 0.2, %
HS Aileron Stop %b/2, 0.4, %

Wing 2 Surface Area, 0, m2
Wing 2 Wing Span, 0, m
Wing 2 SweepLE, 0, deg
Wing 2 Taper Ratio, 0, -
Wing 2 Zero-Lift Drag Coefficient, 0, -
Wing 2 Oswald Efficiency factor, 0, -
Wing 2 DeDa, 0, -
Wing 2 Dihedral Angle, 0, deg
Wing 2 Cl0 of Airfoil, 0, -
Wing 2 Cm0 of Airfoil, 0, -
Wing 2 t/c max, 0, %
Wing 2 stall min, 0, deg
Wing 2 stall max, 0, deg

Stab 1 Surface Area, 5, m2
Stab 1 Wing Span, 10, m
Stab 1 SweepLE, 0, deg
```


Stab 1 Taper Ratio, 1, -
Stab 1 Zero-Lift Drag Coefficient, 0.03, -
Stab 1 Oswald Efficiency factor, 0.8, -
Stab 1 DeDa, 0.1, -
Stab 1 Dihedral Angle, 0, deg
Stab 1 Offset in Y, 0, m
Stab 1 Cl0 of Airfoil, 0.15, -
Stab 1 Cm0 of Airfoil, 0.18, -
Stab 1 t/c max, 0.1, %
Stab 1 stall min, -15, deg
Stab 1 stall max, 15, deg
Elevator Chord Length, 0.1, m

Stab 2 Surface Area, 2, m²
Stab 2 Wing Span, 3, m
Stab 2 SweepLE, 18, deg
Stab 2 Taper Ratio, 0.47, -
Stab 2 Zero-Lift Drag Coefficient, 0.03, -
Stab 2 Oswald Efficiency factor, 0.75, -
Stab 2 DeDa, 0.1, -
Stab 2 Dihedral Angle, 95, deg
Stab 2 Offset in Y, 5.13, m
Stab 2 Cl0 of Airfoil, 0.15, -
Stab 2 Cm0 of Airfoil, 0, -
Stab 2 t/c max, 0.1, %
Stab 2 stall min, -15, deg
Stab 2 stall max, 15, deg
Rudder Chord Length, 0.2, m

Empennage Connection Width, 0, m
Empennage Connection Height, 0, m

Number of Upward Engines, 4, -
Diameter Upward Engines, 1, m
Thrust Coefficient Upward Engines, 0.8, -
Number of Blades Upward Engines, 5, -
Average Blade Chord Upward Engines, 0.16, m

Number of Forward Engines, 1, -
Diameter Forward Engines, 1, m
Thrust Coefficient Forward Engines, 0.8, -
Number of Blades Forward Engines, 5, -
Average Blade Chord Forward Engines, 0.22, m

Fuselage Upward Drag Coefficient, 0.8, -
Fuselage Forward Drag Coefficient, 0.245, -
Fuselage Length X, 5, m
Fuselage Width Y, 2, m
Fuselage Height Z, 2, m

Battery, 254000, Wh
Battery Length X, 1, m
Battery Width Y, 1, m
Battery Height Z, 0.5, m

Location of Battery X, 1, m

Location of Battery Y, 0, m
Location of Battery Z, 0.5, m

Location of Passengers X, 1.5, m
Location of Passengers Y, 0, m
Location of Passengers Z, 1.25, m

Location of Wing 1 X, 3.5, m
Location of Wing 1 Y, 0, m
Location of Wing 1 Z, 2, m

Location of Wing 2 X, 0, m
Location of Wing 2 Y, 0, m
Location of Wing 2 Z, 0, m

Location of Stab 1 X, 8, m
Location of Stab 1 Y, 0, m
Location of Stab 1 Z, 3.5, m

Location of Stab 2 X, 7.76, m
Location of Stab 2 Y, 0, m
Location of Stab 2 Z, 2, m

Location of Upward T1 X, 0.5, m
Location of Upward T1 Y, -3, m
Location of Upward T1 Z, 2, m

Location of Upward T2 X, 6, m
Location of Upward T2 Y, -3, m
Location of Upward T2 Z, 2, m

Location of Upward T3 X, 0.5, m
Location of Upward T3 Y, 3, m
Location of Upward T3 Z, 2, m

Location of Upward T4 X, 6, m
Location of Upward T4 Y, 3, m
Location of Upward T4 Z, 2, m

Location of Upward T5 X, 0, m
Location of Upward T5 Y, 0, m
Location of Upward T5 Z, 0, m

Location of Upward T6 X, 0, m
Location of Upward T6 Y, 0, m
Location of Upward T6 Z, 0, m

Location of Upward T7 X, 0, m
Location of Upward T7 Y, 0, m
Location of Upward T7 Z, 0, m

Location of Upward T8 X, 0, m
Location of Upward T8 Y, 0, m
Location of Upward T8 Z, 0, m

Location of Upward T9 X, 0, m

Location of Upward T9 Y, 0, m
Location of Upward T9 Z, 0, m

Location of Upward T10 X, 0, m
Location of Upward T10 Y, 0, m
Location of Upward T10 Z, 0, m

Location of Upward T11 X, 0, m
Location of Upward T11 Y, 0, m
Location of Upward T11 Z, 0, m

Location of Upward T12 X, 0, m
Location of Upward T12 Y, 0, m
Location of Upward T12 Z, 0, m

Location of Forward Tf1 X, 6, m
Location of Forward Tf1 Y, 0, m
Location of Forward Tf1 Z, 1, m

Location of Forward Tf2 X, 0, m
Location of Forward Tf2 Y, 0, m
Location of Forward Tf2 Z, 0, m

Location of Forward Tf3 X, 0, m
Location of Forward Tf3 Y, 0, m
Location of Forward Tf3 Z, 0, m

Location of Forward Tf4 X, 0, m
Location of Forward Tf4 Y, 0, m
Location of Forward Tf4 Z, 0, m

Location of Forward Tf5 X, 0, m
Location of Forward Tf5 Y, 0, m
Location of Forward Tf5 Z, 0, m

Location of Forward Tf6 X, 0, m
Location of Forward Tf6 Y, 0, m
Location of Forward Tf6 Z, 0, m

Weight of Fuselage, 259, kg
Weight of Passengers, 0, kg
Weight of Battery, 597, kg
Weight of Wing 1, 414, kg
Weight of Wing 2, 0, kg
Weight of Stab 1, 51, kg
Weight of Stab 2, 27, kg
Weight of an Upward Engine, 24.75, kg
Weight of a Forward Engine, 79.625, kg

E.2.2. Output Plots

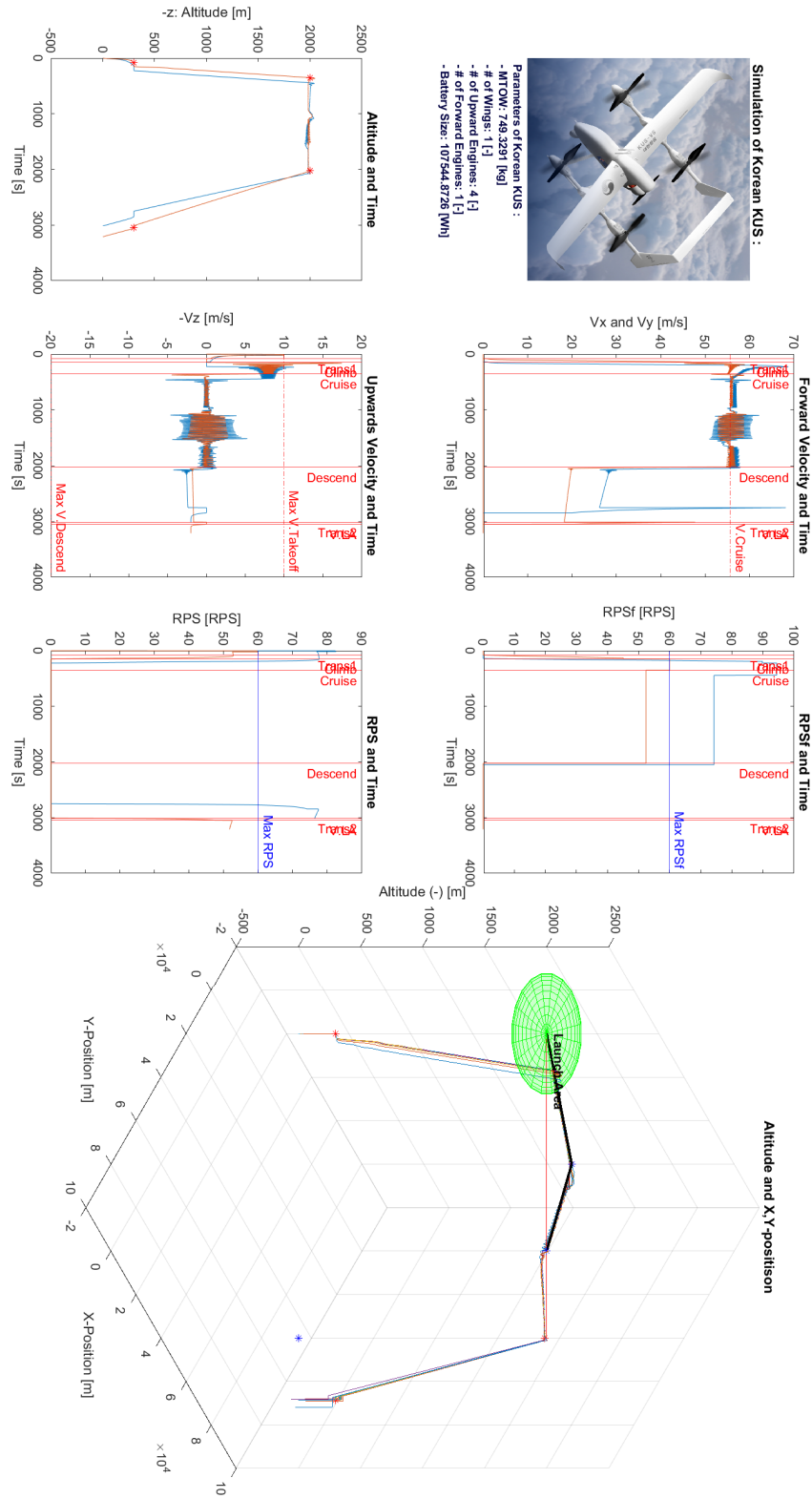


Figure E.7: Optimum Path of Korean KUS

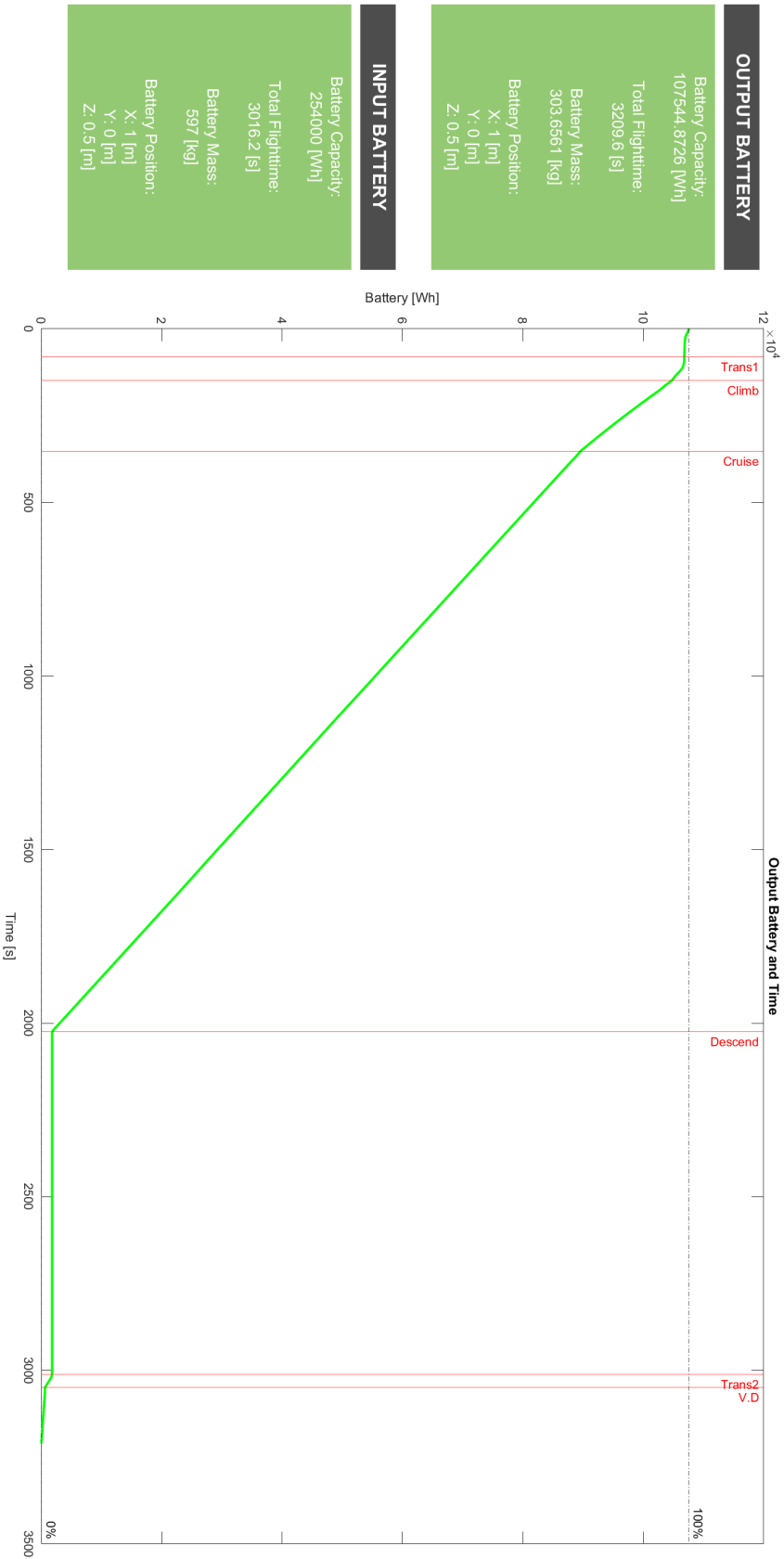


Figure E.8: Optimum Battery of Korean KUS

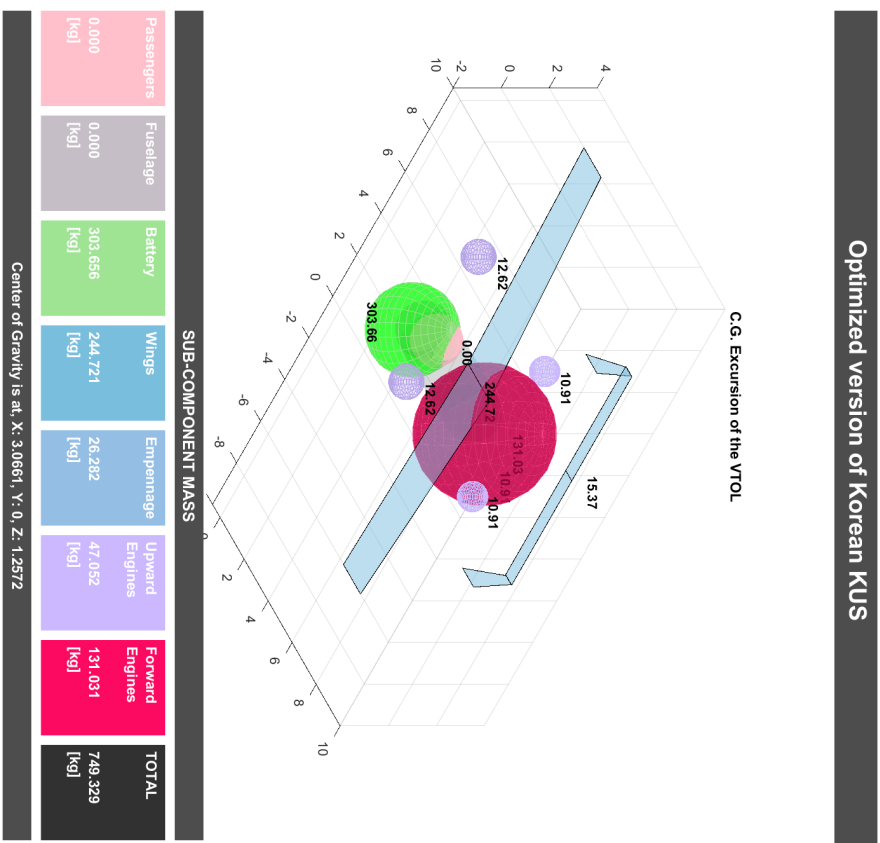
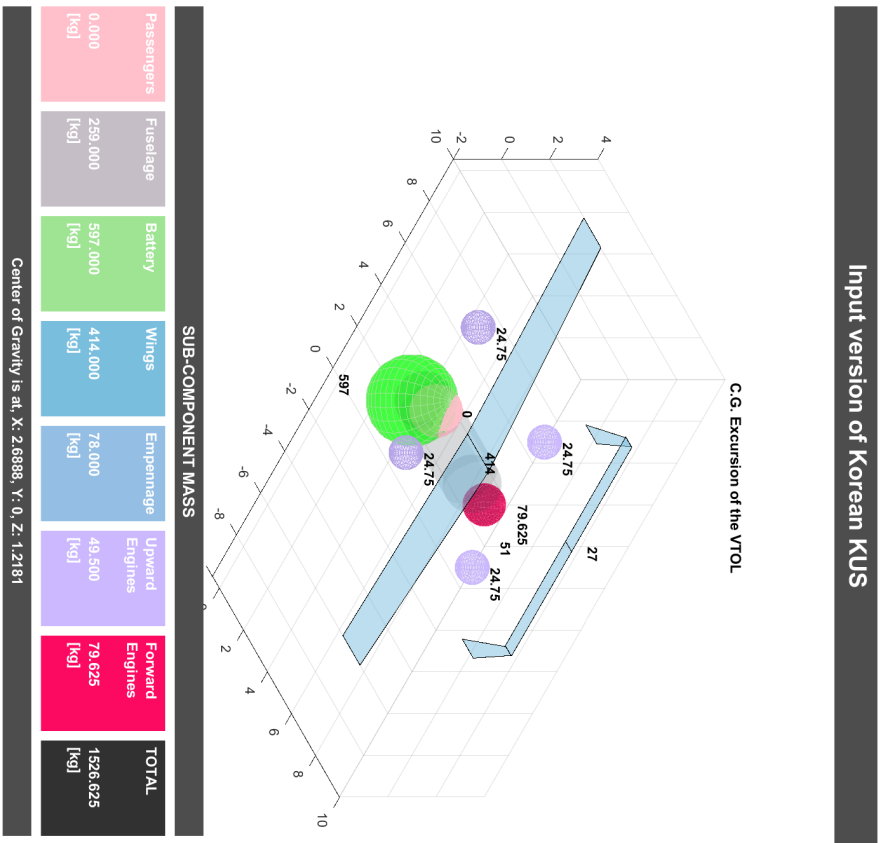


Figure E.9: Optimum Masses of Korean KUS

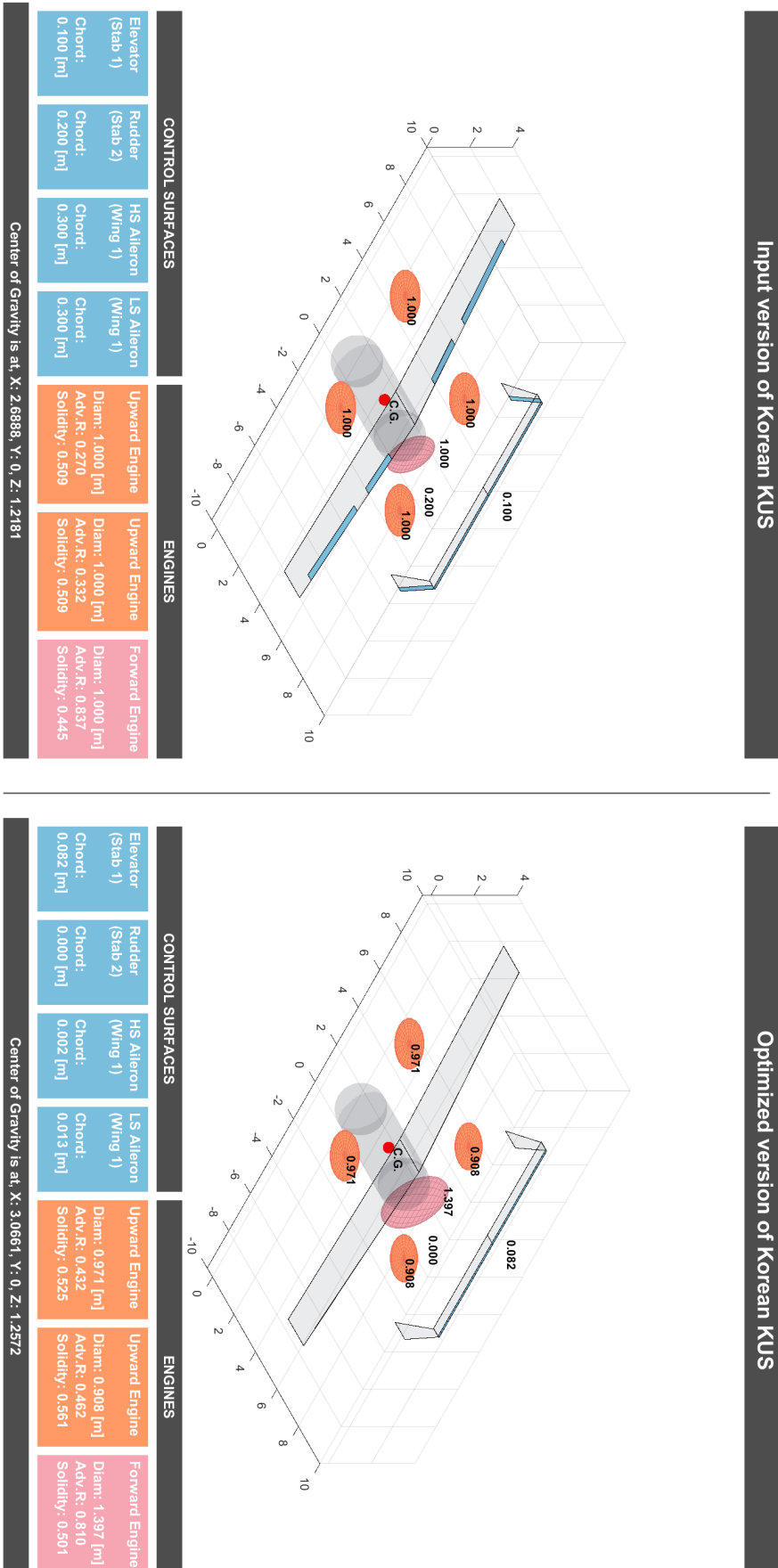
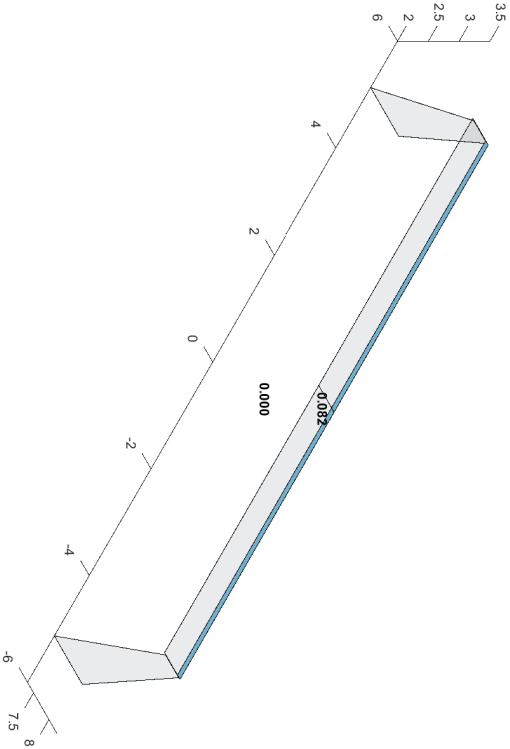
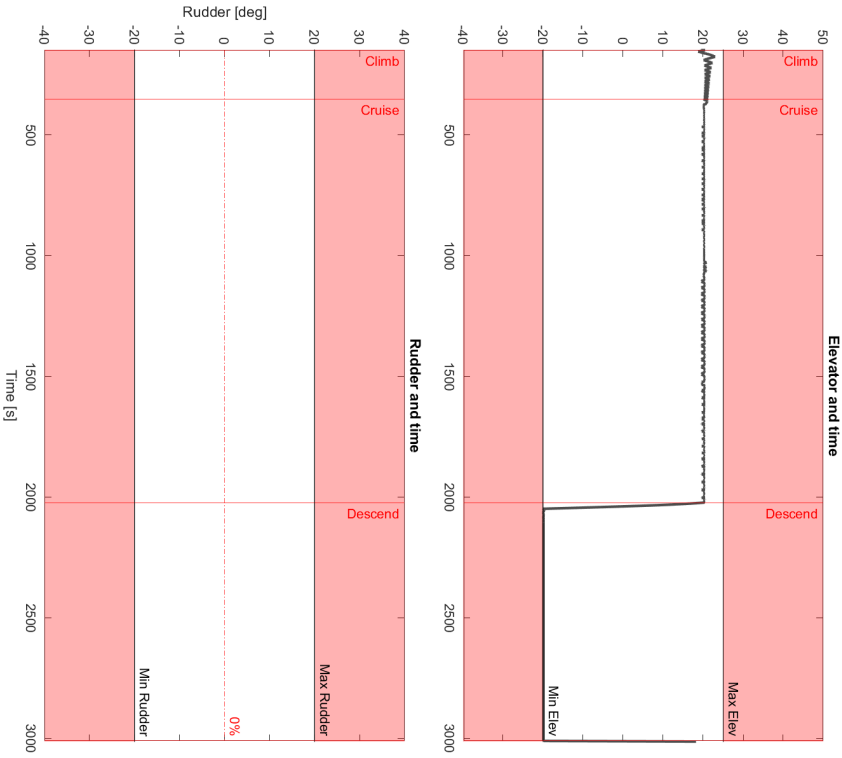


Figure E.10: Optimum Dimensions of Korean KUS



INPUT CONTROL SURFACES		OUTPUT CONTROL SURFACES	
Elevator (Stab 1)	Rudder (Stab 2)	Elevator (Stab 1)	Rudder (Stab 2)
Chord: 0.100 [m]	Chord: 0.200 [m]	Chord: 0.082 [m]	Chord: 0.000 [m]

Figure E.11: Optimum Stabiliser of Korean KUS

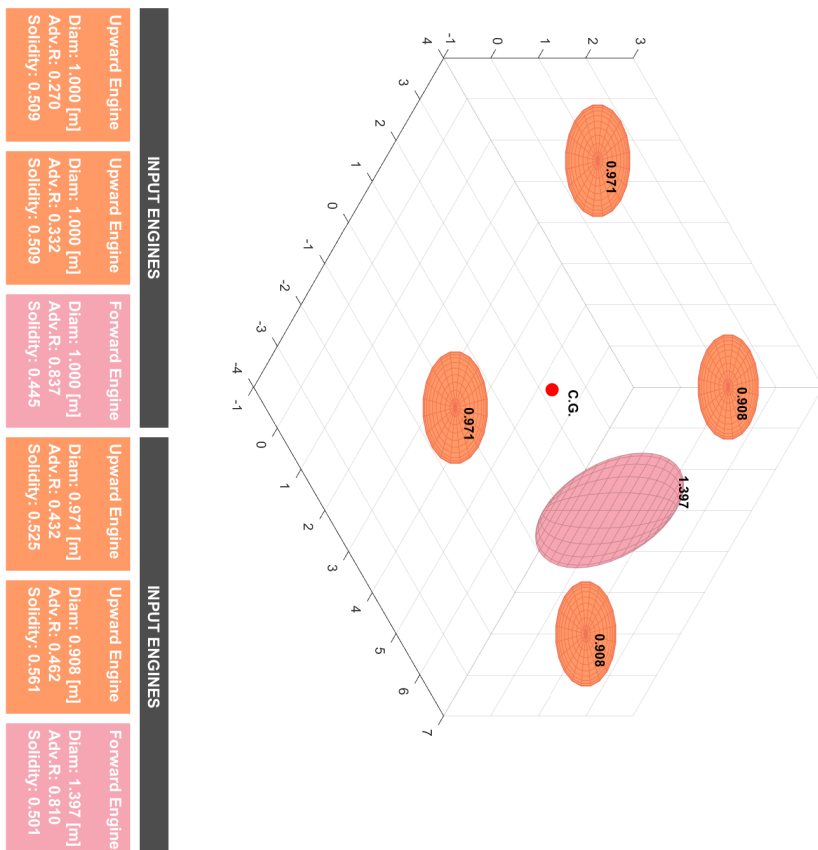
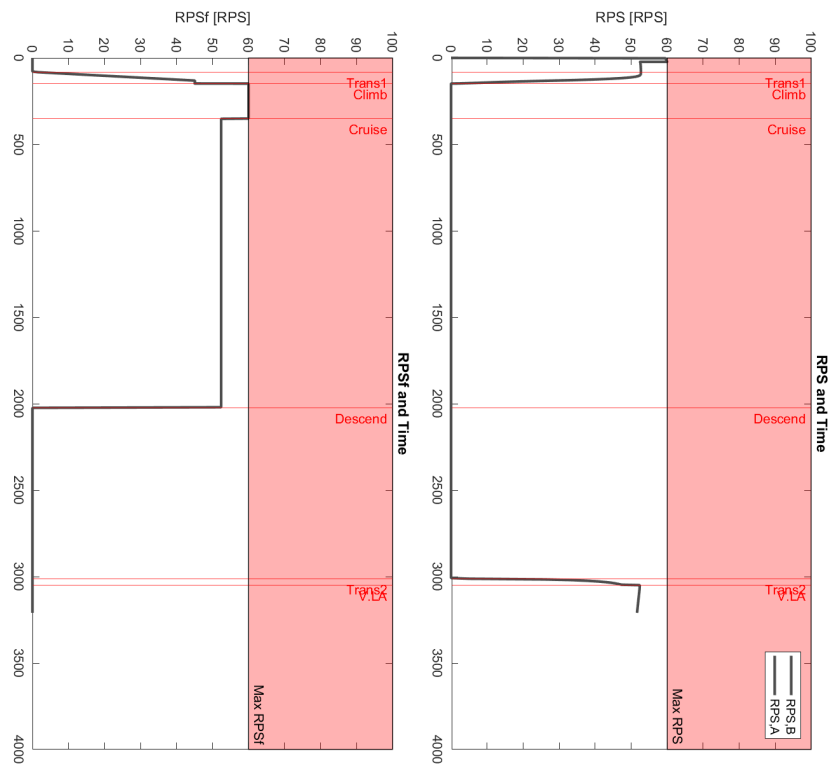


Figure E.12: Optimum Engines of Korean KUS

E.3. Wisk Cora

E.3.1. Input Parameter File

Parameter, Value, Unit

```
#-----
# Notes: The Coordinate system is centered at 0,0,0 on the front, at the
# bottom and in the middle of the fuselage. If the rotors of the aircraft
# can rotate please use the upwards engines and not the forward engines.
# If there is a V-Tail, use Stabilizer 1.
#-----
# General Data
#-----
Mass, 2000, kg
Design Cruise Velocity, 200, km/h
Design Range, 100, km
Number of Passengers, 2, -
Number of Wings, 1, -
Number of Stabilizers, 2, -

Wing 1 Surface Area, 25, m2
Wing 1 Wing Span, 15, m
Wing 1 SweepLE, 3, deg
Wing 1 Taper Ratio, 0.7, -
Wing 1 Zero-Lift Drag Coefficient, 0.03, -
Wing 1 Oswald Efficiency factor, 0.80, -
Wing 1 DeDa, 0, -
Wing 1 Dihedral Angle, 0, deg
Wing 1 Cl0 of Airfoil, 0.15, -
Wing 1 Cm0 of Airfoil, 0.18, -
Wing 1 t/c max, 0.1, %
Wing 1 stall min, -15, deg
Wing 1 stall max, 15, deg
LS Aileron Chord Length, 0.3, m
LS Aileron Start %b/2, 0.5, %
LS Aileron Stop %b/2, 0.9, %
HS Aileron Chord Length, 0.3, m
HS Aileron Start %b/2, 0.2, %
HS Aileron Stop %b/2, 0.4, %

Wing 2 Surface Area, 0, m2
Wing 2 Wing Span, 0, m
Wing 2 SweepLE, 0, deg
Wing 2 Taper Ratio, 0, -
Wing 2 Zero-Lift Drag Coefficient, 0, -
Wing 2 Oswald Efficiency factor, 0, -
Wing 2 DeDa, 0, -
Wing 2 Dihedral Angle, 0, deg
Wing 2 Cl0 of Airfoil, 0, -
Wing 2 Cm0 of Airfoil, 0, -
Wing 2 t/c max, 0, %
Wing 2 stall min, 0, deg
Wing 2 stall max, 0, deg

Stab 1 Surface Area, 5, m2
Stab 1 Wing Span, 6, m
Stab 1 SweepLE, 0, deg
```

Stab 1 Taper Ratio, 1, -
Stab 1 Zero-Lift Drag Coefficient, 0.03, -
Stab 1 Oswald Efficiency factor, 0.8, -
Stab 1 DeDa, 0.1, -
Stab 1 Dihedral Angle, 0, deg
Stab 1 Offset in Y, 0, m
Stab 1 Cl0 of Airfoil, 0.15, -
Stab 1 Cm0 of Airfoil, 0.18, -
Stab 1 t/c max, 0.1, %
Stab 1 stall min, -15, deg
Stab 1 stall max, 15, deg
Elevator Chord Length, 0.2, m

Stab 2 Surface Area, 3.2, m²
Stab 2 Wing Span, 3, m
Stab 2 SweepLE, 18, deg
Stab 2 Taper Ratio, 0.47, -
Stab 2 Zero-Lift Drag Coefficient, 0.03, -
Stab 2 Oswald Efficiency factor, 0.75, -
Stab 2 DeDa, 0.1, -
Stab 2 Dihedral Angle, 95, deg
Stab 2 Offset in Y, 3.13, m
Stab 2 Cl0 of Airfoil, 0.15, -
Stab 2 Cm0 of Airfoil, 0, -
Stab 2 t/c max, 0.1, %
Stab 2 stall min, -15, deg
Stab 2 stall max, 15, deg
Rudder Chord Length, 0.2, m

Empennage Connection Width, 0, m
Empennage Connection Height, 0, m

Number of Upward Engines, 12, -
Diameter Upward Engines, 1, m
Thrust Coefficient Upward Engines, 0.8, -
Number of Blades Upward Engines, 5, -
Average Blade Chord Upward Engines, 0.16, m

Number of Forward Engines, 1, -
Diameter Forward Engines, 1, m
Thrust Coefficient Forward Engines, 0.8, -
Number of Blades Forward Engines, 5, -
Average Blade Chord Forward Engines, 0.22, m

Fuselage Upward Drag Coefficient, 0.8, -
Fuselage Forward Drag Coefficient, 0.245, -
Fuselage Length X, 7, m
Fuselage Width Y, 2, m
Fuselage Height Z, 2, m

Battery, 254000, Wh
Battery Length X, 1, m
Battery Width Y, 1, m
Battery Height Z, 0.5, m

Location of Battery X, 1, m

Location of Battery Y, 0, m
Location of Battery Z, 0.5, m

Location of Passengers X, 1.5, m
Location of Passengers Y, 0, m
Location of Passengers Z, 1.25, m

Location of Wing 1 X, 4, m
Location of Wing 1 Y, 0, m
Location of Wing 1 Z, 2, m

Location of Wing 2 X, 0, m
Location of Wing 2 Y, 0, m
Location of Wing 2 Z, 0, m

Location of Stab 1 X, 10, m
Location of Stab 1 Y, 0, m
Location of Stab 1 Z, 3.5, m

Location of Stab 2 X, 9.76, m
Location of Stab 2 Y, 0, m
Location of Stab 2 Z, 2, m

Location of Upward T1 X, 2, m
Location of Upward T1 Y, -2, m
Location of Upward T1 Z, 2, m

Location of Upward T2 X, 6.5, m
Location of Upward T2 Y, -2, m
Location of Upward T2 Z, 2, m

Location of Upward T3 X, 2, m
Location of Upward T3 Y, -4, m
Location of Upward T3 Z, 2, m

Location of Upward T4 X, 6.5, m
Location of Upward T4 Y, -4, m
Location of Upward T4 Z, 2, m

Location of Upward T5 X, 2, m
Location of Upward T5 Y, -6, m
Location of Upward T5 Z, 2, m

Location of Upward T6 X, 6.5, m
Location of Upward T6 Y, -6, m
Location of Upward T6 Z, 2, m

Location of Upward T7 X, 2, m
Location of Upward T7 Y, 2, m
Location of Upward T7 Z, 2, m

Location of Upward T8 X, 6.5, m
Location of Upward T8 Y, 2, m
Location of Upward T8 Z, 2, m

Location of Upward T9 X, 2, m

Location of Upward T9 Y, 4, m
Location of Upward T9 Z, 2, m

Location of Upward T10 X, 6.5, m
Location of Upward T10 Y, 4, m
Location of Upward T10 Z, 2, m

Location of Upward T11 X, 2, m
Location of Upward T11 Y, 6, m
Location of Upward T11 Z, 2, m

Location of Upward T12 X, 6.5, m
Location of Upward T12 Y, 6, m
Location of Upward T12 Z, 2, m

Location of Forward Tf1 X, 7.5, m
Location of Forward Tf1 Y, 0, m
Location of Forward Tf1 Z, 1, m

Location of Forward Tf2 X, 0, m
Location of Forward Tf2 Y, 0, m
Location of Forward Tf2 Z, 0, m

Location of Forward Tf3 X, 0, m
Location of Forward Tf3 Y, 0, m
Location of Forward Tf3 Z, 0, m

Location of Forward Tf4 X, 0, m
Location of Forward Tf4 Y, 0, m
Location of Forward Tf4 Z, 0, m

Location of Forward Tf5 X, 0, m
Location of Forward Tf5 Y, 0, m
Location of Forward Tf5 Z, 0, m

Location of Forward Tf6 X, 0, m
Location of Forward Tf6 Y, 0, m
Location of Forward Tf6 Z, 0, m

Weight of Fuselage, 259, kg
Weight of Passengers, 200, kg
Weight of Battery, 597, kg
Weight of Wing 1, 414, kg
Weight of Wing 2, 0, kg
Weight of Stab 1, 27, kg
Weight of Stab 2, 51, kg
Weight of an Upward Engine, 24.75, kg
Weight of a Forward Engine, 79.625, kg

E.3.2. Output Plots

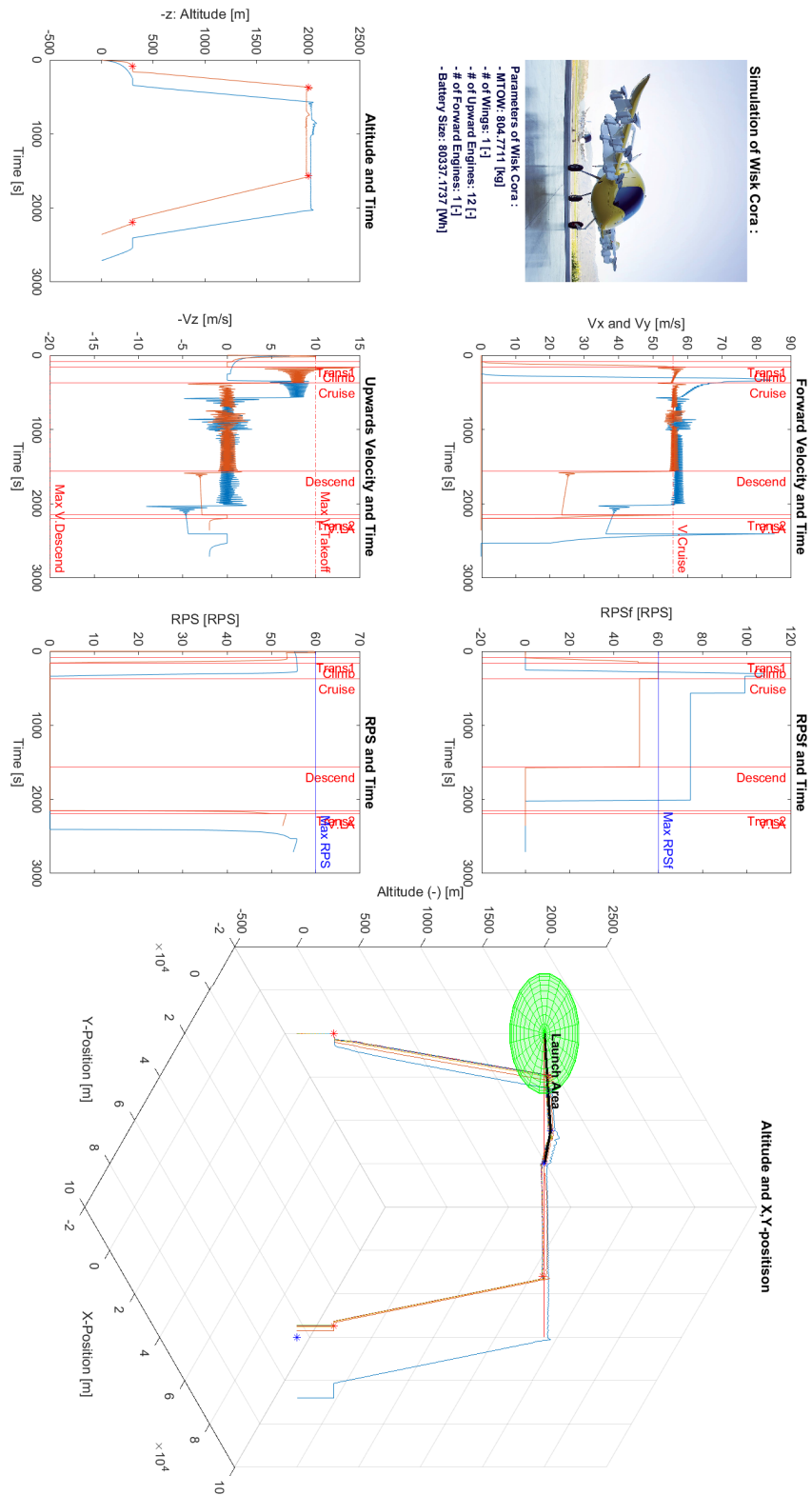


Figure E.13: Optimum Path of Wisk Cora

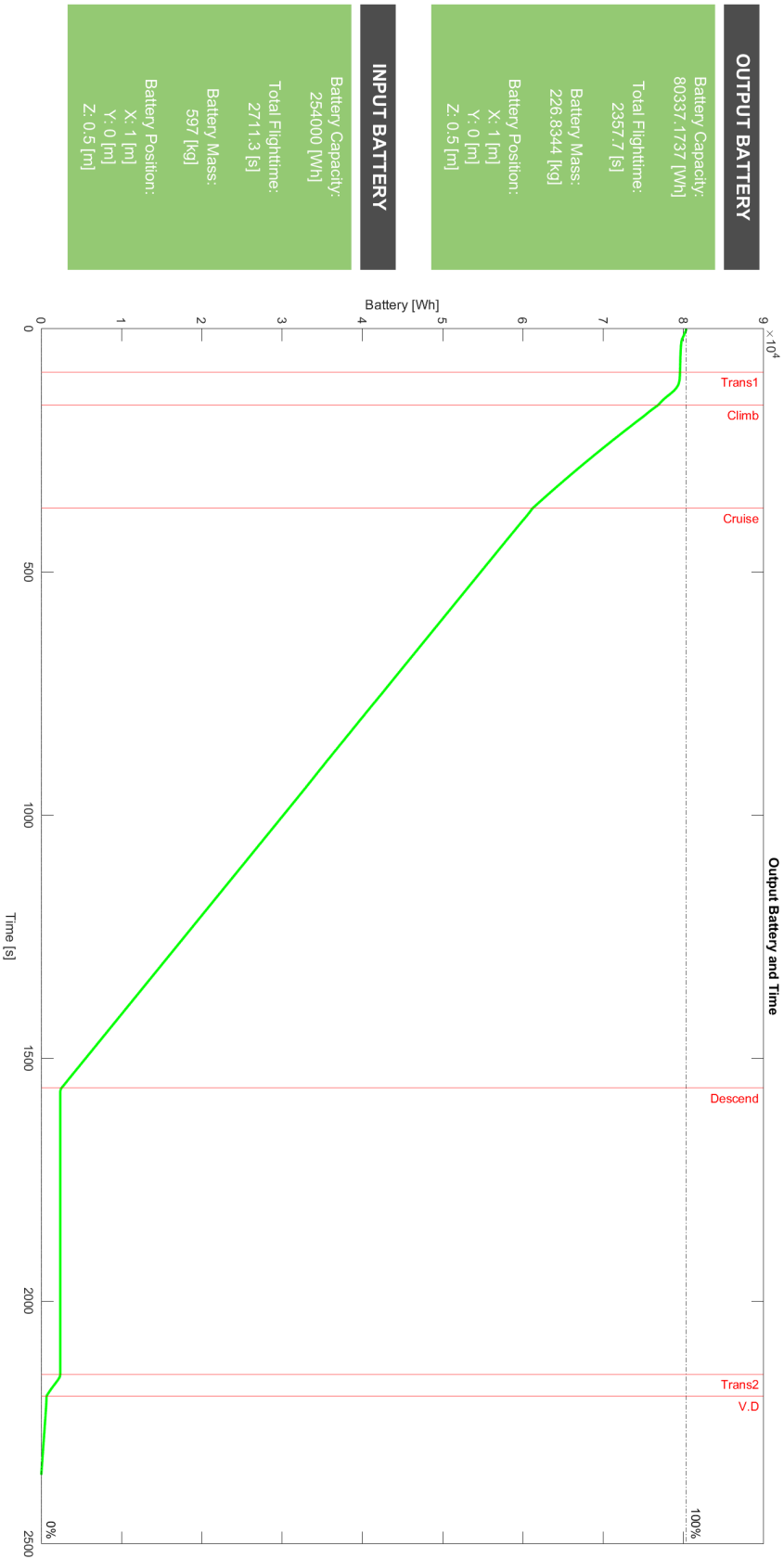


Figure E.14: Optimum Battery of Wisk Cora

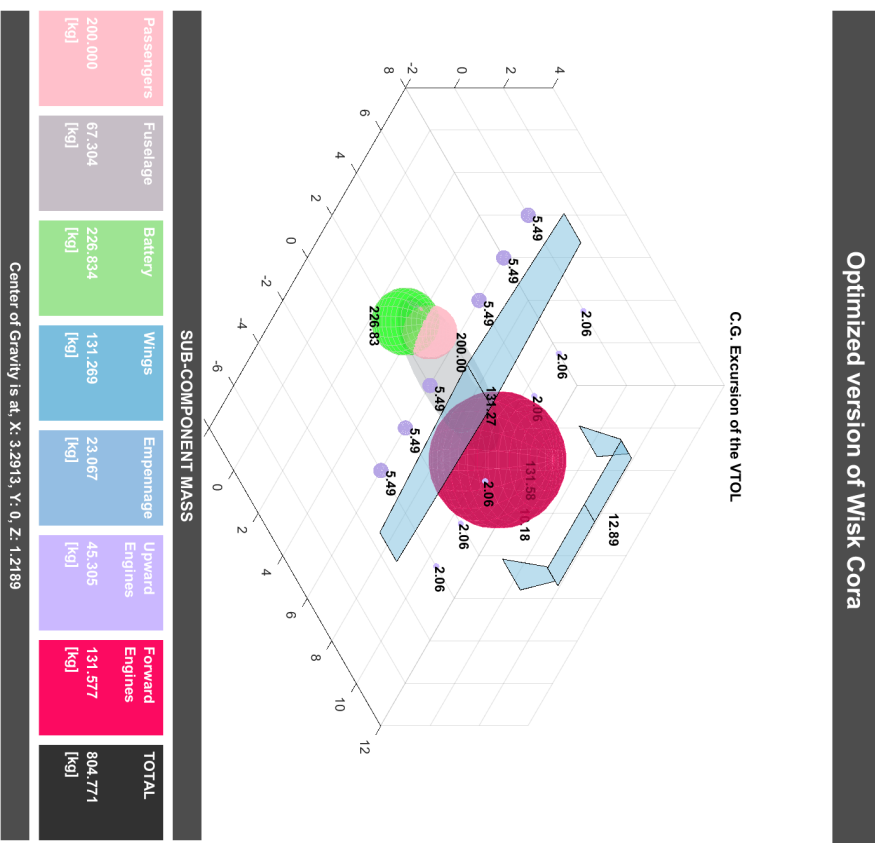
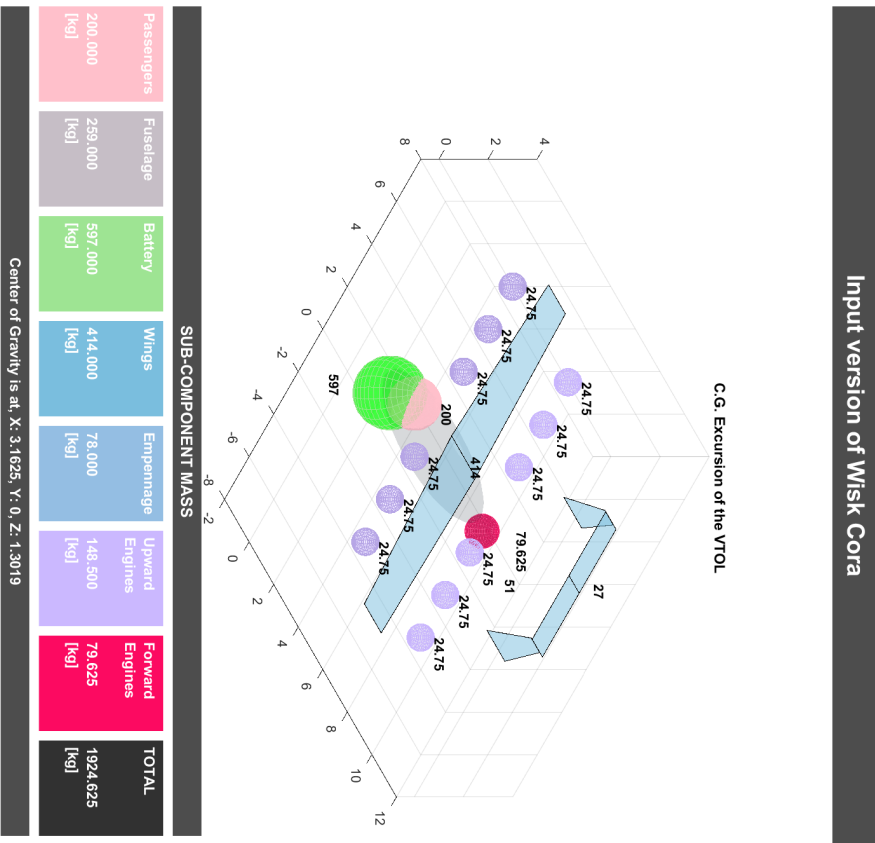


Figure E.15: Optimum Masses of Wisk Cora

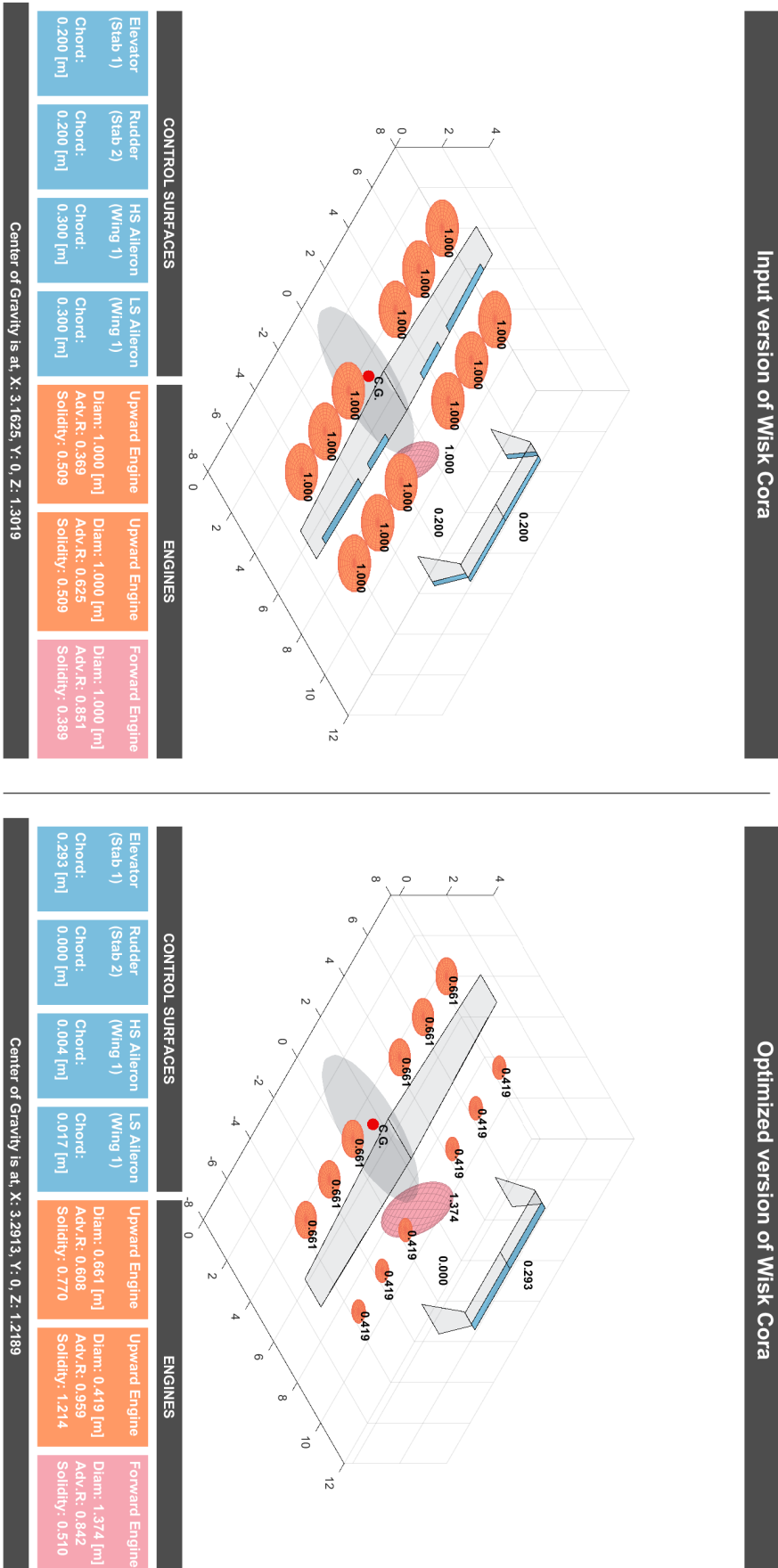
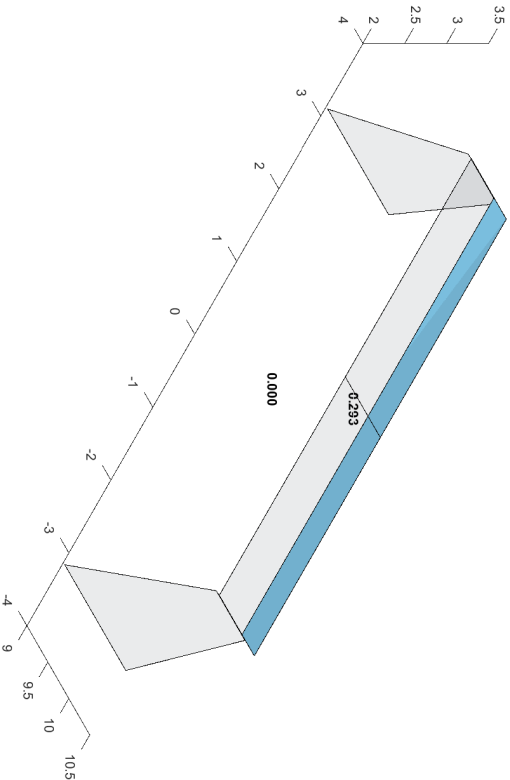
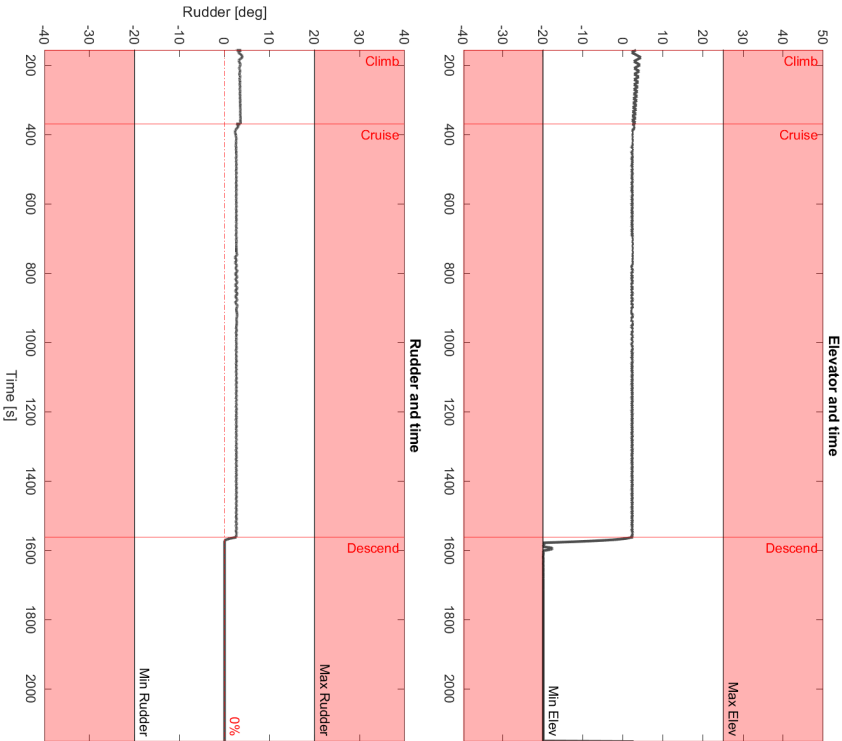
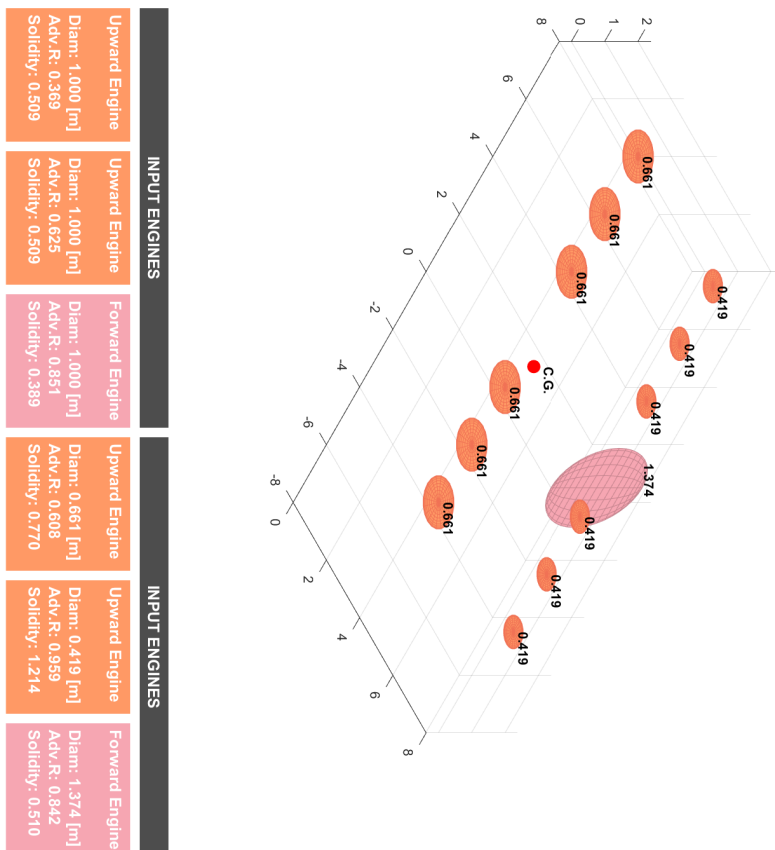
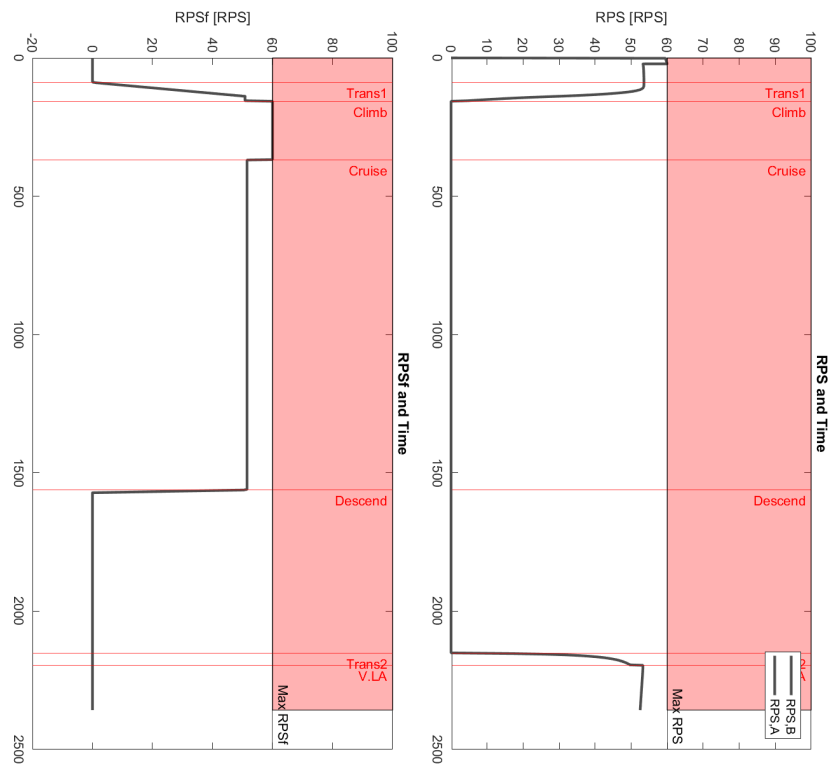


Figure E.16: Optimum Dimensions of Wisk Cora



INPUT CONTROL SURFACES		OUTPUT CONTROL SURFACES	
Elevator (Stab 1)	Rudder (Stab 2)	Elevator (Stab 1)	Rudder (Stab 2)
Chord: 0.200 [m]	Chord: 0.200 [m]	Chord: 0.293 [m]	Chord: 0.000 [m]

Figure E.17: Optimum Stabiliser of Wisk Cora



INPUT ENGINES		INPUT ENGINES	
Upward Engine	Upward Engine	Upward Engine	Upward Engine
Diam: 1,000 [m]	Diam: 1,000 [m]	Diam: 0,661 [m]	Diam: 0,419 [m]
Adv./R: 0,369	Adv./R: 0,625	Adv./R: 0,608	Adv./R: 0,959
Solidity: 0,509	Solidity: 0,509	Solidity: 0,770	Solidity: 1,214
Forward Engine	Forward Engine	Forward Engine	Forward Engine
Diam: 1,000 [m]	Diam: 1,000 [m]	Diam: 1,374 [m]	Diam: 1,374 [m]
Adv./R: 0,851	Adv./R: 0,851	Adv./R: 0,842	Adv./R: 0,842
Solidity: 0,589	Solidity: 0,589	Solidity: 0,510	Solidity: 0,510

Figure E.18: Optimum Engines of Wisk Cora